

Copyright  
by  
Stacy Leona Agar  
2009

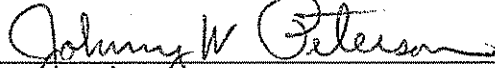
The Dissertation Committee for Stacy Leona Agar Certifies that this is the approved  
version of the following dissertation:

**NEW VIRULENCE MECHANISMS IN *YERSINIA PESTIS*, THE  
PLAGUE (BLACK DEATH)-CAUSING BACTERIUM: A RE-  
EMERGING AND BIOTERROR PATHOGEN**

Committee:



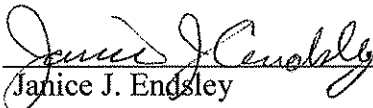
Ashok K. Chopra, Supervisor



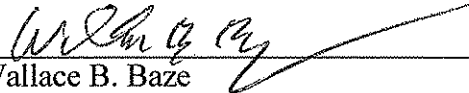
Johnny W. Peterson



Vladimir Motin



Janice J. Endsley



Wallace B. Baze



Dean, Graduate School

**NEW VIRULENCE MECHANISMS IN *YERSINIA PESTIS*, THE  
PLAGUE (BLACK DEATH)-CAUSING BACTERIUM: A RE-  
EMERGING AND BIOTERROR PATHOGEN**

**by**

**Stacy Leona Agar, B.S.**

**Dissertation**

Presented to the Faculty of the Graduate School of  
The University of Texas Medical Branch  
in Partial Fulfillment  
of the Requirements  
for the Degree of

**Doctor of Philosophy**

**The University of Texas Medical Branch  
May, 2009**

## **Dedication**

*Optimus Parentibus*



## **Acknowledgements**

I thank Dr Ashok Chopra for his mentorship and the members of my committee for their guidance. My thanks also go to all of the members of Dr Chopra's laboratory (past and present), to the faculty and staff of the Department of Microbiology and Immunology, and to the Deans and staff of the Graduate School for Biomedical Sciences.

An experience such as graduate school is not possible without the support of friends and family; for me, a group many in number and large in heart. All have played important roles during this time, have seen me through ups and downs, and have remained beside me. For them, I am grateful.

I have also been fortunate to receive intramural funding for 2 years through the NIAID T32 Biodefense and Emerging and Tropical Infectious Diseases Training Grants. My thanks go to Drs Alan Barrett, Steve Higgs, and Scott Weaver for their support.

# NEW VIRULENCE MECHANISMS IN *YERSINIA PESTIS*, THE PLAGUE (BLACK DEATH)-CAUSING BACTERIUM: A RE- EMERGING AND BIOTERROR PATHOGEN

Publication No. \_\_\_\_\_

Stacy Leona Agar, Ph.D.

The University of Texas Medical Branch, 2009

Supervisor: Ashok K. Chopra

**Abstract:** *Yersinia pestis* evolved from *Y. pseudotuberculosis* to become the causative agent of bubonic and pneumonic plague. *Y. pestis* is also a category A select agent based on its potential use as a biological weapon. Currently, there is no vaccine licensed in the United States for use against *Y. pestis* so continued research on understanding the pathogenesis of *Y. pestis* and identifying new virulence factors is warranted. Although the natural route of primary infection with *Y. pestis* results in bubonic plague in humans, it is commonly thought that aerosolized *Y. pestis* will be utilized during a biowarfare attack. Therefore, the purpose of this work was two-fold: to assess the changes in virulence attributable to the deletion of a chromosomal element and a virulence plasmid; and to investigate disease progression following aerosolization of *Y. pestis* in two animal models. First, we characterized *Y. pestis* strains lacking murein, or Braun, lipoprotein (Lpp), an outer membrane protein conserved within the *Enterobacteriaceae* family. We then cured wild-type and  $\Delta lpp$  mutant strains of virulent *Y. pestis* CO92 of one of the virulence plasmids, pPCP1, and assessed how these deletions attenuated the bacterium. Our data indicated that a significant and possibly synergistic attenuation in bacterial virulence occurred in a mouse model of pneumonic plague when both the *lpp* gene and the virulence plasmid pPCP1 encoding the *pla* gene were deleted from *Y. pestis* CO92.

The second half of this work focused on characterizing the dynamics of pneumonic infection following aerosolization of *Y. pestis* CO92 strain in both the mouse and rat models of infection. We exposed mice and rats in a whole-body Madison chamber to various doses of *Y. pestis* CO92 aerosolized by a Collison nebulizer and determined the LD<sub>50</sub> dose, bacterial dissemination, cytokine/chemokine production, and tissue damage over a 72-h course of infection. Plague in mice and rats mimics disease in humans and understanding disease progression in these models will facilitate a better understanding of disease in humans.

## Table of Contents

List of Tables .....	xi
List of Figures .....	xii
Chapter 1 <i>Introduction</i> .....	1
A history of <i>Yersinia pestis</i> .....	1
The pathogenesis of <i>Y. pestis</i> .....	3
<i>PLASMID PCD1</i> .....	3
<i>PLASMID PMT1</i> .....	4
<i>PLASMID PPCP1</i> .....	5
<i>PIGMENTATION LOCUS AND THE HIGH PATHOGENICITY ISLAND</i> .....	7
<i>PH 6 ANTIGEN</i> .....	8
Murein, or Braun, lipoprotein .....	9
Transmission of <i>Y. pestis</i> .....	10
The diseases called plague .....	12
Current animal models of <i>Y. pestis</i> .....	14
Treatment and vaccines .....	16
<i>Y. pestis</i> as an agent of bioterrorism .....	17
Summary .....	18
Chapter 2 <i>Methods and Materials</i> .....	19
Bacterial strains and plasmids .....	19
Bacterial growth for aerosolization .....	21
Generation and characterization of $\Delta lpp$ mutants of <i>Y. pestis</i> and <i>Y. pseudotuberculosis</i> .....	22
<i>COMPLEMENTATION OF THE YERSINIAE <math>\Delta LPP</math> MUTANTS</i> .....	24
<i>WESTERN BLOT ANALYSIS</i> .....	24
<i>PLASMID ISOLATION</i> .....	25
<i>TRANSLOCATION OF T3SS EFFECTORS</i> .....	25
<i>MOTILITY TESTING</i> .....	26

Assessment of the membrane integrity of yersiniae $\Delta lpp$ mutants .....	26
<i>RELEASE OF PERIPLASMIC RNASE I</i> .....	26
<i>RELEASE OF B-LACTAMASE</i> .....	27
<i>SENSITIVITY TO DETERGENT</i> .....	27
<i>SENSITIVITY TO PH AND DETERGENT</i> .....	28
<i>CYTOTOXICITY</i> .....	28
Measurement of minimum inhibitory concentration (MIC) of levofloxacin .....	28
Animal studies .....	29
<i>AEROSOL CHALLENGE OF MICE AND RATS</i> .....	30
Passive transmission of <i>Y. pestis</i> .....	30
Histopathological analyses .....	31
Blood chemistry and blood cell counts .....	32
Bacterial dissemination .....	32
<i>In vivo</i> cytokine and chemokine analyses .....	34
Bacterial invasion/phagocytosis of murine macrophages and intracellular survival .....	34
Statistical analyses .....	35
Chapter 3 <i>Braun Lipoprotein (Lpp) Contributes to the Virulence of Yersiniae:</i> <i>Potential Role of Lpp in Inducing Bubonic and Pneumonic Plague</i> ...	36
<i>Results</i> .....	37
Pneumonic plague in mice .....	37
<i>BLOOD CHEMISTRIES AND CELL COUNT DATA</i> .....	37
<i>HISTOPATHOLOGICAL DATA</i> .....	39
Characterization of $\Delta lpp$ mutants of <i>Yersinia</i> species .....	40
Isolation of virulence plasmids and amplification of plasmid-associated virulence genes .....	44
Translocation of T3SS effectors .....	45
Membrane integrity of the $\Delta lpp$ mutants versus WT bacteria .....	49
Bacterial motility and invasion .....	49
Deletion of the <i>lpp</i> gene attenuates the virulence of <i>Y. pseudotuberculosis</i> in a mouse model .....	50
Lpp contributes to the virulence of <i>Y. pestis</i> .....	52

Histopathological analysis of animal tissues following intranasal inoculation with WT <i>Y. pestis</i> CO92 and its $\Delta lpp$ mutant .....	57
Histopathological analysis of animal tissues following subcutaneous inoculation with WT <i>Y. pestis</i> CO92 and its $\Delta lpp$ mutant .....	58
Histopathological analysis of animal tissues following intraperitoneal inoculation with parental <i>Y. pestis</i> KIM/D27 and its $\Delta lpp$ mutant .....	59
<i>In vivo</i> cytokine analysis .....	63
Colonization and dissemination of WT and $\Delta lpp$ mutant of <i>Y. pestis</i> CO92 in mouse tissues after intranasal challenge in the absence and presence of levofloxacin .....	65
Intracellular survival of WT <i>Y. pestis</i> CO92 as compared to its $\Delta lpp$ mutant <i>in vitro</i> .....	69
<i>Discussion</i> .....	71
Chapter 4 <i>Deletion of Chromosomal Braun Lipoprotein Gene (lpp) and Curing of Plasminogen Activating Protease (Pla)-Encoding Plasmid Dramatically Alter the Virulence of Yersinia pestis CO92 in a Pneumonic Mouse Model</i> .....	79
<i>Results</i> .....	80
<i>Y. pestis</i> pPCP <sup>-</sup> / $\Delta lpp$ mutant CO92 strain was less lethal than was WT <i>Y. pestis</i> or its single pPCP1 <sup>-</sup> and $\Delta lpp$ mutants .....	80
<i>Y. pestis</i> pPCP <sup>-</sup> , $\Delta lpp$ , and pPCP <sup>-</sup> / $\Delta lpp$ mutant strains were as cytotoxic as the WT <i>Y. pestis</i> CO92 strain .....	82
WT <i>Y. pestis</i> CO92-infected mice had more severe tissue injury than did mice infected with the mutant strains .....	83
<i>Y. pestis</i> CO92 cured for the pPCP1 plasmid or deleted for the <i>lpp</i> gene exhibited differential survivability in peripheral organs compared to that in WT-infected mice at 48 h p.i. ....	89
Mice infected with <i>Y. pestis</i> CO92 strains cured of the pPCP1 plasmid containing the <i>pla</i> gene showed lower levels of cytokines and chemokines by 48 h p.i. compared to the levels in WT bacteria-infected mice .....	92
Lack of survivability of <i>Y. pestis</i> CO92 mutants in murine macrophages was more dependent upon the <i>lpp</i> gene than the pPCP1 plasmid .....	101

<i>Discussion</i> .....	102
CHAPTER 5 <i>Characterization of a Mouse Model of Plague after Aerosolization of Yersinia pestis CO92</i> .....	109
<i>Results</i> .....	109
Murine model for developing pneumonic plague by aerosolization of <i>Y. pestis</i> CO92 .....	109
Histopathology following aerosolization .....	112
Bacterial dissemination following aerosolization over a 72-h period .....	115
<i>In vivo</i> cytokine analysis .....	118
<i>Discussion</i> .....	124
Chapter 6 <i>Characterization of the Rat Pneumonic Plague Model: Infection Kinetics Following Aerosolization of Yersinia pestis CO92</i> .....	125
<i>Results</i> .....	125
Calculation of the LD <sub>50</sub> dose for aerosolized <i>Y. pestis</i> CO92 in the rat model .....	125
Tissue injury in rats resulting from aerosolization of <i>Y. pestis</i> CO92 .....	127
Dissemination of aerosolized <i>Y. pestis</i> CO92 in rat tissues .....	132
<i>In vivo</i> cytokine and chemokine analysis .....	136
Passive transmission of <i>Y. pestis</i> .....	141
<i>Discussion</i> .....	143
Chapter 7 <i>Future Directions and Concluding Remarks</i> .....	146
Bibliography .....	148
Vita .....	168

## List of Tables

Table 2.1:	Bacterial strains and plasmids used in these studies.....	20
Table 2.2:	Primers used in these studies. ....	23
Table 2.3:	Abbreviations and acronyms of cytokines and chemokines measured in these studies. ....	33
Table 3.1:	Alterations in blood chemistries following challenge of mice with <i>Y. pestis</i> CO92 <i>via</i> intranasal inoculation.....	38
Table 3.2	Alterations in blood counts following challenge of mice with <i>Y. pestis</i> CO92 <i>via</i> intranasal inoculation.....	39
Table 3.3:	Changes in the levels of cytokines and chemokines in the sera of mice infected with WT or the $\Delta lpp$ mutant of <i>Y. pestis</i> CO92 intranasally.....	66
Table 3.4:	Quantitative analysis of selected organs for bacterial counts from mice infected with WT or <i>lpp</i> mutant of <i>Y. pestis</i> CO92.....	68
Table 4.1:	Cytokine and chemokine levels (pg/ml) in the lung homogenates of mice 48 h after intranasal infection with WT or mutant <i>Y. pestis</i> strains.....	94
Table 4.2:	Cytokine and chemokine levels (pg/ml) in the liver homogenates of mice 48 h after intranasal infection with WT or mutant <i>Y. pestis</i> strains.....	96
Table 4.3:	Cytokine and chemokine levels (pg/ml) in the spleen homogenates of mice 48 h after intranasal infection with WT or mutant <i>Y. pestis</i> strains. ....	98
Table 4.4:	Cytokine and chemokine levels (pg/ml) in the heart homogenates of mice 48 h after intranasal infection with WT or mutant <i>Y. pestis</i> strains.....	99
Table 4.5:	Cytokine and chemokine levels (pg/ml) in the sera of mice 48 h after intranasal infection with WT or mutant <i>Y. pestis</i> strains. ....	100
Table 6.1:	Cytokine and chemokine levels (pg/ml) in tissues following <i>Y. pestis</i> aerosol inoculation. ....	137

## List of Figures

Figure 3.1:	Histopathology following i.n. inoculation of mice with WT <i>Y. pestis</i> CO92.....	41
Figure 3.2:	Nucleotide and amino acid sequence identities/homologies between lipoproteins of <i>Y. pestis</i> CO92 and <i>S. enterica</i> serovar Typhimurium.. .....	43
Figure 3.3:	Western blot analysis showing the expression of the <i>lpp</i> gene in WT yersiniae, <i>lpp</i> mutants, and their corresponding complemented strains.. ....	44
Figure 3.4:	Plasmid profiles of various WT/parental yersiniae and their corresponding $\Delta lpp$ mutant strains.. .....	46
Figure 3.5:	Translocation of Yops (YopE and YopH) in HeLa cells infected with various WT/parental yersiniae and their corresponding $\Delta lpp$ mutant strains.. .....	47
Figure 3.6:	Assessment of the cytotoxicities of the various yersiniae. ....	48
Figure 3.7:	The <i>Y. pseudotuberculosis</i> $\Delta lpp$ mutant is less virulent than WT <i>Y. pseudotuberculosis</i> in a mouse model.....	51
Figure 3.8:	Deletion of the <i>lpp</i> gene attenuates <i>Y. pestis</i> KIM/D27 in the Swiss-Webster (A) and BALB/c (B) mouse models and protects against rechallenge with WT <i>Y. pestis</i> CO92.....	54
Figure 3.9:	A subinhibitory dose of levofloxacin better defines the attenuation of the <i>Y. pestis</i> CO92 $\Delta lpp$ mutant. ....	55
Figure 3.10:	Attenuation of the <i>Y. pestis</i> CO92 $\Delta lpp$ mutant in BALB/c mice inoculated via the s.c. route to mimic bubonic plague.. .....	56
Figure 3.11:	Histopathology of the lungs of Swiss-Webster mice infected with either the WT or the $\Delta lpp$ mutant of <i>Y. pestis</i> CO92 via the i.n. route. ....	60
Figure 3.12:	Histopathology of the spleens of BALB/c mice 120 h p.i. with either the WT or $\Delta lpp$ mutant strain of <i>Y. pestis</i> CO92 via the s.c. route.....	62
Figure 3.13:	Comparison of the survival of the WT or the $\Delta lpp$ mutant of <i>Y. pestis</i> CO92 in murine macrophages.. .....	70
Figure 4.1:	Survival analysis of mice infected with WT and mutant <i>Y. pestis</i> CO92 strains. ....	80



Figure 4.2:	Type 3 secretion system-associated cytotoxicity in HeLa cells infected with WT and mutant <i>Y. pestis</i> strains.....	82
Figure 4.3:	Histopathology of mouse tissues following infection with WT and mutant <i>Y. pestis</i> strains.....	88
Figure 4.4:	Survival of WT and mutant <i>Y. pestis</i> strains 1 h and 48 h p.i. in peripheral organs of mice.....	91
Figure 4.5:	Survival of WT and mutant <i>Y. pestis</i> strains <i>in vitro</i> .....	103
Figure 5.1:	Calculation of the LD <sub>50</sub> for aerosolized <i>Y. pestis</i> CO92..	111
Figure 5.2:	Histopathology of mouse tissue 72 h after exposure to aerosolized <i>Y. pestis</i> .....	113
Figure 5.2:	Dissemination of <i>Y. pestis</i> CO92 through the organs of mice at 1 h and 72 h p.i....	118
Figure 5.4:	Cytokine and chemokine levels in various organ homogenates at 1 h and 72 h p.i....	123
Figure 6.1:	Calculating the LD <sub>50</sub> dose in a rat model using aerosolized <i>Y. pestis</i> CO92.....	126
Figure 6.2:	Histopathology of rat organs at different time points following aerosolization of <i>Y. pestis</i> CO92.....	131
Figure 6.3:	Dissemination of bacteria at various time points p.i. with <i>Y. pestis</i> CO92 in different organs of rats.....	135
Figure 6.4	LINCOp <sub>lex</sub> analysis of cytokine and chemokine levels at 1 h and 48 h post aerosolization with <i>Y. pestis</i> CO92 in rat sera.....	140

# Chapter 1

## *Introduction*

### **A HISTORY OF *YERSINIA PESTIS***

Bacteria of the genus *Yersinia* are Gram-negative bacilli in the family *Enterobacteriaceae*, and 3 of 11 species in this genus are human pathogens. *Y. pseudotuberculosis* and *Y. enterocolitica* are spread *via* the fecal-to-oral route and typically cause self-limiting, enteropathogenic infections characterized by diarrhea, fever, and abdominal pain (142). In 1894, Alexandre Yersin first described *Y. pestis* as a non-motile coccobacillus whose poles absorbed more stain than the center following application of a 1% solution of carbolized thionin to bacteria smeared on a microscope slide (187). *Y. pestis* is transmitted to humans accidentally through the bite of an infected flea or after inhalation of the organisms and manifests as bubonic, pneumonic or septicemic plague (14). *Y. pestis* is historically credited for 200 million deaths world-wide, and, in the pneumonic form, the organism is very virulent and a potential agent of biowarfare or bioterrorism (56, 96, 102). *Y. pestis* can be classified into biological variants (or biovars) based on the ability of the bacteria to ferment carbohydrates and to reduce nitrate to nitrite (10). Antigua variants can ferment glycerol and arabinose and reduce nitrates, Medievalis can ferment glycerol and arabinose but cannot reduce nitrates, while Orientalis can ferment arabinose and reduce nitrates but cannot ferment glycerol (53). Two groups of 'atypical' *Y. pestis* have also been studied. Pestoides, which can ferment melibiose and rhamnose, is of the biovar Antigua and a highly virulent strain despite naturally lacking the virulence plasmid pPCP1 (10, 185). Biovar Microtus contains a 22-kb plasmid, pCRY, not found in the other biovars that encodes a

cryptic type IV secretion system (169). *Microtus* is avirulent in humans but found in voles in China and cannot ferment arabinose or reduce nitrate but can ferment glycerol (169, 194). Discovery of these atypical strains suggests how little we know about *Y. pestis* and its characteristics as an emerging pathogen.

One of the oldest written accounts of the disease called plague is described in the Bible in the First Book of Samuel and occurred in Israel 1000 years before the Common Era (BCE) in Israel (145). Another account described by Thucydides occurred in 432 BCE and was thought to have killed a third of the population of Athens (187). Thucydides apparently had the illness responsible for the epidemic and reported having violent headaches, a “fiery redness” in his eyes, inflammation, sneezing, a loss of voice, coughing, and vomiting (174). There is evidence to suggest that some of these earlier epidemics were not caused by *Y. pestis* but by another common pestilence (145). Historians are quite certain, however, that *Y. pestis* was responsible for 3 natural plague pandemics dating back about 2500 years ago. The Justinian plague, named for the Byzantine emperor Justinian I, is thought to have begun in 541 AD in Egypt and continued through 700 AD (2). As many as 60% of the populations of the “known” world (Europe, Northern Africa, parts of Asia and Arabia) died during this pandemic as a result of either plague or another predominate disease of the time (e.g. small pox) (131). The second plague pandemic, the first epidemic of which was called the Black Death, began in the 14<sup>th</sup> century (circa 1330) in Asia and continued into the 17<sup>th</sup> century after killing over 28 million people in Europe (131). The third pandemic began in the late 19<sup>th</sup> century in China and is currently ongoing, evidenced by sporadic outbreaks world-wide (96). It is during the third pandemic in 1894 that Alexandre Yersin (191) and Shibasaburo Kitasato (33) independently isolated the bacterium initially named *Bacterium pestis*, then *Pasteurella*

*pestis* after Yersin's mentor Pasteur, and finally *Yersinia pestis* (131). Additionally, the importance of the flea vector in the transmission of *Y. pestis* was independently described by Masanori Ogata and Paul-Louis Simond in 1897 (33, 160). Based on historical records and epidemiological studies, it was thought that biovars Antiqua, Medievalis, and Orientalis caused the three pandemics, respectively (2). Recent evidence from the dental pulp of unearthed victims from the first two pandemics, however, has suggested that biovar Orientalis caused all three historical pandemics (55).

### **THE PATHOGENESIS OF *Y. PESTIS***

*Y. pestis* causes a disease that is quite distinct from the other two yersinia human pathogens, yet the bacterium shares some virulence-associated systems (mechanisms) with the other two pathogenic *Yersinia* species. The virulence plasmid pCD1 is a 70-kb plasmid encoding 71 genes and is similar in all three pathogenic species (94). This virulence plasmid is designated as pYVe in *Y. enterocolitica*, and pYV in *Y. pseudotuberculosis* (95, 131). In addition to plasmid pCD1, *Y. pestis* harbors another two plasmids that are absent in the enteropathogenic yersinia (66, 138). *Y. pestis* is thought to have acquired the two virulence plasmids pPCP1 and pMT1 sometime between 1500 and 20,000 years ago when this species diverged from *Y. pseudotuberculosis* (1).

### **PLASMID PCD1**

Plasmid pCD1, also known as pCad for calcium dependence, encodes the low-calcium response stimulon (LCRS) comprised of the host cell contact-dependent type three secretion system (T3SS) and is absolutely required for virulence of the yersinia (20, 26, 46). In the absence of calcium and at 37°C, growth of *Yersinia* is halted and the low calcium

response antigen (LcrV), needle-like secretion apparatus (Ysc, or injectisome), translocator and effector *Yersinia* outer membrane proteins (Yops), and the specific Yop chaperone proteins (Syc) are all expressed (131). The Ysc injectisome is made up of 29 proteins that form a barrel through which the effector Yops travel from the bacterium into the host cell cytoplasm (47). The tip of this injectisome needle is the result of a polymerization of the protein YscF (47). Yops B and D and LcrV form the channel on the surface of the host cell membrane through which the needle travels (147). The effector Yops – YopH, YopT, YopJ, YopO/YpkA YopE, YopM - are translocated into the host cytosol upon docking of the bacterium to the host cell (176). The Yops are responsible for resisting phagocytosis of immune cells (146, 177), subverting the normal proinflammatory response in the host and suppressing the host immune system (24, 128), and blocking apoptosis (149, 150), thereby successfully establishing infection in the host.

There is also a chromosomally encoded T3SS homologous to one encoded by a pathogenicity island in *Salmonella enterica* serovar Typhimurium (41, 52, 130). It appears to encode Ysc injectisome components, but its role in the pathogenesis of *Y. pestis* has not been clarified (141).

### ***PLASMID PMT1***

Plasmid pMT1 is a 110-kb plasmid encoding 115 genes (115). Also known in the literature as pFra, pMT1 is the largest of the 3 virulence plasmids and encodes the genes responsible for the formation of the glycoprotein capsular antigen F1, *cafI*, and murine toxin, *ymt* (102). Capsular antigen F1 is expressed at 37°C, and its expression is thought to facilitate the resistance of the bacterium to the phagocytosis by immune cells (12, 38). F1 is a protective antigen and is the focus of current vaccine development, but some F1<sup>-</sup> strains have

been isolated in nature (180, 186).

In 2000, Hinnebusch and others noted that murine toxin, Ymt, has phospholipase D activity that contributes to its toxic effects in mice but was not necessary for the virulence of *Y. pestis* in mice (93). Expression of Ymt is greater at 26°C than at 37°C, so its physiological importance resides in its activity in the flea vector (131), explained in greater detail below.

### ***PLASMID PPCP1***

Plasmid pPCP1, also known in the literature as pPla and the smallest of the 3 virulence plasmids, is 9.5 kb and it contains three genes encoding proteins with distinctly different functions. Pesticin, encoded for by the *pst* gene, causes cell wall lysis and the death of neighboring bacteria by hydrolyzing the bond between N-acetylglucosamine and N-acetylmuramic acid, thus degrading the glycan backbone of murein (Braun) lipoprotein (65). It is hypothesized that *Y. pestis* uses this bacteriocin to kill neighboring cells in which the pPCP1 plasmid is absent while, at the same time, protecting itself with pesticin immunity protein, encoded for by the *pim* gene on pPCP1 plasmid (168).

Also present on the pPCP1 plasmid is plasminogen activating protease (Pla), a surface protein consisting of two subunits,  $\alpha$ - and  $\beta$ -, with molecular sizes of 37 and 35 kDa, respectively (105, 166). The *pla* gene is under the transcriptional control of the cyclic AMP receptor protein (101). Pla's function has been well characterized, and its role in the invasiveness and dissemination of *Y. pestis* extensively studied *in vivo* and *in vitro* (3, 5, 25). Pla also functions in the adherence of *Y. pestis* to host cells (100), and its ability to attach to the host extracellular matrix and basement membranes facilitates tissue invasion (108). In the two enteropathogenic species, the virulence determinants Yad (*Yersinia* adherence protein, formerly designated as YopA) and invasin protein (Inv) play a crucial role in bacterial

colonization and invasion of the intestinal epithelium, but are not functional in *Y. pestis* (131). Pla also subverts the innate immune response by degrading complement proteins, thus reducing the ability of phagocytes to opsonize and phagocytize *Y. pestis* and by preventing the chemotaxis of other inflammatory cells to the site of infection (168).

Pla is a member of the omptin family of aspartate proteases expressed on the surface of many members of the *Enterobacteriaceae* family and possesses a proteolytic function characteristic of these proteases (121, 167). Pla of *Y. pestis* shares significant amino acid homology to PgtE of *Salmonella enterica* serovar Typhimurium (71%) and OmpT of *Escherichia coli* (47.5%), but its function in the pathogenesis of plague infections differs from that of the other omptins (107, 167).

The human blood coagulation and fibrinolysis pathways are naturally active during times of tissue regeneration and wound repair (21). Many bacterial pathogens, however, subvert the natural pathways and utilize hemostatic factors (like plasminogen and plasmin) to migrate from the original site of infection and disseminate through the tissues (51). Pla of *Y. pestis* proteolytically activates plasminogen and anchors it to the bacterial surface (17). Human plasminogen activators convert plasminogen into plasmin, which *Y. pestis* uses to gain access to deeper tissue layers and to colonize and disseminate through the host (168).

The above-mentioned hemostatic system is a tightly regulated process, and production of plasmin is controlled by  $\alpha 2$ -antiplasmin and other inactivators present in the blood (21). To maintain control of plasmin for its own purposes, Pla also functions in the inactivation of  $\alpha 2$ -antiplasmin (103). Furthermore, the proteolytic activity of Pla is diminished if the necessary interactions between Pla and the lipid A moiety of lipopolysaccharide (LPS) are sterically hindered by complete O-antigen side chains (104).

Consequently, *Y. pestis* has a “rough” LPS coat lacking O-antigen, and it is thought that this absence of O-antigen in LPS facilitates the invasiveness of the plague bacterium (161).

Since Pla plays an important role in human infection and avoidance of the immune system, significant work has been performed to better understand the role of both the *pla* gene and the pPCP1 plasmid on the pathogenesis of *Y. pestis* infections. For example, the loss of the pPCP1 plasmid or the *pla* gene attenuates *Y. pestis* administered by the subcutaneous (s.c.) route to mice and guinea pigs (29, 153, 168, 179, 181), and by the intradermal (i.d.) (156) and intranasal (i.n.) (110) routes in mice but bacterial dissemination that occurs in intranasally-infected mice was not noted in subcutaneously-infected animals. No change in the LD<sub>50</sub> was observed in mice inoculated with the wild-type (WT) versus *pla*-minus mutant by either the intraperitoneal (i.p.) (179, 181) or the intravenous (i.v.) (168) routes of infection. Reports on the virulence of strains lacking this plasmid and delivered *via* the aerosol route of infection are not consistent and are possibly dependent upon the strains of *Y. pestis* used in the studies (153, 179, 181). These data indicated that mutant strains evoked an earlier inflammatory response than did the WT strains, and animals were able to clear the infection sooner resulting in a higher mouse survival rate in mutant versus WT bacteria-infected mice (110, 168, 181).

#### ***PIGMENTATION LOCUS AND THE HIGH PATHOGENICITY ISLAND***

The *Y. pestis* chromosome also encodes for a 102-kb pigmentation (*pgm*) locus that is silent in *Y. pseudotuberculosis*, and deletion of this element from the chromosome of *Y. pestis* attenuates its virulence (95). *Y. pestis* strains that possessed a pigmented phenotype (Pgm<sup>+</sup>) when grown in the presence of hemin or Congo-red agar at 28°C were pathogenic in mice when administered subcutaneously (31, 32). Strains deemed Pgm<sup>-</sup> were not pathogenic



unless hemin or iron salts were injected into mice at the time of infection and then they were fully virulent in mice (32). Furthermore, it was noted that this pigmentation phenotype was linked to the presence of a 102-kb region on the chromosome, later named the *pgm* locus, bordered by an insertion sequence, *IS100*, that allowed its spontaneous deletion from the chromosome at a rate of  $10^5$  (28, 67). An attenuated strain used in our laboratory and in others, *Y. pestis* KIM/D27, is lacking the *pgm* locus (73) and is highly attenuated in the mouse model of infection *via* subcutaneous (32, 158) but not intravenous inoculation (175). The ability to form pigmented colonies is not, however, what makes this chromosomal region physiologically important. Included within this 102-kb segment is the high pathogenicity island containing the hemin storage, *hms*, operon encoding genes responsible for the biosynthesis and regulation of the siderophore, yersiniabactin (91). Iron is a cofactor necessary in many biological functions including enzymatic and metabolic pathways (79). Bacterial siderophores sequester iron from the host cells, and the presence of siderophores in *Y. pestis* (178) and in the enteropathogenic yersiniae were determined to be required for bacterial virulence (86). The *hms* operon also encodes genes responsible for the iron storage capability of *Y. pestis* and for the biofilm formation that facilitates colonization of the bacteria in the flea proventriculus (16, 69, 91, 113, 132).

### ***PH 6 ANTIGEN***

In the early 1960s, it was noted that in *Y. pestis* strains grown at temperatures in the range of 35-37°C and in acidic media, a change occurred in the electrophoretic mobility of the bacterium (19). These changes appeared to be associated with the formation of a surface antigen on the bacterium later described as fimbriae (19, 116). Further, the cytotoxic effect that bacteria grown under these conditions had on monocytes suggested a role for this surface

antigen in the pathogenesis of *Y. pestis* (23), and the suspected environment within the host cell where these interactions took place was the phagolysosome (114). Future work described a loss of virulence in strains that contained a mutation in the genes associated with the pH 6 antigen, *psaE* and *psaA*, or persistent expression of genes in tissues, suggesting a role for this antigen in the pathogenesis of various forms of plague (43, 114). However, recent work was not able to show a loss of virulence in mice subcutaneously inoculated with strains of *Y. pestis* containing mutations or deletions in the *psa* gene (9). So the role of Psa in the pathogenesis of *Y. pestis*, if any, is still not clear.

#### **MUREIN, OR BRAUN, LIPOPROTEIN**

The outer membrane of Gram-negative bacteria is comprised of many different proteins that help maintain the structural integrity of the bacterial cell envelope. Some of these proteins are covalently modified by the addition of a lipid, N-acyl-S-diacylglyceryl cysteine, and such modified proteins are collectively known as lipoproteins (118). One particularly abundant lipoprotein, designated as murein (or Braun) lipoprotein (Lpp), is associated with the outer membrane of bacteria within the *Enterobacteriaceae* family. Originally identified in *Escherichia coli*, Lpp links the murein (peptidoglycan) layer to the outer bacterial membrane (84). Lpp has previously been demonstrated to play a role in the host's immune response against infections with some Gram-negative enteric pathogens, such as *E. coli*, *Salmonella enterica* serovar Typhimurium, and *Y. enterocolitica* (192). Our laboratory's earlier studies indicated that Lpp (6.3 kDa) purified from *E. coli* and *Y. enterocolitica* not only synergized with LPS to induce septic shock but also evoked the production of tumor necrosis factor-alpha (TNF- $\alpha$ ) and interleukin (IL)-6 in both LPS-responsive and LPS non-responsive mice and in mouse peritoneal exudate macrophages,

suggesting an alternative signaling mechanism for Lpp (193). In fact, a subsequent study showed that Lpp signals through Toll-like receptor (TLR)-2 and not TLR-4 (6), which LPS utilizes for cell signaling.

Lpp clearly plays a role in the immune response, so it is possible that Lpp is a virulence factor not previously explored in *Y. pestis*. As deadly as *Y. pestis* has been in the past, the continued investigation of new virulence factors and virulence-associated systems is warranted to fully elucidate the mechanisms of yersinia pathogenesis.

### **TRANSMISSION OF *Y. PESTIS***

*Y. pestis* currently exists in concurrent enzootic and epizootic transmission cycles, and endemic regions of the United States (U.S.) include Arizona, New Mexico, California, Oregon and Colorado (39). *Y. pestis* can infect almost every mammal species, and over 80 species of fleas have been implicated as vectors, but plague is typically associated with rodent hosts because they can reach a high enough titer for their fleas to transmit the bacteria (59). Enzootic cycles maintain *Y. pestis* in the environment and, when the infection is transferred from enzootic hosts to more susceptible hosts, rapid die-offs of the infected rodents can induce epizootic episodes to occur (71). *Y. pestis* does not naturally exist outside of this vector/mammal cycle (162).

Transmission of plague by fleas was eloquently described in 1914 by Bacot and Martin (12). As a flea feeds on a mammal, the blood meal travels from the mouth parts through the esophagus, into the proventriculus, and then into the midgut (88). Bacot and Martin noted that the proventriculi and midguts of infected fleas contained a solid mass within which they found the *Yersinia* bacilli (12). They described the architecture of the proventriculus as including curved, chitin-covered projections, called spines, that were lined

in rows and wrapped in a muscular layer (12). They determined that this muscular band acted as a valve to prevent blood from traveling back towards the esophagus (12). In infected fleas, however, this bacilli-containing blood mass was also unable to move through the midgut, and, over time, these “blocked” fleas starved to death (12). Transmission of bacteria to naïve animals occurred as the infected and hungry fleas continued to feed on the animals and regurgitated infected blood into the bite area (12). Originally, it was hypothesized that only blocked fleas could transmit *Y. pestis* (137), but recent work has contradicted this hypothesis (58). Additional work deciphered the molecular mechanisms controlling the formation of this infectious mass in the blocked flea. Earlier, it was hypothesized that the procoagulant ability of Pla, encoded for on the pPCP1 plasmid, was responsible for the formation of the jelly-like mass in blocked fleas (37). Hinnebusch and others later discovered that *Y. pestis* strains with partial or complete deletions of pPCP1 were still able to colonize in fleas, while strains with pMT1 deletions were not (90). Plasmid pMT1 encodes a protein named murine toxin, Ymt, for its lethal effect in mice. As a result, it was hypothesized that Ymt played an important role in the pathogenicity of *Y. pestis*. Ymt mutant strains, however, had a similar LD<sub>50</sub> in mice as did WT strains (92). Ymt mutant strains were not able to colonize in flea, while WT strains predictably and consistently colonized in the midgut of the flea (92).

Furthermore, it was determined that strains lacking the chromosomal locus responsible for the pigmentation phenotype, *hms*, were unable to colonize in the flea (106). Using fluorescence microscopy, Hinnebusch and others were able to definitively prove that *hms*<sup>+</sup> strains of *Y. pestis* colonized the spines of the proventriculus facilitating the characteristic blockage, while *hms*<sup>-</sup> strains were unable to do so (91). Additionally, it was noted that genes located on the *hms* operon were responsible for a biofilm formation in the

flea (49) and that *hms*–dependent extracellular matrix formation only occurs at 26°C and not at 37°C, so is not essential for *Y. pestis* pathogenesis in the mammalian host (113). Colonization of bacteria in the flea begins in the midgut and then moves in a retrograde fashion to the proventriculus (137). *Y. pestis* strains lacking both *hms* and *ymt* were not able to colonize either site in the flea and, thus, prevented transmission of the bacteria to the mammalian host (92). Taken together, these data indicated an important role for these genes in the flea vector and in the transmission of the bacteria to mammals (89).

### THE DISEASES CALLED PLAGUE

The term plague is derived from the Latin ‘plaga’ meaning ‘a stroke from a whip’ referring to the common philosophy that this disease was a punishment from God for the sins of mankind (174). Also known as ‘the sweating sickness’ and ‘a crisis of distemper’, the spread of plague was described in 1744 by Mead as being caused by a “corrupted state of air” that was “necessary to give these contagious atoms their full force” (122). Mead and his contemporaries were not completely disconnected from our current understanding how the earlier pandemics spread *via* the shipping industry when he wrote in 1744:

“That when the constitution of the *Air* happens to favor *Infection*, it rages there with great Violence: that at times more especially diseased Persons give it to one another, and from them *Contagious Matter* is lodged in Goods of a loose and soft Texture, which being packed up and carried in other Countries, let it out, when opened, the imprisoned Seeds of *Contagion*, and produce the Disease whenever the *Air* is disposed to give them force.” (122, page 78)

Since 1744, much research has elucidated the cause, spread, and pathogenesis of *Y. pestis* and

the diseases collectively referred to as ‘plague.’

Following flea-bite transmission of *Y. pestis*, by far the most common method of transmission, the fully virulent bacterium replicates at the site of infection within macrophages before being transported to the lymph nodes *via* the lymphatic system (131). *Y. pestis* is a facultative intracellular pathogen (131). It replicates intracellularly until the Yops, encoded for on pCD1, and capsular antigen, encoded for on pMT1, are produced at 37°C and then replicates extracellularly (27). After a 2-8 day incubation period, patients usually report having a high fever, chills, headache, malaise, and weakness (96). Growth of bacteria in the lymph nodes and the ensuing inflammatory response causes swelling and bubo formation characteristic of bubonic plague (131). The bacteria disseminate from the lymph nodes to peripheral organs, and progression to systemic infection is manifested by the T3SS encoded for on virulence plasmid pCD1 (27). Systemic infection results in septicemia and disseminated intravascular coagulation (DIC). Gangrene resulting from necrosis of the small vessels in the extremities and digits along with DIC causes a blackish appearance to the skin, the origin of the moniker ‘black death’ given to the disease during the Middle Ages in England (96). Many antibiotics are typically used to treat bubonic plague (explained in greater detail below), yet insufficient treatment may facilitate hematogenous dissemination of the bacteria to the meninges resulting in meningial plague, rarely a primary infection (33). If left untreated, bubonic plague is fatal in 50-90% of the cases (140).

Septicemic plague not only arises secondarily to bubonic plague, but also primarily following flea-bite transmission if the bacteria by-pass the lymphatic system and directly enter the blood stream (96). In the case of primary septicemic plague, no bubo is formed, and the mortality is much higher than bubonic plague if treatment is not started soon after the

onset of symptoms (96).

Pneumonic plague can either arise secondarily following flea-bite transmission, in a minority of the cases, or primarily following an aerosol exposure to the bacteria (77). After a 1-3 day incubation period (123), initial symptoms of pneumonic plague can be gastrointestinal in nature; e.g. vomiting and diarrhea (54). High fever, chest pain, dyspnea, and coughing (with and without the presence of blood in the sputum) quickly follow as the disease progresses (145). Treatment must be started 24-48 h following exposure as the mortality of pneumonic plague approaches 100% if treatment is delayed (145, 158).

Additionally, inflammation of the pharynx resembling tonsillitis has, in rare cases, occurred in conjunction with pneumonic infection of *Y. pestis* (33). Plague pharyngitis has a cultural disposition and has been noted in women who kill presumably infected fleas groomed from another's hair by biting down on the insect (33).

Diagnosis of *Y. pestis* infections is most easily performed using antigen detection protocols, immunostaining, polymerase chain reaction (PCR), or by performing a Gram-stain on blood or cerebral spinal fluid and noting the characteristic bipolar, 'safety-pin', staining of the coccobacillus (96). Any technique that diagnoses the infection using antibodies may delay treatment as antibodies may take weeks to develop (96).

#### **CURRENT ANIMAL MODELS OF *Y. PESTIS***

Plague research has benefited tremendously by the use of animal models that mimic human infection. Bubonic infection characterized in rodents is similar to that reported in humans (163), and disease progression during bubonic infection, a more natural presentation of the disease, has been studied quite extensively in many animal models (111, 155, 157). The rat model is a preferred model to study of bubonic plague because, unlike in the mouse

model of infection, the regional lymph nodes of rats became enlarged, swollen, painful, and hemorrhagic, similar in pathology to the buboes seen in human bubonic infection (155).

Wu Lien-Teh's account of the progression of pneumonic plague in humans *via* autopsies on deceased patients provided valuable information regarding the pathogenesis of *Y. pestis* to the medical and research community (112). Furthermore, the pathology of *Y. pestis* following aerosol infection in Rhesus monkeys was artfully described by Finegold and others in 1968 (68). In comparison with these findings, data acquired from the study of pneumonic infection in rodents (30, 109, 110, 158) have indicated that the progression of pneumonic plague, both *via* i.n. and aerosol administration, is also similar between these species and humans (163). Smith *et al.* earlier reported the development of pneumonic plague in mice *via* the aerosolization of *Y. pestis* (165), and, since then, several studies have utilized an aerosol model to test the efficacies of plague vaccine combinations (7, 8, 75, 85, 87, 99, 184). Intranasal or aerosol entry facilitates channeling of the bacteria into the bloodstream and bypassing the lymphatics, the most common route following intradermal administration and results in a rapid dissemination of bacteria to the body's other organs. Additionally, a biphasic response (an anti-inflammatory phase followed by a proinflammatory one) was noted after intranasal administration of *Y. pestis* CO92 (isolated from a fatal case of pneumonic plague referenced in (54)) to mice, which was indicative of a delay in the host's response to infection (109). Although difficult to test as T3SS-negative strains of *Y. pestis* do not establish serious infections *in vivo*, it was presumed that the early anti-inflammatory response (24-36 h p.i.) was induced by the T3SS and its associated effectors, while the later proinflammatory response (36-72 h p.i.) was due to the production of various cytokines/chemokines (e.g., IL-6, macrophage chemoattractant protein [MCP]-1, etc.).



## TREATMENT AND VACCINES

Most strains of *Y. pestis* can be killed with antibiotic therapy such as streptomycin, gentamicin, doxycycline, ciprofloxacin, or chloramphenicol (96). However, multiple drug resistant strains have been isolated in Madagascar and were described in 1997 and 2001 (72, 81). Until 1999, a formaldehyde-killed, whole cell vaccine, prepared using a highly virulent *Y. pestis* strain 195/P, was used for military personnel, but its production was halted because of severe side effects and of its short-lived protection in humans (151). In addition, the above-mentioned vaccine provided protection against bubonic, but not against pneumonic plague (173). Although the use of a live attenuated plague vaccine is not approved in the U.S. and many other countries because of safety reasons (172), a *pgm* locus-minus mutant of *Y. pestis* strain EV76 has been used in the countries of the former Soviet Union (173). This vaccine was found to be effective against both bubonic and pneumonic plague (64, 152). However, most of these EV76 derivatives can cause severe local and systemic reactions and gross tissue changes independent of their route of inoculation, thus limiting their use worldwide (173). Recent studies have indicated that the subunit vaccines containing *Y. pestis* antigens (e.g., LcrV and F1) have immunogenic properties in mice and macaques (50, 183, 190) and appear very promising. In fact, one preparation is currently in phase II clinical trials (85, 140, 172). Additionally, fusion vaccines using recombinant F1 and LcrV (143) and fusions of F1 and LcrV with flagellin as the adjuvant (124) have also shown protection in mice and non-human primates.

In an effort to further attenuate *Y. pestis* EV76, the *lpxM* gene (encoding lipid A myristoyl transferase) was deleted, and the generated  $\Delta lpxM$  mutant synthesized a less toxic penta-acylated LPS, compared to the more toxic hexa-acylated LPS in the parental strain (11,

64). More importantly, the overall virulence potential of  $\Delta lpxM$  mutant of *Y. pestis* EV76 was reduced, and the mutant strain even provided a better level of protective immunity in immunized hosts (64).

#### ***Y. PESTIS* AS AN AGENT OF BIOTERRORISM**

In 2002, the U.S. Public Health Security and Bioterrorism Preparedness Act deemed *Y. pestis* a select agent thereby regulating research performed on the bacterium and restricting who in the U.S. had access to bacterial preparations and stocks (140). *Y. pestis* has furthermore been characterized as a category A select agent based on the pathogen's disseminative capability, high mortality rate, and its potential impact on the public health infrastructure of the U.S. (78). *Y. pestis* makes a likely candidate for a bioterrorism attack based on its availability in endemic areas of the world, the simplicity of microbiological techniques necessary to culture it, and the speed at which pulmonary infection develops (140). Additionally, *Y. pestis* was one of many pathogens whose weaponizable capability was researched by the biological weapons programs of both the U.S. and former Soviet Union (96). Aerosolization of *Y. pestis* is the most likely method of dissemination that would be used to institute a biological attack (96) although other methods have been used in the past. In the 14<sup>th</sup> century, Tartars attacking the port of Caffa (now Feodosia, Ukraine) hurled the bodies of plague victims over the city walls resulting in an outbreak of plague within the city (145). During World War II, the Japanese army released *Y. pestis*-infected fleas over China causing an outbreak in the targeted villages (96). Unless one suspected a release of *Y. pestis*, one would not assume that the symptoms he/she was experiencing could be attributed to plague; some of the initial symptoms (e.g. fever, headache, malaise) are nonspecific. This

delay in both diagnosis and treatment would be detrimental to the affected population. The World Health Organization estimated in 1970 that if 50 kg of aerosolized *Y. pestis* were released over a city with a population of 5 million, the resulting pneumonic plague would have an infectivity rate of 3% (150,000 illnesses) and a mortality of 24% (182).

## **SUMMARY**

Annual morbidity and mortality of *Y. pestis* infections do not approach the deadly epidemics of the past but many factors suggest that *Y. pestis* is still a dangerous emerging pathogen. *Y. pestis* will never be eradicated because both the flea vector and rodent hosts are common in many countries of the world. The bacterium is readily accessible in nature and its use as a bioweapon has already been established. Based on these factors, continuing research on this bacterium is warranted.

## Chapter 2

### *Methods and Materials*

#### **BACTERIAL STRAINS AND PLASMIDS**

Bacterial strains and plasmids (52, 54, 57, 76, 130) used in these studies are listed in Table 2.1. *Yersinia* were grown in Brain Heart Infusion (BHI) or Heart Infusion Broth (HIB) medium (Difco, Voigt Global Distribution Inc, Lawrence, KS) at 26-28°C with constant shaking (180 rpm) and/or on BHI/HIB agar plates, while Luria-Bertani (LB) medium was used for growing other bacterial cultures (e.g., recombinant *E. coli*) at 37°C with shaking.

In some preparations, in order to maximize bacterial titrations, we used a modification of protocol described previously (7). Briefly, 10 µl of bacterial glycerol stock was streaked onto a 5% sheep blood agar (SBA) plate (Teknova, Hollister, CA) and incubated at 28°C for 48 h. Colonies were removed from the plate using a sterile loop, and a suspension was made using 4 ml of HIB. After mixing well, 100 µl of the suspension was added to 10 ml of HIB to obtain an optical density at 620 nm of 1.0. Finally, 200 µl of the diluted suspension was used to inoculate 10 ml of HIB and grown for 24 h at 30°C and 180 rpm. Following incubation, the suspension was centrifuged at 5000 rpm for 10 min in an Avanti J-20 refrigerated centrifuge fitted with HEPA filters (Beckman-Coulter, Fullerton, CA), and the pellet was washed twice in HIB before being resuspended in 10 ml of HIB (yielding approximately 10<sup>10</sup> colony forming units [cfu]/ml as determined by growth of serial dilutions on SBA). Appropriate dilutions were made in PBS in order to obtain the inoculation

dose for each study.

Strains/Plasmids	Description and Source	Reference
<i>Y. pestis</i> strain CO92	Virulent WT <i>Y. pestis</i> isolated in 1992 from a fatal pneumonic plague case, biovar Orientalis, and naturally resistant to polymyxin B.	36, 54, 130, CDC <sup>a</sup>
<i>Y. pestis</i> strain KIM/D27	An attenuated strain of <i>Y. pestis</i> KIM (Kurdistan Iran man) containing a deletion of the pigmentation locus ( $\Delta pgm$ ), biovar Mediaevalis.	52, Laboratory stock
<i>Y. pseudotuberculosis</i> YPIII	WT <i>Y. pseudotuberculosis</i> , <i>phoP</i> minus, with pYV plasmid.	ATCC <sup>b</sup> , 76
<i>Salmonella enterica</i> serovar Typhimurium strain 14028	WT <i>S. Typhimurium</i> .	ATCC <sup>b</sup>
$\Delta lpp$ D27	The <i>lpp</i> gene deletion mutant of <i>Y. pestis</i> KIM/D27.	158
$\Delta lpp$ CO92	The <i>lpp</i> gene deletion mutant of <i>Y. pestis</i> CO92.	158
pPCP <sup>+</sup> CO92	<i>Y. pestis</i> CO92 cured of virulence plasmid pPCP1.	3
pPCP <sup>+</sup> / $\Delta lpp$ CO92	$\Delta lpp$ mutant strain of <i>Y. pestis</i> CO92 cured of virulence plasmid pPCP1.	3
$\Delta lpp$ pseudo	The <i>lpp</i> gene deletion mutant of <i>Y. pseudotuberculosis</i> YPIII.	158
$\Delta lpp$ D27compl	The complemented <i>Y. pestis</i> <i>lpp</i> deletion mutant ( $\Delta lpp$ D27) via plasmid pBRY <i>lpp</i> . Tc <sup>r</sup> .	158
$\Delta lpp$ pseudocompl	The complemented <i>Y. pseudotuberculosis</i> YPIII <i>lpp</i> deletion mutant ( $\Delta lpp$ pseudo) via plasmid pBRY <i>lpp</i> . Tc <sup>r</sup> .	158
$\Delta lpp$ D27/pBR322	The <i>Y. pestis</i> <i>lpp</i> deletion mutant ( $\Delta lpp$ D27) containing plasmid pBR322. Tc <sup>r</sup> , Ap <sup>r</sup> .	158
$\Delta lpp$ pseudo/pBR322	The <i>Y. pseudotuberculosis</i> YPIII <i>lpp</i> deletion mutant ( $\Delta lpp$ pseudo) containing plasmid pBR322. Tc <sup>r</sup> , Ap <sup>r</sup> .	158
<i>Y. pestis</i> strain KIM/D27/pBR322	The <i>Y. pestis</i> KIM/D27 strain containing plasmid pBR322. Tc <sup>r</sup> , Ap <sup>r</sup> .	158
<i>Y. pseudotuberculosis</i> YPIII/pBR322	WT <i>Y. pseudotuberculosis</i> YPIII containing plasmid pBR322. Tc <sup>r</sup> , Ap <sup>r</sup> .	158
pDMS197	Suicide vector with a conditional R6K origin of replication ( <i>ori</i> ) and a levansucrase gene ( <i>sacB</i> ) from <i>Bacillus subtilis</i> used for homologous recombination.	57
pBR322	The cloning vector for complementation.	GE Healthcare
pDMS197KIMUD	Recombinant plasmid containing the <i>lpp</i> gene up- and down-stream flanking DNA fragments from <i>Y. pestis</i> KIM/D27 cloned into the pDMS197 suicide vector.	158
pDMS197CO92UD	Recombinant plasmid containing the <i>lpp</i> gene up- and down-stream flanking DNA fragments from <i>Y. pestis</i> CO92 cloned into the pDMS197 suicide vector.	158
pDMS197pseudoUD	Recombinant plasmid containing the <i>lpp</i> gene up- and down-stream flanking DNA fragments from <i>Y. pseudotuberculosis</i> cloned into the pDMS197 suicide vector.	158
pBRY <i>lpp</i>	Recombinant plasmid containing the <i>lpp</i> gene coding region and its putative promoter in vector pBR322 used to complement the $\Delta lpp$ mutants of yersinae.	158

<sup>a</sup>Centers for Disease Control and Prevention, Atlanta, GA

<sup>b</sup>American Type Culture Collection, Manassas, VA

Table 2.1: Bacterial strains and plasmids used in these studies.

## BACTERIAL GROWTH FOR AEROSOLIZATION

To prepare *Y. pestis* CO92 for aerosolization, we followed the protocol published by Anderson and others (7) with some modifications to yield a concentration of  $1 \times 10^{10}$  cfu/ml. Briefly, 10  $\mu$ l of bacterial glycerol stock was streaked onto an SBA plate and incubated at 28°C for 48 h. Colonies were removed from the plate using a sterile loop and suspended well in 4 ml of HIB. The optical density of the bacterial suspension at 620 nm was adjusted to 1.0 (a 1:7 dilution, yielding approximately  $10^9$  cfu/ml). Finally, 2 ml of the diluted suspension was used to inoculate 100 ml of HIB, in a 1 liter plastic Erlenmeyer flask, supplemented with 0.2% xylose (DL-xylose, Sigma-Aldrich, St. Louis, MO). The culture was grown for 24 h at 30°C and 100 rpm. We preferred to grow bacteria at 30°C over 37°C to avoid possible complications of aerosolizing *Y. pestis* with capsule, as the latter is optimally synthesized at 37°C. Further, 30°C being closer to the optimal growth temperature of yersiniae, we were able to achieve higher bacterial concentrations needed for aerosolization. Following incubation, the suspension was centrifuged at 5000 rpm for 10 min at 4°C in a HEPA filter-fitted Avanti J-20 refrigerated centrifuge, and the pellet was washed twice in sterile water before being resuspended in 10 ml of sterile water (yielding approximately  $10^{10}$  cfu/ml). Subsequently, bacterial dilutions were made in sterile water to obtain the concentrations we used to precisely calculate the aerosolized *Y. pestis* CO92 LD<sub>50</sub> dose in mice and rats. Antifoam A emulsion 240 (30  $\mu$ l, Sigma-Aldrich) was added to each bacterial suspension to prevent foaming during nebulization of the bacterial culture. The bacterial cultivation was conducted in our restricted entry Biosafety Level (BSL)-2 laboratory approved by the CDC.

## GENERATION AND CHARACTERIZATION OF $\Delta LPP$ MUTANTS OF *Y. PESTIS* AND *Y. PSEUDOTUBERCULOSIS*

Based on the genome sequence of *Y. pestis* (KIM and CO92) and *Y. pseudotuberculosis*, the *lpp* gene coding region (237 bp) and its upstream flanking DNA sequences were identical (GenBank accession numbers NC\_003143, NC\_004088 and NC\_006155) (40, 52, 130). However, the downstream flanking DNA sequences to the *lpp* gene were somewhat different in these two *Y. pestis* strains (KIM and CO92) as well as in *Y. pseudotuberculosis* YPIII. By using different primer sets (Table 2.2), the *lpp* flanking DNA fragments from each of the corresponding yersiniae were PCR amplified and cloned into the pDMS197 suicide vector (57), resulting in recombinant plasmids pDMS197KIMUD, pDMS197CO92UD, and pDMS197pseudoUD, respectively (Table 2.1). By electroporation (Genepulser Xcell, Bio-RAD, Hercules, CA), the recombinant plasmids were transformed into their corresponding WT/parental strains for homologous recombination. The transformants were plated onto the BHI agar plates containing 5% sucrose and screened by colony blot hybridization (136) with the *lpp* gene probe which was PCR amplified *via* specific primers *lppF/lppR* (Table 2.2) from the genomic DNA (gDNA) of *Y. pestis* CO92. The colonies which did not react with the *lpp* gene probe were potential *lpp* mutants, and their identity was confirmed by Southern blot analysis using the *lpp* gene probe and suicide vector pDMS197 plasmid as a probe (159). The resulting mutants were designated as  $\Delta lppD27$ ,  $\Delta lppCO92$ , and  $\Delta lpppseudo$ , respectively (Table 2.1).

Primer Position	Primer name and sequence <sup>a</sup>	Purpose
5'	<i>lpp</i> up-F/XbaI 5' GCTCTAGAGCTTGATCGGTATGGAAGTC 3'	Primer pair for amplification of the <i>lpp</i> gene upstream flanking DNA
3'	<i>lpp</i> up-R/BamHI 5' CGGGATCCCGTTAATCTCCATGTAGCCTTAC 3'	fragment: both <i>Y. pestis</i> and <i>Y. pseudotuberculosis</i> .
5'	<i>lpp</i> /pestis/down-F/BamHI 5' CGGGATCCCGAAGTAATATTACTTCCTG 3'	Primer pair for amplification of the <i>lpp</i> gene downstream flanking DNA
3'	<i>lpp</i> /pestis/down-R/SacI 5' ACCGAGCTCGAACAGCAACGACACGTGAAG 3'	fragment: <i>Y. pestis</i> only.
5'	<i>lpp</i> F: 5' ATGAATCGTACTAAACTTGATAC 3'	Primer pair involved in the amplification of the <i>lpp</i> gene from the genome of <i>Y. pestis</i> CO92, which was used as probe in the screening of <i>lpp</i> gene deletion mutants of <i>Yersinae</i> .
3'	<i>lpp</i> R: 5' TTACTTCTTGTAAGCTTTGAG 3'	
5'	<i>lpp</i> /pseudo/down-F/BamHI 5' CGGGATCCCGAAGTAATATTACTTCCTG 3'	Primer pair for amplification of the <i>lpp</i> gene downstream flanking DNA
3'	<i>lpp</i> /pseudo/down-R/SacI 5' ACCGAGCTCGACTACAAACCGACAGAGAGTCAG 3'	fragment: <i>Y. pseudotuberculosis</i> only.
5'	<i>lpp</i> -N/PvuII: 5' ATCGATCGCACCTTACAAATAAGACTAGTC 3'	Primer pair for amplification of the coding region of the <i>lpp</i> gene and its potential promoter region for complementation of the <i>lpp</i> mutants of <i>Yersinae</i> .
3'	<i>lpp</i> -C/PstI: 5' AACTGCAGTTACTTCTTGTAAGCTTGAGCT 3'	
5'	<i>lcrV</i> -F 5' CCAGCTAGCATTAGAGCCTACGAACA 3'	Primer pair for amplification of the coding region of the <i>lcrV</i> gene to verify the existence of plasmid pCD1/pYV <sup>b</sup> in the <i>lpp</i> mutants of <i>Yersinae</i> .
3'	<i>lcrV</i> -R 5' AACAGATCTGTGTCATTACCCAGACG 3'	
5'	<i>cafI</i> -F 5' TCTCGCTAGCAAAAAAATCAGTTCCG 3'	Primer pair for amplification of the coding region of the <i>cafI</i> gene to verify the existence of plasmid pMT1 <sup>c</sup> in the <i>lpp</i> mutants of <i>Y. pestis</i> .
3'	<i>cafI</i> -R 5' CTGAGATCTGGATTATTGGTTAGATA 3'	
5'	<i>pla</i> -F 5' ATGAAGAAAAGTTCATTATTGTG 3'	Primer pair for amplification of the coding region of the <i>pla</i> gene to verify the existence of plasmid pPCP1 <sup>d</sup> in the <i>lpp</i> mutants of <i>Y. pestis</i> .
3'	<i>pla</i> -R 5' TCAGAAGCGATATTGCAGAC3 '	

<sup>a</sup> Underlined bases denote restriction enzyme site in the primer.

<sup>b</sup> pCD1 is a 70 kb plasmid encoding the type 3 secretion system proteins and effectors including LcrV.

<sup>c</sup> pMT1 is a 100 kb plasmid encoding murine toxin and capsular antigen, CafI.

<sup>d</sup> pPCP1 is a 10 kb plasmid encoding pesticin and plasminogen activating protein, Pla.

Table 2.2: Primers used in these studies.



### **COMPLEMENTATION OF THE *YERSINIAE* $\Delta$ LPP MUTANTS**

We used specific primers (*lpp*-N/PvuI and *lpp*-C/PstI, Table 2.2) to amplify a DNA fragment that contained the coding region of the *lpp* gene (237 bp), as well as its potential promoter region (200 bp upstream of the start codon of the *lpp* gene) from the gDNA of *Y. pseudotuberculosis*. The amplified DNA fragment was cloned into the pBR322 vector, generating the recombinant plasmid pBRY*lpp* (Table 2.1). By electroporation, the plasmid pBRY*lpp* was transformed into the *lpp* mutants of *Y. pestis* KIM/D27 and *Y. pseudotuberculosis* for complementation. The pBR322 vector alone was also introduced into the parental strains and into the *lpp* mutants to serve as proper controls. These yersiniae were grown in BHI or HIB medium in the presence of tetracycline (15 µg/ml).

Restriction endonucleases and T4 DNA ligase were obtained from Promega (Madison, WI). The Advantage® cDNA PCR Kit was purchased from Clontech (Palo Alto, CA). The digested plasmid DNA or DNA fragments from agarose gels were purified using QIAquick® Kits (Qiagen, Inc., Valencia, CA).

### **WESTERN BLOT ANALYSIS**

WT/parental *Y. pestis* KIM/D27 and CO92, as well as WT *Y. pseudotuberculosis* YPIII, their corresponding  $\Delta$ *lpp* mutants and complemented strains were grown in 3 ml of BHI medium at 28°C overnight with shaking. The bacteria were harvested and Western blot analysis was performed with specific primary mouse anti-Lpp monoclonal antibodies (1:2000 dilution), followed by horseradish peroxidase (HRP)-labeled, goat anti-mouse secondary antibodies. The blots were developed using a SuperSignal® West Pico Chemiluminescent Substrate (45, 159). All of the sample preparations were conducted in our approved,

restricted-entry BSL-2 laboratory where needed.

To detect the secreted form of LcrV (low-calcium response antigen), the above, overnight-grown yersiniae cultures were diluted (in a total volume of 10 ml of the medium) to an optical density (OD) of 0.2 at 600 nm (OD<sub>600nm</sub>), and EGTA was added to a final concentration of 5 mM. After 4 to 6 h of growth at 37°C, the culture supernatants (10 ml each) were collected, filter-sterilized (0.22 µm) and precipitated with trichloroacetic acid (TCA; 10% final concentration). The precipitated proteins were resuspended in 100 µl of SDS-PAGE loading buffer, and an aliquot (25 µl) from each of these samples was used for Western blot analysis with specific anti-LcrV antibodies (125).

#### ***PLASMID ISOLATION***

The WT/parental yersiniae and their  $\Delta lpp$  mutant cultures were grown at 28°C overnight. Approximately 10-15 ml of each culture was used to isolate the plasmid DNA (pCD1, pYV, pMT1, and pPCP1) using the Qiagen plasmid isolation kit with slight modifications. Briefly, after the addition of neutralizing solution P3, the supernatants were separated from the pellet and extracted with phenol. The plasmid DNA was then directly precipitated with an equal volume of isopropyl alcohol and resolved using 0.7% agarose gel electrophoresis with Tris-acetate buffer (119).

#### ***TRANSLOCATION OF T3SS EFFECTORS***

A modified protease protection and digitonin extraction assay (41) was used to evaluate the translocation ability of T3SS effectors, Yops, in *Yersinia*  $\Delta lpp$  mutants. Briefly, duplicate wells of HeLa cells (in a 6-well plate) were infected with different *Yersinia* strains

(WT/parental and their  $\Delta lpp$  mutant strains) at an MOI (multiplicity of infection) of 10. After 2-3 h of infection at 37°C, cells were treated with 1 ml of proteinase K (100 µg/ml in phosphate-buffered saline [PBS]), followed by the addition of 500 µl of freshly prepared phenylmethylsulfonyl fluoride (4 mM in PBS), to block protease activity. One set of the cells was lysed with 200 µl of digitonin (1% in PBS), and the other set was incubated with 200 µl of PBS without digitonin. Cells were dislodged from the surface of the plate, collected, and centrifuged. The supernatants were collected and subjected to Western blot analyses using antibodies to YopE (Santa Cruz Biotechnology, Santa Cruz, CA) and YopH (Agrisera, Stockholm, Sweden).

### ***MOTILITY TESTING***

Overnight-grown WT *Y. pseudotuberculosis*,  $\Delta lpp$  mutant and its complemented strain were adjusted to similar optical densities, and equal numbers of bacteria ( $1 \times 10^6$  cfu) were stabbed into 0.35% BHI-agar plates (159). The migration of organisms from the center to the periphery of the plates was measured after incubation for 48 h at 28°C.

### **ASSESSMENT OF THE MEMBRANE INTEGRITY OF YERSINIAE $\Delta LPP$ MUTANTS**

Different methods were used to measure the membrane integrity of yersinia  $\Delta lpp$  mutant strains, as described below.

### ***RELEASE OF PERIPLASMIC RNASE I***

WT/parental yersinia strains and their corresponding  $\Delta lpp$  mutants were grown overnight and then diluted to an OD<sub>600nm</sub> of 0.2. An aliquot (10 µl) of each diluted culture

was spotted in triplicate onto BHI agar plates containing 1.5% Torula yeast RNA (Sigma-Aldrich, St. Louis, MO). Plates were incubated overnight at 26-28°C, after which 10% TCA was poured in the plates. As RNase I degrades the yeast RNA substrate on the plate, a clear zone around the bacterial growth was formed after application of TCA. Therefore, the size of the clear zone represented the amount of RNase I released from the bacterial periplasmic space and was indicative of cell membrane integrity (22).

#### ***RELEASE OF $\beta$ -LACTAMASE***

The plasmid pBR322, a source of  $\beta$ -lactamase, was transformed into WT/parental *Y. pestis* KIM/D27, *Y. pseudotuberculosis* YPIII, and their corresponding  $\Delta lpp$  mutant strains. The membrane integrity of  $\Delta lpp$  mutants was assessed by measuring the percentage of  $\beta$ -lactamase activity in the culture supernatant/cell extract and comparing it to the corresponding parental strains as we previously described (159).

#### ***SENSITIVITY TO DETERGENT***

Triton X-100 (TX-100) was used in this assay as previously described (159). Briefly, WT/parental yersiniae and their  $\Delta lpp$  mutant strains were grown to an OD<sub>600nm</sub> of 0.4-0.5 and diluted 50-fold. TX-100 was then added at various final concentrations (0, 1, 2 and 5%), and the cultures were incubated at 26-28°C for 3 h with shaking after which the OD<sub>600nm</sub> was measured. TX-100-treated cultures were compared to corresponding cultures without TX-100 in three independent experiments. A 50% reduction in the OD indicated a sensitivity of the bacterium to detergent treatment and a breach in membrane integrity (35).

### ***SENSITIVITY TO PH AND DETERGENT***

The WT/parental *Yersinia* and their  $\Delta lpp$  mutant strains were grown at 28°C or 37°C overnight. The cultures were then pelleted and resuspended in BHI medium with different pH (3.0 or 5.0) and TX-100 (0.5% or 2.0%) combinations for 5 min at room temperature (13). The normal BHI medium (pH 7.0 without the addition of TX-100) served as a control. The bacterial samples were utilized in triplicate in each treatment, and the surviving bacteria were counted by serial dilution and plating. The bacterial survival rates were calculated as the percentage of viable bacteria from the control groups.

### ***CYTOTOXICITY***

Cultures of WT/parental *Yersinia* and their  $\Delta lpp$ , pPCP<sup>-</sup>, and pPCP<sup>-</sup>/ $\Delta lpp$  mutant strains were grown overnight at 28°C. A 1:4 dilution was made of the overnight cultures in fresh broth, and incubation was continued at 28 °C for 30 min and then at 37°C for 1 h. HeLa cells were infected with *Yersinia* at various MOIs (0.5, 1, 10, and 20) for 2-3 h at 37°C. The cell morphology (cytotoxicity) was monitored and recorded by using light microscopy.

### **MEASUREMENT OF MINIMUM INHIBITORY CONCENTRATION (MIC) OF LEVOFLOXACIN**

The MIC of levofloxacin against WT *Y. pestis* CO92 and the  $\Delta lpp$  mutant was determined by using the E-Test (AB Biodisk North America Inc, Culver City, CA) (127). Briefly, the overnight-grown *Yersinia* cultures were diluted (1:4) with fresh BHI medium and continued to grow at 28°C for 2 h (OD<sub>600nm</sub> of 0.6). The bacterial cultures were then spread evenly onto the Mueller–Hinton agar plates (Becton Dickinson, Cockeysville, MD) or on SBA plates, and the predefined levofloxacin (range of 0.002 to 32 µg/ml) E-strips were

placed onto the plates. Plates were incubated for 48 h at 28°C, and the MIC values were recorded.

## ANIMAL STUDIES

All animal experiments were performed using protocols approved by the UTMB Institutional Animal Care and Use and Institutional Biological Safety Committees in Animal BSL (ABSL) - 2/3 laboratories. Female 5-to-6 week old Swiss-Webster or BALB/c mice (20-25 g) and inbred Brown Norway rats, weighing either 50-75 g or 150-175 g, were purchased from Charles River Laboratories (Wilmington, MA). Animals were challenged *via* the i.p. (62), i.n. (133, 134, 158), or s.c. (134) routes of infection or *via* aerosol challenge (described below) with various doses of different species and strains of WT/parental *Yersinia* or the  $\Delta lpp$ , pPCP<sup>-</sup>, and pPCP<sup>-</sup>/ $\Delta lpp$  mutant strains and complemented strains as is indicated with each experiment. In some experiments, mice received a sub-inhibitory dose of levofloxacin (0.3–0.5 mg/kg/day, unpublished data) starting 24 h p.i. by the i.p. route for a maximum period of 6 days. This has been indicated with each individual experiment. Levofloxacin is a homolog of ciprofloxacin with a longer half life and has recently been approved by the Food and Drug Administration for use against anthrax (63). Mice were assessed for morbidity or mortality over the duration of each experiment or were sacrificed, and the sera and organs were harvested at the indicated time points. In animal experiments in which complemented strains were used, mice were given tetracycline in water (5 mg/ml) 48 h prior to challenge and continued throughout the experiment to maintain the plasmid in bacteria.

### ***AEROSOL CHALLENGE OF MICE AND RATS***

The aerosol unit was decontaminated with formaldehyde gas and any remaining gas residues were removed using an air flush immediately prior to the nebulization of *Y. pestis*. Animals were exposed to *Y. pestis* CO92 aerosols in a whole-body Madison chamber (Madison, WI) attached in tandem to a class III biological glove cabinet (Baker Company IsoGARD 14, Sanford, ME) and then to a class II biological safety cabinet, as previously described (133). For LD<sub>50</sub> determination, groups of 10 mice or rats were challenged with various concentrations of *Y. pestis* CO92 aerosolized using a three-jet Collison nebulizer (BGI Incorporated, Waltham, MA) in the ABSL-3 facility (5, 133). Animals were exposed to the pathogen for 15 min while the aerosol chamber was flushed with air at a flow rate of 50-65 liters/min, as described recently for *B. anthracis* spores (133). Air flow to the nebulizer was 6.5 L/min, and the temperature of the air inside the chamber was observed to be 72 °F with 50 % humidity. Samples of bacteria at each run were collected in SKC BioSamplers (Eighty Four, PA) using an airflow of 12.5 L/min for 5 min. The animals were housed in our ABSL-3 laboratory for the duration of this study and given food and water *ad libitum*.

### ***PASSIVE TRANSMISSION OF Y. PESTIS***

Rats of comparable size and age and from the same batch were inoculated intranasally in groups of eight with either a 25 LD<sub>50</sub> or a 2500 LD<sub>50</sub> dose of *Y. pestis* CO92. Two infected rats were housed in a cage with one uninfected rat immediately following challenge and monitored for mortality. Organs harvested from dead animals in this experiment were homogenized in sterile water, serially diluted, and cultured on SBA plates to identify the presence of *Y. pestis*. Total DNA from selected colonies from the organs was

subjected to polymerase chain reaction (PCR) for the detection of genes encoding capsular antigen (F1), type 3 secretion system (T3SS)-associated low calcium response antigen (LcrV), and plasminogen-activated protease (Pla) (158). These three genes are present on distinct plasmids found in *Y. pestis* (131).

## **HISTOPATHOLOGICAL ANALYSES**

At various time points indicated with each experiment, 5 *Y. pestis*-infected animals per group were humanely euthanized (mice: ketamine [90 mg/kg] and xylazine [10 mg/kg]; rats: ketamine [50 mg/kg] and xylazine [7 mg/kg]), and the lungs, liver, spleen, and heart tissues were collected at necropsy and immersion fixed in 10 % neutral buffered formalin in screw-cap containers. Uninfected animals were used as controls. After 3 days, the tissues were moved to new containers with fresh formalin, processed, sectioned at 5  $\mu$ m, mounted on glass slides, and stained with hematoxylin and eosin (H&E). Tissues were processed and analyzed by the pathology department at the University of Texas M.D. Anderson Cancer Center in Bastrop, TX. The sterility of the fixed tissues was confirmed by plate counts before histopathologic examination. Light microscopic evaluation of the tissues was performed. Lesions considered distinctive for *Y. pestis* infection included: (1) the presence of massive numbers of organisms; (2) inflammatory changes, such as edema and cellular infiltrates; and (3) tissue and/or blood vessel necrosis, with congestion and hemorrhage. Lesions were graded based on a severity scale of minimal, mild, moderate, and severe. The scale correlated to estimates of lesion distribution and extent of tissue involvement (minimal = 2-10 %; mild  $\geq$  10-20 %; moderate  $\geq$  20-50 %; severe  $\geq$  50 %).

In general, acute inflammation was characterized by the presence of neutrophils while



subacute inflammation indicated a mixture of neutrophils and mononuclear cells (macrophages and lymphocytes). Edema and/or necrosis were present in some acute and subacute lesions, particularly if moderate-to-severe lesions were observed. Bacteria seen in tissues were consistent with *Y. pestis* based on their morphology, although special staining was not performed except in some cases where bacteria were stained with Giemsa. We analyzed tissues from 3-5 animals per group for histopathology (indicated with each experiment), and data from representative tissues were presented.

#### **BLOOD CHEMISTRY AND BLOOD CELL COUNTS**

Swiss-Webster mice were inoculated *via* the i.n. route with a 5 LD<sub>50</sub> dose ( $1.7 \times 10^3$  cfu) of WT *Y. pestis* CO92. After 24, 48 and 96 h p.i., blood was drawn *via* cardiac puncture, and 3-5 animals were used for each time point. The blood chemistries and cell counts were analyzed by using a Drew Scientific ProChem Blood Analyzer and Drew Scientific Hemavet 950 Hematology System (Drew Scientific Inc., Dallas, TX), respectively. The results were compared to both the Mouse Baseline Clinical Chemistry Values published by Charles River and to the 0 h control. Data for all animals at each time point were averaged, and a standard deviation (SD) was calculated.

#### **BACTERIAL DISSEMINATION**

Mice and rats were exposed to various doses of *Y. pestis* CO92 or one of the mutant strains *via* the aerosolized or i.n. routes of infection. In some experiments, mice received a sub-inhibitory dose of levofloxacin after 24 h p.i., but this is indicated with the appropriate experiment. At various timepoints (indicated with each experiment), groups of 3-5 animals

were euthanized (mice: ketamine [90 mg/kg] and xylazine [10 mg/kg]; rats: ketamine [50 mg/kg] and xylazine [7 mg/kg]), and blood from the heart was drawn *via* cardiac puncture. The lungs, liver, spleen, and heart were removed immediately after ensuring death by cervical dislocation. The organs were weighed and homogenized in either 1 ml of sterile water containing 25 µg/ml of polymyxin B (to facilitate specific growth of *Y. pestis* CO92) or sterile water alone using tissue grinders (Kendall, Mansfield, MA). The blood and tissue homogenates were serially diluted in sterile water with polymyxin B or in sterile water alone and cultured on SBA plates. Plates were incubated at 28°C for 48 h after which bacterial colonies were counted and cfu per gram of tissue or per ml of blood was calculated.

Abbreviation or Acronym	Definition	Cellular Source
Eotaxin	eosinophil chemotactic protein	monocytes
G-CSF	granulocyte-colony stimulating factor	macrophages
GM-CSF	granulocyte monocyte-colony stimulating factor	macrophages and T cells
IFN- $\gamma$	interferon-gamma	T cells and NK cells
IL	interleukin (many types)	Many sources: T cells, macrophages, B cells
IP-10	IFN- $\gamma$ inducible protein-10	monocytes
KC	keratinocyte-derived chemokine	monocytes
LIF	leukemia inhibitory factor	T cells, monocytes, fibroblasts
LIX	lipopolysaccharide-induced CXC chemokine	monocytes
MCP-1	macrophage chemotactic protein-1	monocytes
M-CSF	monocyte-colony stimulating factor	monocytes
MIG	monocyte induced by interferon-gamma	monocytes
MIP	macrophage inflammatory protein	T cells, monocytes, neutrophils
RANTES	regulated upon activation, normal T cell expressed and secreted	T cells
TNF- $\alpha$	tumor necrosis factor-alpha	macrophages, mast cells, lymphocytes
VEGF	vascular endothelial growth factor	keratinocytes
GRO-KC	growth-related oncogene/keratinocyte-derived chemokine	monocytes

Table 2.3: Abbreviations and acronyms of cytokines and chemokines measured in these studies.

## **IN VIVO CYTOKINE AND CHEMOKINE ANALYSES**

Mice and rats were exposed to various doses of *Y. pestis* CO92 or one of the mutant strains *via* the aerosolized or i.n. routes of infection. In parallel with the bacterial dissemination experiment described above, blood was drawn *via* cardiac puncture from euthanized animals at various time points. Sera were filtered once through a 0.45- $\mu$ m and then once through a 0.22- $\mu$ m syringe filter before culturing on SBA plates to confirm that bacteria had been successfully removed from the samples prior to analysis.

The levels of cytokines and chemokines were measured using the multiplex assay with either Bio-Plex (mouse, Bio-RAD, Hercules, CA), LINCoplex (rats, Millipore, Billerica, MA) or Milliplex (mouse, Millipore). The abbreviations and acronyms of cytokines and chemokines measured in these studies are described in Table 2.3.

## **BACTERIAL INVASION/PHAGOCYTOSIS OF MURINE MACROPHAGES AND INTRACELLULAR SURVIVAL**

RAW 264.7 murine macrophages were seeded in 6-well plates and incubated until they reached 60-70% confluence (approximately  $3 \times 10^6$  cells/well) (61, 62, 159). Different yersiniae, grown in HIB medium at either 28°C or 37°C, were used to infect macrophages at an MOI of 1. Plates were centrifuged at 1500 rpm for 10 min to facilitate binding of the bacteria to the host cells and were then incubated at 37°C in 5% CO<sub>2</sub> for the duration of the experiment. After 30 min of incubation, the medium was aspirated and the cells carefully washed 2x with PBS. DMEM supplemented with either 100  $\mu$ g/ml or 200  $\mu$ g/ml gentamicin was added to each well to kill extracellular bacteria. After 1 h, the medium was removed, and an aliquot (100  $\mu$ l) from each well was spread onto SBA plates to determine whether all of

the extracellular bacteria were killed by the gentamicin treatment. Subsequently, the infected RAW cells were carefully washed 2x with PBS before DMEM containing 10 µg/ml of gentamicin was added to each well. The 0 h plates, representing host cells that were infected with bacteria for 30 min and then treated with gentamicin for 1 h, were harvested at this time to determine the number of initially invaded/phagocytosed bacteria. At the designated time points (between 0 and 24 h), host cell viability was assessed using a light microscope after which the monolayers were carefully washed 2x with PBS. Macrophages were then lysed with 300 µl of sterile water and shaken to ensure complete disruption of the host cells. Suspensions of lysed macrophages were serially diluted ten-fold and cultured on SBA plates for determining colony counts after incubation at 28°C for 24-48 h. The original bacterial suspension was also serially diluted and plated in order to calculate the percentage of invasion/phagocytosis.

#### **STATISTICAL ANALYSES**

Kaplan-Meier survival estimate of 10 animals per group for each dose of bacteria was used for comparison of the LD<sub>50</sub> survival curves, and these experiments were repeated three times. Whenever appropriate, the student's *t*-test or ANOVA with Bonferroni post-test were utilized for statistical analysis between groups. For studies on bacterial dissemination and cytokine profiling, tissues and blood were collected from 5 animals at each time point unless otherwise noted. Cytokine analyses were repeated twice to determine statistical significance of the data.

## Chapter 3\*

### ***Braun Lipoprotein (Lpp) Contributes to the Virulence of Yersiniae: Potential Role of Lpp in Inducing Bubonic and Pneumonic Plague***

Murein, or Braun, lipoprotein (Lpp) is associated with the outer membrane of bacteria within the *Enterobacteriaceae* family. Lpp has previously been demonstrated to play a role in the host's immune response against infections with some gram-negative enteric pathogens, such as *E. coli*, *Salmonella enterica* serovar Typhimurium, and *Y. enterocolitica* (192). In fact, we recently reported that both single and double *lpp* gene deletions from the chromosome of *S. Typhimurium* resulted in attenuation of the bacteria in terms of their motility, invasiveness, cytokine/chemokine production, and such mutants were avirulent in mice when administered by systemic and oral routes when compared to the WT bacterium (61, 62, 159).

After searching the National Center for Biotechnology Information (NCBI) database, we identified a homolog of the *Salmonella enterica* serovar Typhimurium lipoprotein (*lpp*) gene in the genome of all three pathogenic yersiniae (40, 52, 130). We prepared *lpp* gene deletion mutants of *Y. pseudotuberculosis* YPIII, *Y. pestis* KIM/D27 (*pgm* locus-minus), and *Y. pestis* CO92 in order to study the affect this deletion has on the virulence in *Yersinia* infections. To our knowledge, this is the first systematic study illustrating the role of Lpp in the pathogenesis of yersiniae infection.

---

\* Copyright © American Society for Microbiology, *Infection and Immunity*, vol 76, p 1390-1409, 2008. Used with permission.

## ***Results***

### **PNEUMONIC PLAGUE IN MICE**

Primary pneumonic plague is highly contagious and almost always fatal (109, 131). To better understand the progression of the disease and the host responses, we used an established mouse model in which animals were intranasally challenged with WT *Y. pestis* CO92 (109). The LD<sub>50</sub> dose of WT *Y. pestis* varies, depending on bacterial growth conditions (such as temperature) and routes of infection (131). In our study, WT *Y. pestis* CO92 was grown at 28°C in BHI or HIB medium. The intranasal LD<sub>50</sub> dose (144) of BHI-grown cells was determined to be 340 bacteria for Swiss-Webster mice and approximately 100 cfu in BALB/c mice. Similar LD<sub>50</sub> doses in mice were reported in the literature for this highly virulent strain of *Y. pestis* by the i.n. route (109).

### ***BLOOD CHEMISTRIES AND CELL COUNT DATA***

To study systemic effects in mice during the course of *Y. pestis* infection, animals were inoculated *via* the i.n. route with 5 LD<sub>50</sub> of WT *Y. pestis* CO92. Blood chemistry analysis of sera from infected mice showed minimal changes during the first 48 h following challenge; however, marked changes were observed late in the infection at 60 h (Table 3.1). The albumin, globulin, and total protein values gradually increased through the course of infection. A similar increasing trend was seen with electrolytes, such as calcium, chloride, potassium and magnesium; although in some cases the values remained within the mouse normal range, but above the average values (e.g., potassium). The bicarbonate values, on the other hand, decreased through the course of infection (Table 3.1). The triglycerides, creatinine (a breakdown product of creatine), alanine transaminase (ALT) and aspartate

aminotransferase (AST) levels also increased (Table 3.1). The latter changes indicated advancing kidney and liver damage, edema, and dehydration of mice due to WT *Y. pestis* infection. For example, the albumin level increased from 3.1 to 5.3 g/dl (average normal value is 3.3) from 0 h to 60 h p.i. Likewise, AST increased from 133 to 669 (U/L) and creatinine from 0.4 to 4.8, when the normal values for them were 137 and 0.6, respectively.

Test	0 h	36 h	48 h	60 h**	Normal Range*
Albumin (g/dL)	3.1 ± 0.9	3.1 ± 0.3	3.5 ± 0.4	5.3	2.9-3.7 (3.3)
Bicarbonate (mmol/L)	21.0 ± 2.9	21.2 ± 2.5	19.3 ± 2.3	5.0	NA
Calcium (mg/dL)	10.7 ± 1.5	10.9 ± 1.2	10.5 ± 0.8	15.0	8.4-10.2 (9.3)
Chloride (mmol/L)	137.3 ± 4.8	124.0 ± 8.7	124.0 ± 6.2	141.0	109.0-119.0 (114)
Magnesium (mg/dL)	2.9 ± 0.2	1.8 ± 1.0	2.4 ± 0.9	6.0	1.2-3.7 (2.45)
Total Protein (g/dL)	5.8 ± 0.9	5.3 ± 0.4	7.0 ± 0.4	12.0	4.2-5.2 (4.7)
Triglycerides (mg/dL)	71 ± 15	74.8 ± 37	41.3 ± 23	263	NA
Potassium (mmol/L)	4.2 ± 0.5	4.5 ± 0.5	5.0 ± 0.6	5.9	4.2-6.2 (5.2)
ALT (U/L)	34.8 ± 9.8	38.5 ± 9.5	27.0 ± 1.7	82.0	56.0-159.0 (103)
AST (U/L)	133.0 ± 83.0	119.3 ± 33.0	125.0 ± 39.0	669.0	87.0-187.0 (137)
Globulin (g/dL)	2.7 ± 1.2	2.2 ± 0.4	3.5 ± 0.4	9.0	1.2-1.6 (1.4)
Creatinine	0.4 ± 0.2	0.5 ± 0.4	0.47 ± 0.3	4.8	0.4-0.8 (0.6)

\*Numbers in parentheses denote the average value.

\*\*SD was not calculated because moribund mice made it necessary to pool the samples.

NA: values not available.

Table 3.1: Alterations in blood chemistries following challenge of mice with *Y. pestis* CO92 *via* intranasal inoculation.

The hematology results (Table 3.2) showed an increase in white (WBC) and red blood cells (RBC), and in hemoglobin (Hb) and hematocrit (Hct) levels. Likewise, platelets increased from 276 to 687, 702, and 417 at 0, 36, 48, and 60 h p.i., respectively, while mean platelet volume (MPV) decreased from 15.5 to 5.3-6.7 over the period of infection. These changes in blood cell counts began at 36 h p.i., with maximum changes occurring at 60 h p.i. Further, alterations in blood chemistries and blood cell counts also correlated with the

development of behavioral changes in the infected mice; the animals became listless, hunched up and huddled together at 48-60 h p.i. before eventually dying by 72-96 h after infection.

Test	0 h	36 h	48 h	60 h	Normal Range*
White Blood Cell Count (WBC)	5.4 ± 3.5	5.6 ± 0.6	6.9 ± 0.6	6.9 ± 0.4	1.0-5.0 (3.0)
Red Blood Cell Count (RBC)	6.3 ± 2.7	8.4 ± 0.6	8.9 ± 0.9	9.7 ± 0.2	4.7-6.5 (5.61)
Hemoglobin (Hb)	8.6 ± 4.6	14.1 ± 1.3	14.5 ± 1.1	16.6 ± 0.1	13.0-16.6 (14.8)
Hematocrit (HCT)	31.5 ± 15	39.4 ± 3.2	40.6 ± 3.3	45.2 ± 0.9	38.0-48.0 (43)
Mean Cell Volume (MCV)	49.5 ± 1.8	46.7 ± 2.6	45.5 ± 2.5	46.5 ± 0.1	69.0-85.0 (76)
Mean Cell Hemoglobin (MCH)	13.2 ± 1.6	16.6 ± 0.9	16.3 ± 0.9	17.0 ± 0.3	23.0-29.0 (26)
Mean Cell Hemoglobin Concentration	26.5 ± 2.4	35.7 ± 1.4	35.7 ± 0.7	36.7 ± 0.6	31.0-39.0 (35)
Red Cell Distribution Width (RDW)	17.7 ± 1.3	19.6 ± 0.3	20.0 ± 1.0	19.5 ± 0.1	12.4-27.0 (19.7)
Platelets (PLT)	276.3 ± 131	687.0 ± 55.0	702.2 ± 365.0	417.0 ± 71.0	10.0-14.0 (12)
Mean Platelet Volume (MPV)	15.5 ± 8.0	5.3 ± 0.18	5.9 ± 0.3	6.7 ± 0.3	5.0-20.0 (12.5)

\*Numbers in parentheses denote the average value.

Table 3.2: Alterations in blood counts following challenge of mice with *Y. pestis* CO92 via intranasal inoculation.

### ***HISTOPATHOLOGICAL DATA***

Uninfected control mice had no lesions in the lungs, liver, or spleen (Fig 3.1, Panels A, F, and K, respectively). However, at 12 h p.i. with a 5 LD<sub>50</sub> dose of WT *Y. pestis* CO92 administered by the i.n. route, the bronchial epithelium of mice revealed mild vacuolation with minute amounts of polymorphonuclear leukocytes (PMNs) seen in peribronchial areas, focally, while the liver and spleen did not show any histopathologic changes (data not shown). At 24 h p.i., the lungs revealed a mild infiltration of alveolar septa by PMNs and capillary dilation (data not shown). No histopathologic changes were noticed in the liver, while the lymphoid follicles in the spleen showed mildly increased apoptotic bodies in the germinal centers. At 36 h p.i., the lungs revealed more prominent peribronchial infiltrates



composed of PMNs, accompanied by patchy edema in the alveolar spaces (data not shown). The alveolar septa were also more congested and more heavily infiltrated by PMNs, involving more distal airways, as compared with earlier time points. The liver revealed occasional PMNs and lymphocytes in the sinusoids, while the spleen changes were essentially the same as 24 h p.i.

At 48 h p.i. with WT *Y. pestis* CO92, the lungs (Fig 3.1, Panels B and C) revealed diffuse vascular congestion in alveolar septa with more PMNs in the interstitium, and patchy areas of bronchopneumonia with microabscess formation and necrosis. The liver (Fig 3.1, Panels G and H) revealed the early formation of microabscesses, located randomly in the parenchyma, with focal hepatocyte cell death. The spleen (Fig 3.1, Panel L) showed prominent apoptotic bodies in germinal centers and a more distinct marginal layer in the lymphoid follicles. The red pulp showed mild increases in PMNs. At 60 h p.i., the lungs (Fig 3.1, Panels D and E) revealed extensive pulmonary edema, more extensive bronchopneumonia and visualization of bacterial clumps in the areas of necrosis. Bronchi also showed luminal secretions with PMNs. The liver (Fig 3.1, Panels I and J) showed well-formed microabscesses with necrosis of hepatic parenchyma. The changes in the spleen (Fig 3.1, Panel M) were more prominent than at 48 h.

#### **CHARACTERIZATION OF $\Delta$ LPP MUTANTS OF *YERSINIA* SPECIES**

Compared with the two functional copies of the *lpp* gene in the genome of *S. Typhimurium* (159), Lpp of *Y. pestis* exhibited 89% and 91% identity and homology at the DNA and amino-acid levels, respectively, with LppA of *S. Typhimurium*, while the

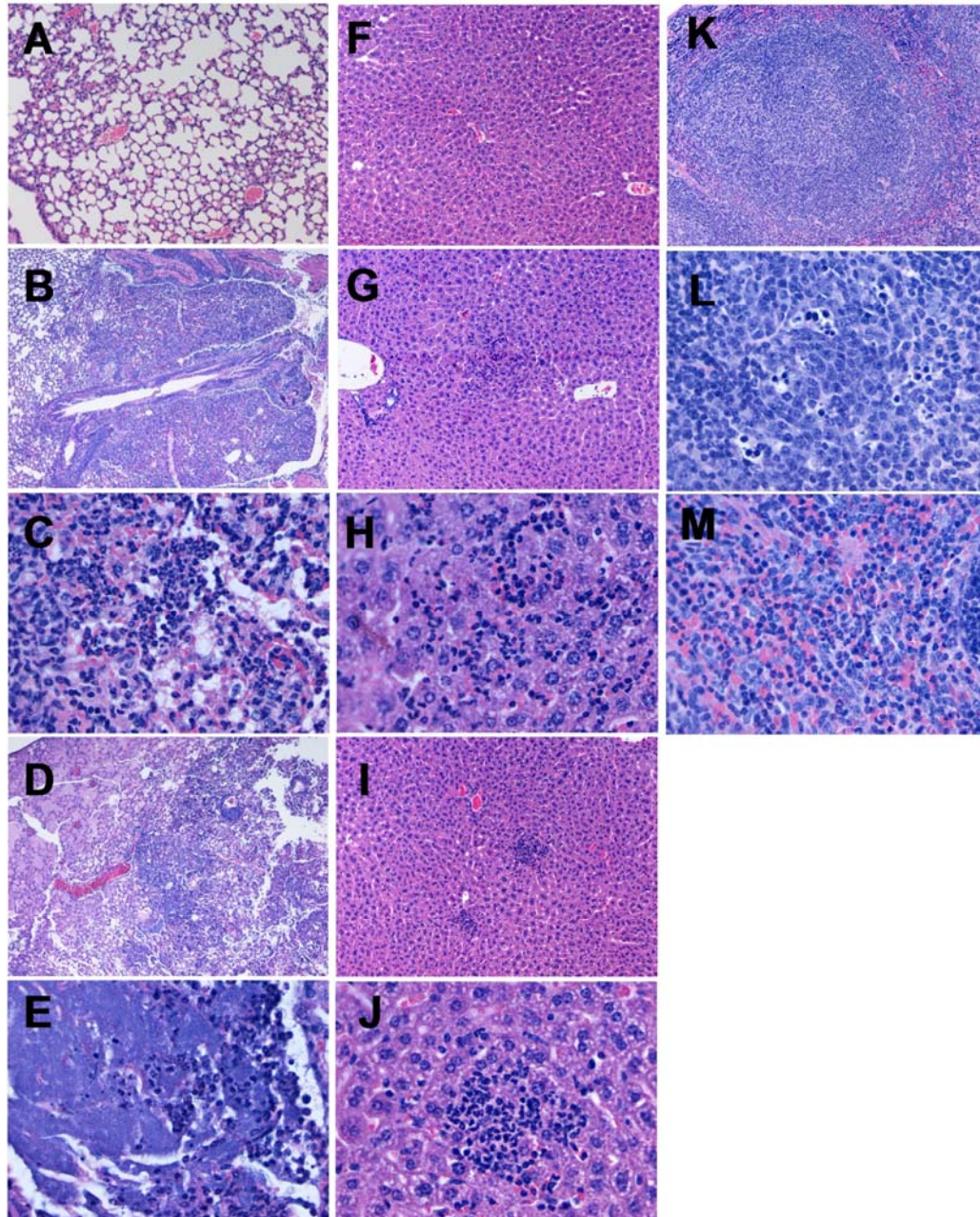


Figure 3.1: Histopathology following i.n. inoculation of mice with WT *Y. pestis* CO92.

Panel A: Control mouse, peripheral section of lung showing thin-walled alveolar spaces, normal vascular structures and indistinct interstitium. Panel B: Section from the lung at 48 h p.i. demonstrating areas of marked

inflammatory infiltrate occupying alveolar spaces around vessels and airways, with focal areas of abscess formation. Panel C: Inflammatory infiltrate at 48 h p.i. in lungs is mostly composed of PMNs. Panel D: Section from the lung at 60 h p.i. showing marked pulmonary edema (left upper corner) and marked inflammatory infiltrate with abscess formation. Panel E: PMNs at 60 h p.i. in lungs are mixed with innumerable bacterial colonies in the background. Panel F: Section of liver from control animal demonstrating normal hepatic cords and sinusoids. Portal triads and central veins are indistinct. Panel G: Section from liver at 48 h p.i. revealing early abscess formation focally in the hepatic parenchyma. Panel H: Focal hepatocyte cell death (shrunken eosinophilic hepatocytes) with PMNs at 48 h p.i.. Panel I: Liver section at 60 h p.i. with focal microabscesses occupying liver parenchyma. Panel J: PMNs and microabscess at high power in liver at 60 h p.i.. Panel K: Section from a normal spleen showing a well-defined germinal center, mantle zone and a normal red pulp. Panel L: Section of spleen at 48 h p.i. demonstrating increased numbers of apoptotic bodies in the germinal center, which is a hallmark of immune activation. Panel M: Section from the spleen at 60 h p.i. demonstrating infiltration of red pulp by PMNs. All sections were stained with hematoxylin and eosin.

corresponding identity and homology were 85% and 84% with LppB of *S. Typhimurium* (Fig 3.2). To study the role of Lpp in the yersiniae infections, we deleted the *lpp* gene from *Y. pestis* KIM/D27 and CO92 strains, as well as from *Y. pseudotuberculosis* YPIII, thus generating  $\Delta lppD27$ ,  $\Delta lppCO92$ , and  $\Delta lpppseudo$  mutants (Table 2.1). Western blot analysis

with anti-Lpp specific antibodies showed that the expression of the *lpp* gene was correspondingly abrogated in the  $\Delta lpp$  mutants, but restored in their complemented strains (Fig 3.3) (159).

*Y. pestis* Lpp                    MNRT-KLVLGAVILA    STMLAG    C    SSNAKIDQ    LSSDVQTLNAKVDQL  
*S. Typhimurium* LppA    MNRT-KLVLGAVILG    STLLAG    C    SSNAKIDQ    LSSDVQTLNAKVDQL  
*S. Typhimurium* LppB    MNRTQQLLGAVVLG    STLLAG    C    SSNAKIDQ    LSSDVQTLSAKVEQL

*Y. pestis* Lpp                    SNDVNAVRADVQAAK    DDAARANQRLDNQAQ    AYKK  
*S. Typhimurium* LppA    SNDVNAVMSDVQAAK    DDAARANQRLDNQAT    KYRK  
*S. Typhimurium* LppB    SNDVNAVMSDVQAAK    DDAARANQRLDNKVF    RICK

Organism	Nucleotide ( <i>lpp</i> )	Amino Acid (Lpp)
<i>Y. pestis</i> <i>lpp</i> (Lpp) <i>S. Typhimurium</i> <i>lppA</i> (LppA)	89%	91%
<i>Y. pestis</i> <i>lpp</i> (Lpp) <i>S. Typhimurium</i> <i>lppB</i> (LppB)	85%	84%
<i>S. Typhimurium</i> <i>lppA</i> (LppA) <i>S. Typhimurium</i> <i>lppB</i> (LppB)	79%	86%

*Y. pestis* KIM/D27 and CO92 *lpp* genes are identical

Figure 3.2: Nucleotide and amino acid sequence identities/homologies between lipoproteins of *Y. pestis* CO92 and *S. enterica* serovar Typhimurium. The N-acyl-S-diacylglycerol lipid modification occurs at the first cysteine residue (boxed) of Lpp. Previous studies from our laboratory indicated two copies of the *lpp* gene in *S. Typhimurium*. The percentage of homologies and similarities between Lpp of *Y. pestis* CO92 and LppA/LppB of *S. Typhimurium* are shown. Underlined letters indicate those amino acid residues that are different in Lpp of *Y. pestis* and *S. Typhimurium*.

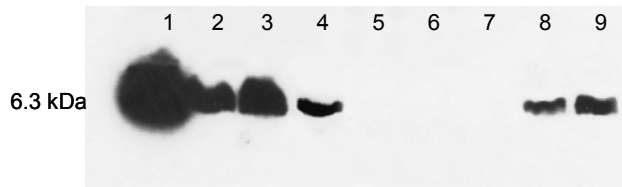


Figure 3.3: Western blot analysis showing the expression of the *lpp* gene in WT yersiniae, *lpp* mutants, and their corresponding complemented strains. Bacteria grown overnight at 26-28°C with shaking (180 rpm) were lysed and separated by SDS-15% PAGE. The proteins were transferred to a nitrocellulose membrane and probed with an anti-Lpp monoclonal antibody (58, 65) as described in the Chapter 2. Lanes 1- 4 represent WT *S. Typhimurium* (positive control) (lane 1); *Y. pseudotuberculosis* (lane 2); *Y. pestis* KIM/D27 (lane 3); and *Y. pestis* CO92 (lane 4). Lanes 5-7 represent the *lpp* isogenic mutants of *Y. pseudotuberculosis* (lane 5); *Y. pestis* KIM/D27 (lane 6); and *Y. pestis* CO92 (lane 7). Lanes 8 and 9 contain the complemented  $\Delta lpp$  mutant strains of *Y. pseudotuberculosis* (lane 8) and *Y. pestis* KIM/D27 (lane 9). The size of Lpp is 6.3 kDa.

#### ISOLATION OF VIRULENCE PLASMIDS AND AMPLIFICATION OF PLASMID-ASSOCIATED VIRULENCE GENES

To further characterize *Yersinia*  $\Delta lpp$  mutants, we performed plasmid isolation and PCR analyses with specific primers for the *lcrV*, *pla* and *cafI* genes encoded on the plasmids

(Table 2.2). There is always a concern that mutagenesis procedures could either result in the loss of plasmids or that a portion of it could be integrated into the chromosome (131). As shown in Fig 3.4, the plasmids harbored in the  $\Delta lpp$  mutant strains were intact and exhibited sizes similar to those seen in their corresponding WT/parental strains (131). As could be noted from lanes 3 and 4, *Y. pseudotuberculosis* harbored only the pYV plasmid, while *Y. pestis* KIM/D27 (lanes 1 and 2) and *Y. pestis* CO92 (lanes 5 and 6) contained two additional plasmids, representing pMT1 and pPCP1. Likewise, we could successfully PCR amplify *lcrV* (981 bp), *pla* (939 bp), and *cafI* (513 bp) genes from the total DNA of *Y. pestis* WT/parental and mutant strains as well as the *lcrV* gene from the WT and the  $\Delta lpp$  mutant of *Y. pseudotuberculosis* (data not shown).

#### TRANSLOCATION OF T3SS EFFECTORS

We detected a similar amount of the secreted form of LcrV in the  $\Delta lpp$  mutants, as compared to the corresponding WT/parental strains of yersiniae by Western blot analysis (data not shown). However, to determine that the T3SS was indeed intact in the  $\Delta lpp$  mutants of yersiniae, we assessed the ability of YopE and YopH effectors to be translocated into HeLa cells. As shown in Fig 3.5, the  $\Delta lpp$  mutants (lanes 3, 7, and 11) delivered a similar amount of Yops (i.e., YopE and YopH) into the cytosol of infected HeLa cells when compared to their corresponding WT/parental strains (lanes 1, 5 and 9). As can also be seen from this figure, minimal levels of YopE and YopH were detected in HeLa cells infected with the WT/parental (lanes 2, 6, and 10) or the  $\Delta lpp$  mutants (lanes 4, 8, and 12) of yersiniae that were not treated with digitonin. These data indicated that we, indeed, measured the translocated effectors, as digitonin lysed the host cells without affecting bacterial cell

integrity. More importantly, the HeLa cells infected with *Yersinia*  $\Delta lpp$  mutant strains exhibited a similar T3SS associated-cytotoxicity, as noted for the HeLa cells infected with the WT/parental *Yersinia* strains and presumably died as a result of apoptosis (Fig 3.6). We examined different MOIs of infection and time of incubation for evaluating cytotoxicity with essentially similar data for the WT/parental versus the mutant strains. These data further confirmed the proper translocation of the T3SS effectors in the  $\Delta lpp$  mutants of yersiniae.

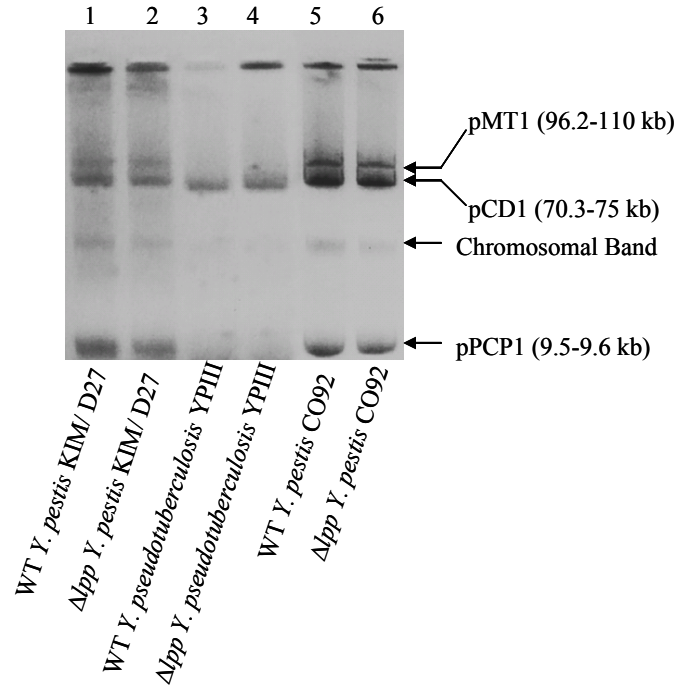


Figure 3.4: Plasmid profiles of various WT/parental yersiniae and their corresponding  $\Delta lpp$  mutant strains. The isolated plasmids were separated by electrophoresis using 0.7% agarose gel and visualized by ethidium bromide staining. Lanes 1 and 2: WT *Y. pestis* KIM/D27 and its  $\Delta lpp$  mutant. Lanes 3 and 4: WT *Y. pseudotuberculosis* YPIII and its  $\Delta lpp$  mutant. Lanes 5 and 6: WT *Y. pestis* CO92 and its  $\Delta lpp$  mutant. Various plasmids harbored by yersiniae are shown.

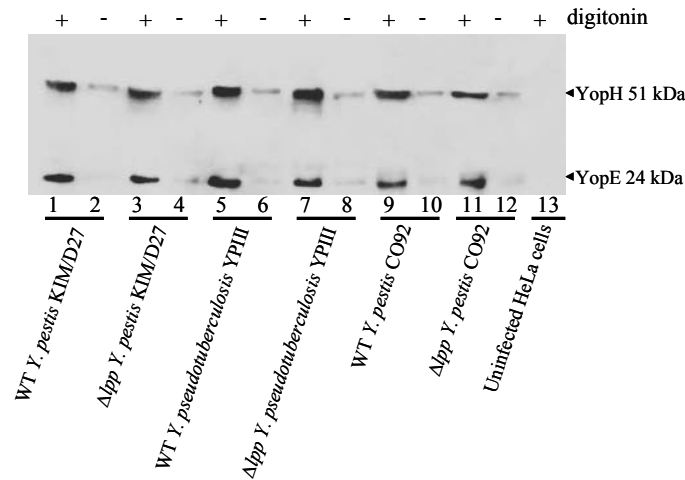


Figure 3.5: Translocation of Yops (YopE and YopH) in HeLa cells infected with various WT/parental yersiniae and their corresponding  $\Delta lpp$  mutant strains. For each *Yersinia* strain, duplicate wells of HeLa cells were used. After a 3-h infection at an MOI of 10, HeLa cells were treated with proteinase K (digesting the extracellularly located Yops), followed by the addition of PMSF (4 mM in PBS) to block the remaining protease activity. One set of HeLa cell cultures was lysed with 1% digitonin (+), while no digitonin was added to the other set (-). The supernatants were collected by centrifugation and subjected to Western blot analyses using antibodies to YopE and YopH. The estimated molecular weights are 24 kDa and 51 kDa for YopE and YopH, respectively. Lanes 1-4: HeLa cells infected with parental *Y. pestis* KIM/D27 and its  $\Delta lpp$  mutant. Lanes 5-8: HeLa cells infected with WT *Y. pseudotuberculosis* YPIII and its  $\Delta lpp$  mutant. Lanes 9-12: HeLa cells infected with WT *Y. pestis* CO92 and its  $\Delta lpp$  mutant. Lane 13: Uninfected HeLa cells were used as a negative



control.

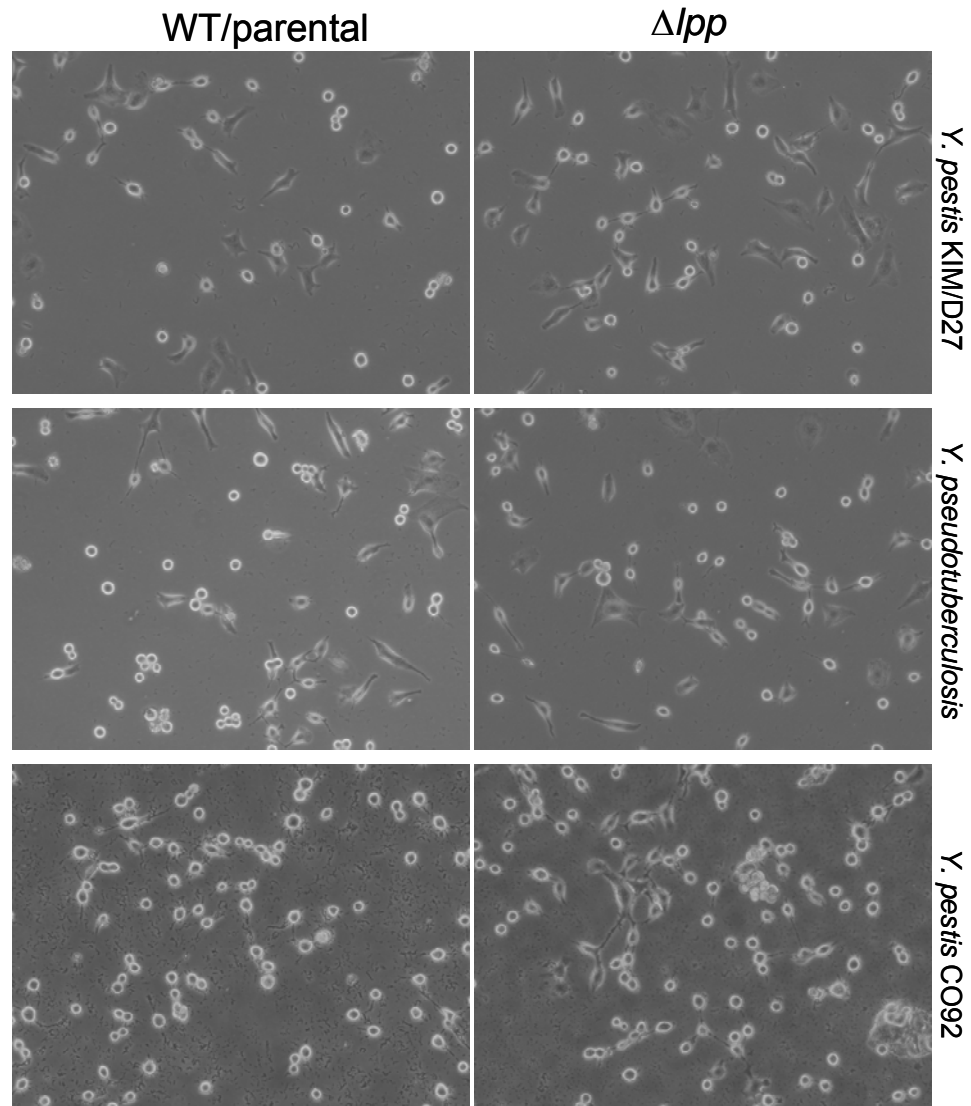


Figure 3.6: Assessment of the cytotoxicities of the various yersiniae. HeLa cells were infected with either WT/parental or  $\Delta/pp$  mutant yersiniae at an MOI of 10 for approximately 3 h. Following this incubation period, the cytotoxicity of the host cells was assessed using light microscopy. At least 8-10 fields were

examined and a typical field is shown. The HeLa were infected with various MOIs and examined over a period of 30 min to 3 h to assess any differences in cytotoxic effects caused by the WT versus  $\Delta lpp$  mutants of yersiniae. Uninfected HeLa cells did not show any toxicity over the course of the experiment (data not shown) whereas approximately 80-90% of the cells treated with WT/parental or its  $\Delta lpp$  mutant died within 3 h.

#### **MEMBRANE INTEGRITY OF THE $\Delta LPP$ MUTANTS VERSUS WT BACTERIA**

We further assessed the integrity of the bacterial membrane in the  $\Delta lpp$  mutants versus WT/parental yersiniae by measuring the release of periplasmic RNase I and  $\beta$ -lactamase, as well as by testing their sensitivity to the detergent TX-100. No obvious differences were noted between WT/parental strains and their corresponding  $\Delta lpp$  mutant strains in any of these assays (data not shown). We then analyzed these  $\Delta lpp$  mutants under the low pH conditions with or without 0.5-2% TX-100 to mimic the harsh environment in the phagosomes and observed a similar survival rate between the  $\Delta lpp$  mutants and their corresponding WT/parental strains (data not shown). These data indicated that the membrane integrity in these *Yersinia*  $\Delta lpp$  mutants was not affected.

#### **BACTERIAL MOTILITY AND INVASION**

Unlike the non-motile bacterium *Y. pestis* (131), the motility of the *Y. pseudotuberculosis*  $\Delta lpp$  mutant was reduced to 59% ( $8.5 \pm 0.7$  mm), compared to its WT bacterium ( $14.5 \pm 2.1$  mm), and this reduction in motility phenotype could be fully

complemented ( $15.5 \pm 0.7$  mm). As we reported previously, the *lppAB* mutant of *S. Typhimurium* had no motility (159), thus correlating with our observation in *Y. pseudotuberculosis*. However, we observed earlier that deletion of the *lpp* genes from *S. Typhimurium* significantly reduced bacterial invasion in the human colonic epithelial cell line T-84 (61, 62, 159), but the invasive capacity of the *Y. pseudotuberculosis*  $\Delta lpp$  mutant remained unaltered, compared to that of the WT bacterium, in both T-84 and HeLa cells (data not shown). These data suggested some diversity in the functions of Lpp in these two related pathogens. In the *Yersinia* model, it is possible that the deletion of Lpp facilitates a susceptibility of these bacteria for destruction by the host cells mechanism moreso than in WT bacteria.

#### **DELETION OF THE *LPP* GENE ATTENUATES THE VIRULENCE OF *Y. PSEUDOTUBERCULOSIS* IN A MOUSE MODEL**

To assess the overall virulence of the  $\Delta lpp$  mutant strain, mice were infected *via* the i.p. route with WT, the  $\Delta lpp$  mutant, and/or the  $\Delta lpp$ -complemented strain of *Y. pseudotuberculosis* YPIII, a *phoP* mutant strain (76), using various doses. As shown in Fig 3.7, all mice inoculated with the highest challenge dose ( $5 \times 10^6$  cfu) of the WT strain and its  $\Delta lpp$  mutant strain died from infection, but a somewhat delayed time to death was observed in the  $\Delta lpp$  mutant-inoculated group. At lower challenge doses of  $1 \times 10^6$  and  $1 \times 10^5$  cfu, consistent and statistically significant, higher survival rates (30-40%) were observed in the  $\Delta lpp$ -infected group compared to the respective WT-infected mice. Further, at the dose of  $1 \times 10^5$  cfu, the mice infected with the complemented strain group had a mortality rate (30%) similar to that of the WT-infected group (40%), while no deaths were observed in the  $\Delta lpp$  mutant-infected mice at this dose, indicating a specific role of Lpp in the virulence of *Y.*

*pseudotuberculosis*.

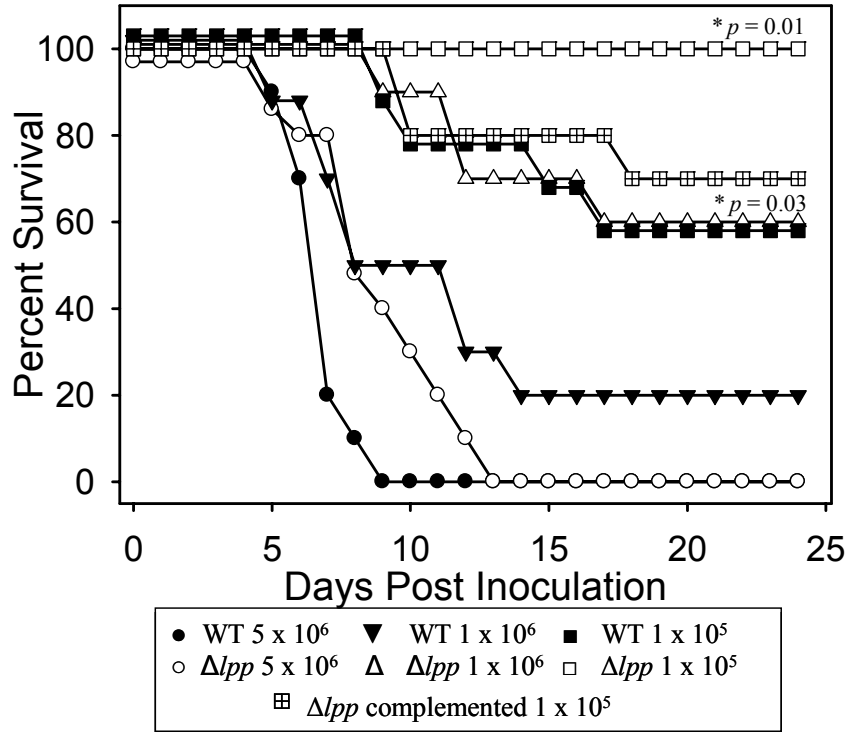


Figure 3.7: The *Y. pseudotuberculosis*  $\Delta lpp$  mutant is less virulent than WT *Y. pseudotuberculosis* in a mouse model. Groups of female Swiss-Webster mice (n=10/group) were infected *via* the i.p. route with various doses of *Y. pseudotuberculosis* strains. The  $\Delta lpp$  mutant was complemented with the corresponding gene using the pBR322 vector. Both the  $\Delta lpp$  mutant and its corresponding WT *Y. pseudotuberculosis* also were transformed with the empty pBR322 vector for this comparative study. \*denotes statistically significant differences in the survival of mice infected with  $\Delta lpp$  mutant over WT bacteria by the Kaplan-Meier survival estimate with log rank analysis. The actual *p*-values are shown on the figure.

## LPP CONTRIBUTES TO THE VIRULENCE OF *Y. PESTIS*

Although *Y. pestis* has evolved from *Y. pseudotuberculosis* (2), the diseases caused by these two bacteria differ tremendously (102). Consequently, we first evaluated the virulence potentials of the parental *Y. pestis* KIM/D27 strain (154), its  $\Delta lpp$  mutant and/or the  $\Delta lpp$ -complemented strain in the mouse model of infection. As shown in Fig 3.8A, Swiss-Webster mice infected by the i.p. route with doses of  $5 \times 10^7$  and  $1 \times 10^8$  cfu of the parental KIM/D27 bacterium died within 5-6 days, while 60% and 100% of the animals inoculated with  $1 \times 10^8$  cfu and  $5 \times 10^7$  cfu of the  $\Delta lpp$  mutant strain, respectively, survived the initial 30 days of observation. Importantly, the complemented  $\Delta lpp$  mutant strain of KIM/D27 was as virulent as the WT bacterium in the mouse model of lethality.

A similar pattern was noticed when BALB/c mice were used for infection (Fig 3. 8B). In this experiment, 100% of the mice from the parental strain-infected groups at the doses of  $5 \times 10^6$  and  $1 \times 10^6$  cfu died, while an 80-100% survival rate was seen in the corresponding  $\Delta lpp$  mutant-infected groups (Fig 3.8B). In the lowest-dose group ( $5 \times 10^5$  cfu), 60% of the mice survived in the parental strain-infected group and 100% in the  $\Delta lpp$  mutant-infected group (Fig 3.8B). Twenty-four to 30 days following the initial inoculation, we rechallenged the survivors (Swiss-Webster [Fig 3.8A] and BALB/c mice [Fig 3.8B]) from both WT and  $\Delta lpp$  mutant groups with a 5 LD<sub>50</sub> dose of the highly virulent WT *Y. pestis* CO92 strain *via* the i.n. route. As could be noted in Figs 3.8A and B, 70-100% of the mice survived rechallenge, indicating that immunity was established in the mice following the initial infection. A group of mice that were given PBS served as an appropriate age-matched control, and these mice were challenged with a 5 LD<sub>50</sub> dose of *Y. pestis* CO92 *via* the i.n. route at the same time immunized mice (with parental or  $\Delta lpp$  mutant KIM/D27) were

subjected to challenge with *Y. pestis* CO92 (Figs 3.8A and B). These control mice showed the usual death curve: 90-100% mortality within 3-4 days.

To confirm the role of Lpp in the virulence of *Yersinia*, an  $\Delta lpp$  mutant of the highly virulent *Y. pestis* CO92 strain was generated. Mice were intranasally challenged with various doses of the WT or  $\Delta lpp$  mutant to mimic pneumonic plague. We could not demonstrate any differences in virulence between the WT and  $\Delta lpp$  mutant of *Y. pestis* CO92 in terms of death rate when tested at doses of  $5 \times 10^2$  and  $5 \times 10^3$  cfu, which represented close to 1 and 10 LD<sub>50</sub> doses (Fig 3.9). These results were not entirely surprising, as the *Y. pestis* CO92 strain is highly virulent and produces many other virulence factors. In an effort to increase the sensitivity of our animal assay for evaluation of virulence factors, we dosed some of the mice with a sub-inhibitory dose of levofloxacin and repeated the challenge study with 1 and 10 LD<sub>50</sub> doses of WT *Y. pestis* CO92 and its  $\Delta lpp$  mutant. The rationale for this experiment was to demonstrate whether Lpp contributes to the bacterial virulence in a pneumonic plague model.

As shown in Fig 3.9, the mice infected with  $\Delta lpp$  mutant bacteria and receiving a sub-inhibitory dose of levofloxacin for 6 days beginning 24 h after infection had significantly higher survival rates -- 100% and 80% -- at the challenge doses of  $5 \times 10^2$  and  $5 \times 10^3$  cfu, respectively. In contrast, animals infected with the WT *Y. pestis* CO92 experienced a higher rate of mortality as 60% and only 10% of the mice infected with  $5 \times 10^2$  and  $5 \times 10^3$  cfu, respectively, survived infection (Fig 3.9) when given the same regimen of the antibiotic treatment.

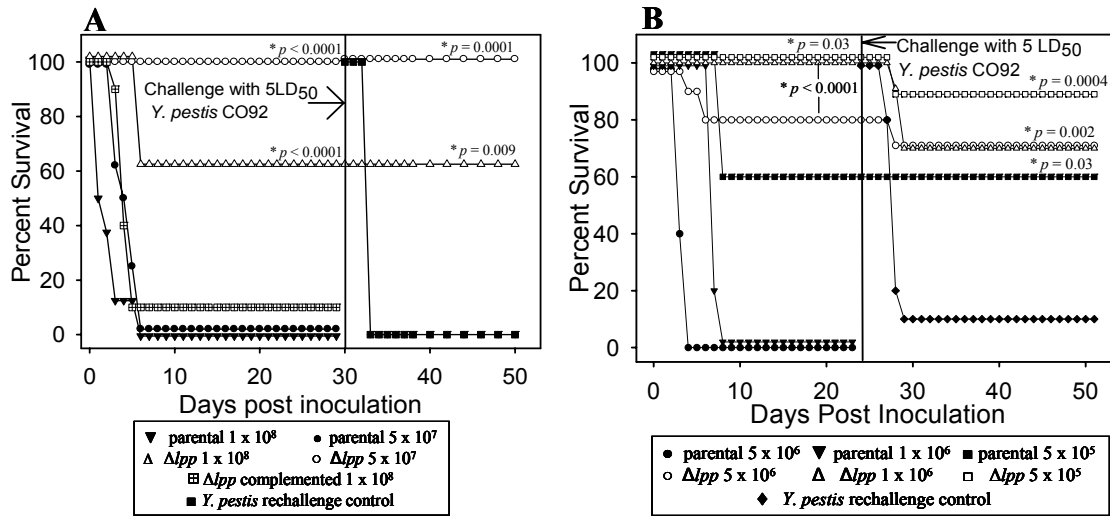


Figure 3.8: Deletion of the *lpp* gene attenuates *Y. pestis* KIM/D27 in the Swiss-Webster (A) and BALB/c (B) mouse models and protects against rechallenge with WT *Y. pestis* CO92. Groups of female Swiss-Webster or BALB/c mice (n=10/group) were inoculated *via* the i.p. route with various doses of *Y. pestis* KIM/D27 strains. The  $\Delta lpp$  mutant was complemented with the corresponding gene using the pBR322 vector. Both the  $\Delta lpp$  mutant and its corresponding parental *Y. pestis* KIM/D27 strain were also transformed with the empty pBR322 vector for this comparative study. Twenty-four to thirty days after initial inoculation, the survivors were challenged *via* the i.n. route with a 5-LD<sub>50</sub> dose of WT *Y. pestis* CO92. \*denotes significant protection as determined by the Kaplan-Meier survival estimate with log rank analysis. The actual *p*-values are shown on the figure.

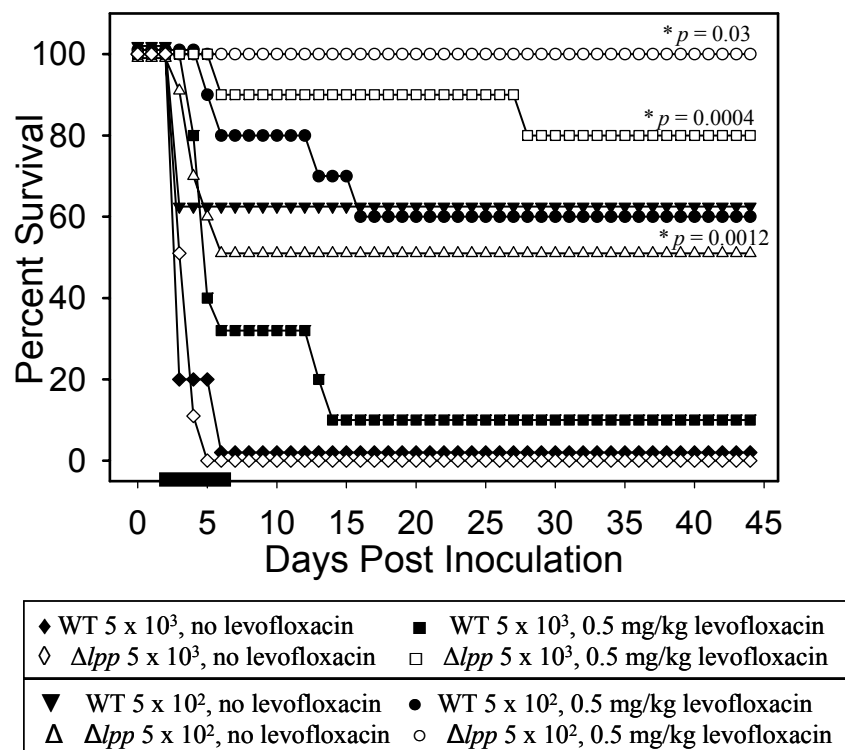


Figure 3.9: A subinhibitory dose of levofloxacin better defines the attenuation of the *Y. pestis* CO92  $\Delta lpp$  mutant. Female Swiss-Webster mice (n=20/group) were inoculated *via* the i.n. route with either  $5 \times 10^3$  cfu or  $5 \times 10^2$  cfu of WT or  $\Delta lpp$  mutant of *Y. pestis* CO92. At 24 h p.i. and for a total of 6 days, half of the mice were given a sub-inhibitory dose (0.3-0.5 mg/kg/day) of the antibiotic levofloxacin (dosing schedule is indicated by the black bar, —). \*denotes statistically significant differences in the survival of mice infected with  $\Delta lpp$  mutant over WT bacteria by the Kaplan-Meier survival estimate with log rank analysis. The actual *p*-values are shown on the figure.



As bubonic plague is most commonly encountered in humans (145), we assessed the role of Lpp in the development of this form of the disease. Mice were subcutaneously challenged with either WT *Y. pestis* CO92 or its  $\Delta lpp$  mutant. Based on the literature and our own studies, the LD<sub>50</sub> of *Y. pestis* CO92 via the s.c. route was between 2.8-9.2 bacteria (131). Therefore, two doses (5 and 20 cfu) were used in this experiment. As shown in Fig 3.10, 30-50% of the mice inoculated with the  $\Delta lpp$  mutant of *Y. pestis* CO92 survived, while only 10% of the mice from the WT-infected group survived 30 days following infection.

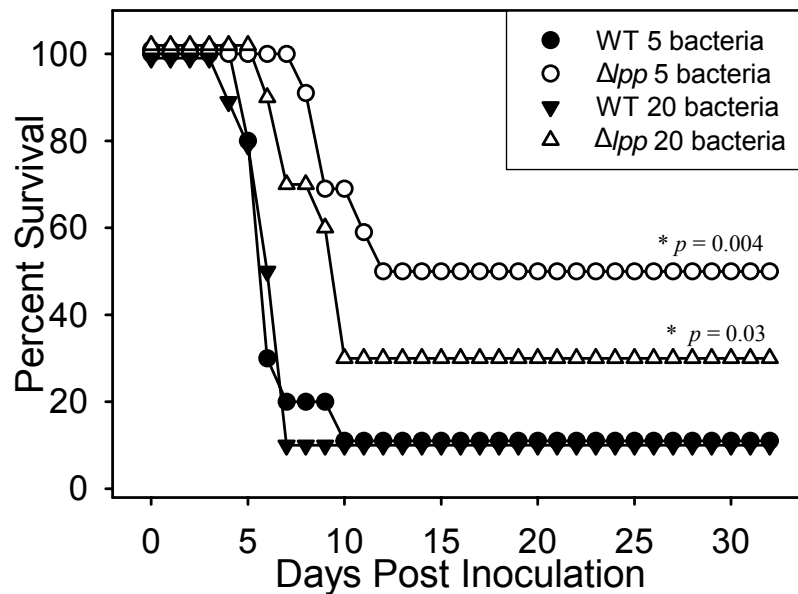


Figure 3.10: Attenuation of the *Y. pestis* CO92  $\Delta lpp$  mutant in BALB/c mice inoculated via the s.c. route to mimic bubonic plague. Mice (n=10/group) inoculated with 5 or 20 cfu of  $\Delta lpp$  mutant of *Y. pestis* CO92 showed higher survival rates than did their WT-infected counterparts. \*denotes statistically significant differences in the survival of mice infected with  $\Delta lpp$  mutant over WT bacteria by the Kaplan-Meier survival estimate with log rank analysis. The actual  $p$ -values are shown on the figure.

As also noted in this study, the mean time to death increased in the  $\Delta lpp$  mutant-versus WT- infected mice. In this set of experiments, no antibiotic treatment was given to the animals. Taken together, these data indicated that Lpp plays a role in the development of both pneumonic and bubonic plague; however, the dose of bacteria or its virulence is critical in discerning the effect of Lpp in overall bacterial virulence attenuation.

#### **HISTOPATHOLOGICAL ANALYSIS OF ANIMAL TISSUES FOLLOWING INTRANASAL INOCULATION WITH WT *Y. PESTIS* CO92 AND ITS $\Delta LPP$ MUTANT**

We compared the differences in histopathology of tissues from the WT *Y. pestis*-infected animals with those infected with the  $\Delta lpp$  mutant at 48 and 72 h p.i. (5 LD<sub>50</sub> dose) in the presence of a sub-inhibitory dose of levofloxacin (Fig 3.11). Uninfected control mice had no significant lesions in the lungs either in the absence (Panel A) or the presence (Panel B) of levofloxacin. At 48 h p.i., all of the WT-infected mice had lesions characteristic of *Y. pestis* infection. We noted mild-to-moderate edema and acute inflammation with masses of bacteria in the lungs of the mice (Panel C, inset at arrow). The livers of the WT-infected mice showed signs of minimal inflammation and necrosis, while the spleens exhibited mild inflammation in the red pulp and lymphoid cell necrosis in the white pulp. No heart lesions were present at 48 h p.i. (data not shown).

Although at 48 h p.i., the animals infected with the  $\Delta lpp$  mutant strain of *Y. pestis* CO92 showed signs of mild-to-moderate inflammation in the lungs (Panel D), there was neither edema nor the presence of masses of bacteria in most of the sections examined and hence these bacteria (which were more dispersed) could not be easily visualized in histopathology pictures, as could be seen in the lungs of WT bacteria-infected mice (Panel C). In the  $\Delta lpp$  mutant-infected mice, we observed minimal liver necrosis, while the red pulp

in the spleen was mildly inflamed, as was also noted in the WT bacteria-infected mice (data not shown). Although lymphoid cell necrosis was noted in the white pulp of the spleen in WT-infected mice, only mild lymphoid depletion was observed in the white pulp of the  $\Delta lpp$  mutant-infected animals. There were no significant lesions in the heart of the  $\Delta lpp$  mutant-infected animals (data not shown).

At 72 h p.i., the mice infected with WT *Y. pestis* CO92 had severe inflammation in the lung and lining surface (pleura) with edema, masses of bacteria (Panel E, inset at arrow) as well as extensive bronchopneumonia. The liver was acutely inflamed, with clumps of bacteria, and necrosis. The red pulp of the spleen was moderately inflamed and had bacteria, and there was lymphoid depletion in white pulp. The heart had low numbers of intravascular bacteria and minimal neutrophilic infiltrates.

Importantly, tissue damage was minimal in mice at 72 h p.i. with the  $\Delta lpp$  mutant of *Y. pestis* CO92. The lungs (Panel F and inset) had essentially normal architecture with no edema, no masses of bacteria (although more dispersed bacteria could be seen under high power magnification, they were not easily visualized in histopathology pictures), or inflammation in most of the sections examined, while the spleen was mildly inflamed. There were no significant lesions consistent with *Y. pestis* infection in the liver or the heart.

#### **HISTOPATHOLOGICAL ANALYSIS OF ANIMAL TISSUES FOLLOWING SUBCUTANEOUS INOCULATION WITH WT *Y. PESTIS* CO92 AND ITS $\Delta LPP$ MUTANT**

Since mice succumbed to infection by days 4-5 after challenge with *Y. pestis* CO92 by the s.c. route (Fig 3.10), we collected tissues at 120 h p.i. from uninfected control mice and animals infected with a 5 LD<sub>50</sub> dose of either WT *Y. pestis* CO92 or its  $\Delta lpp$  mutant (Fig

3.12). The control mice had no significant lesions in any tissue, although data from the spleen are shown in this figure (Panel A). Minimal-to-mild inflammation with neutrophilic infiltrates was observed in the lungs of the mice infected with WT *Y. pestis* CO92. The liver was mildly inflamed and bacteria were present. The spleen showed lymphoid depletion (Panel B, inset at arrow) and, in concert with bacteria (Panel C, at arrow), the red pulp was acutely inflamed and lymphoids were moderately depleted in the white pulp (Panels B and C). These data indicated that systemic infection also damaged the lungs as well as in the liver.

In mice infected with the  $\Delta lpp$  mutant strain of *Y. pestis* CO92, the lungs had minimal-to-mild inflammation with neutrophilic infiltrates. The liver was minimally inflamed and no bacteria were present. The red pulp of the spleen was mildly inflamed and the white pulp had moderate lymphoid depletion, without the presence of bacteria (Panel D and inset).

#### **HISTOPATHOLOGICAL ANALYSIS OF ANIMAL TISSUES FOLLOWING INTRAPERITONEAL INOCULATION WITH PARENTAL *Y. PESTIS* KIM/D27 AND ITS $\Delta LPP$ MUTANT**

Previous studies from our laboratory indicated that 90-100% of the mice inoculated with  $1 \times 10^7$  cfu of the parental strain or the  $\Delta lpp$  mutant of *Y. pestis* KIM/D27 survived the duration of the experiment, which was 21 days (data not shown). Therefore, the tissue sections were subjected to histopathology 7 days p.i..

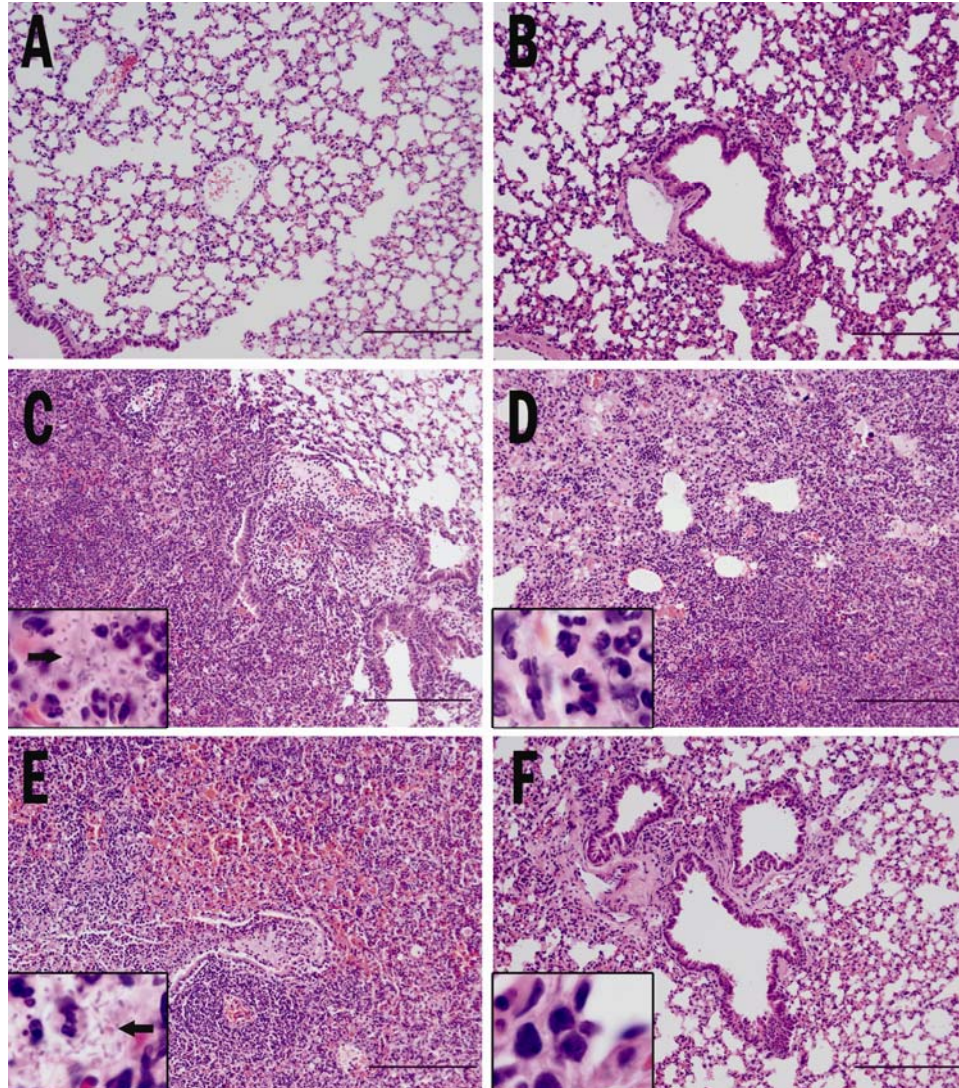


Figure 3.11: Histopathology of the lungs of Swiss-Webster mice infected with either the WT or the  $\Delta lpp$  mutant of *Y. pestis* CO92 *via* the i.n. route. Mice were sacrificed at 48 and 72 h p.i. and the lungs, liver, spleen and heart were immediately harvested. Panel A represents a normal lung from an uninfected mouse that was not given the antibiotic levofloxacin. Panel B represents a normal lung from an uninfected mouse that was given a sub-inhibitory dose of

levofloxacin. At 48 h p.i., mice infected with WT bacteria (Panel C) showed signs of acute inflammation, accompanied by edema and bacteria in the lungs (at arrow in inset), whereas  $\Delta lpp$  mutant-infected mice (Panel D) had acute inflammation without masses of bacteria present in the section shown (inset). At 72 h p.i., mice infected with WT *Y. pestis* CO92 strain (Panel E) also had acute inflammation, accompanied by edema and bacteria in the lungs (at arrow in inset). However, in contrast, no masses of bacteria were present in the lungs of mice infected with *Y. pestis* CO92  $\Delta lpp$  mutant in the section shown, and the tissue appeared normal (Panel F, inset). All sections were stained with H&E. The bar in the photographs represents 200  $\mu\text{m}$ .



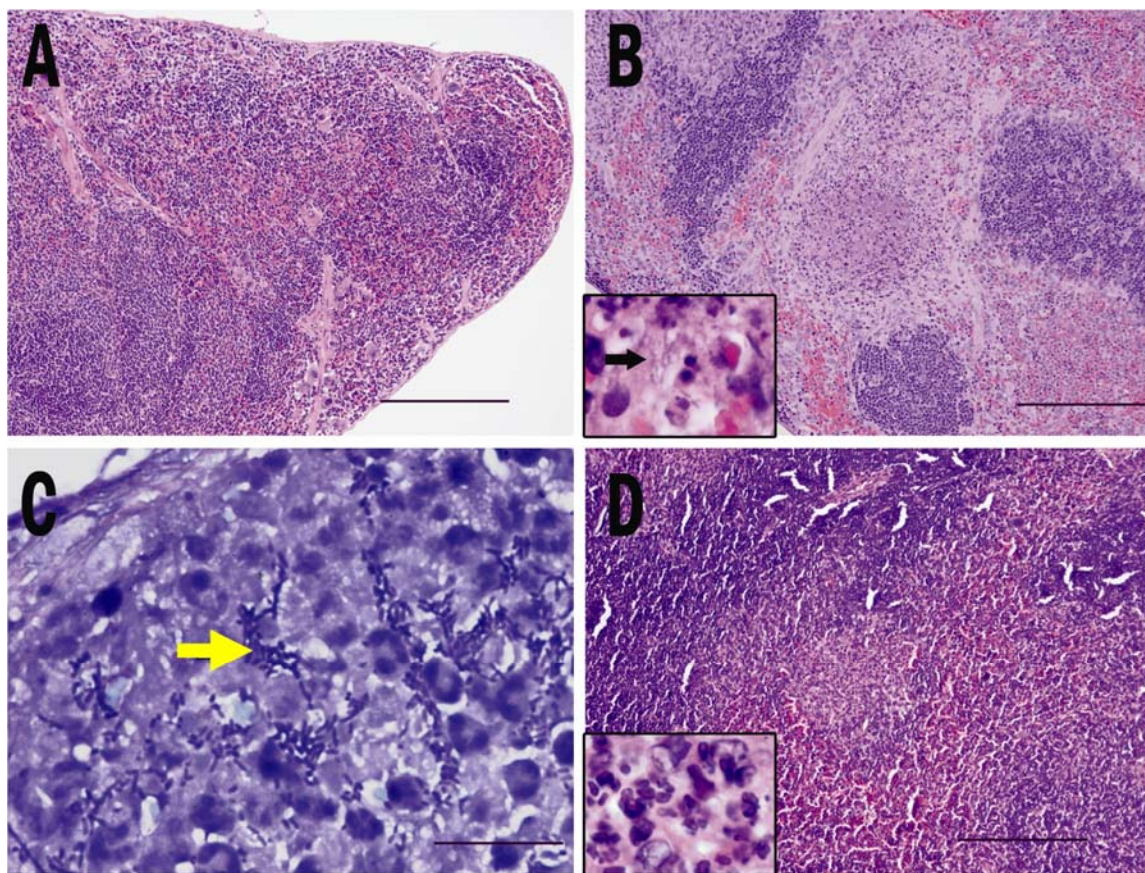


Figure 3.12: Histopathology of the spleens of BALB/c mice 120 h p.i. with either the WT or  $\Delta lpp$  mutant strain of *Y. pestis* CO92 via the s.c. route. Panel A shows the normal spleen of an uninfected mouse. Panel B shows the spleen of a mouse infected with WT *Y. pestis* CO92 strain with signs of acute inflammation and lymphoid depletion. The arrow in the inset photograph points to areas of lymphoid depletion with bacteria present. In Panel C, the bacteria (at arrow) in the spleen at 120 h p.i. with WT *Y. pestis* CO92 are evident using Giemsa stain. The bar represents 20  $\mu\text{m}$ . In Panel D, the spleen of a mouse infected with the  $\Delta lpp$  mutant of *Y. pestis* CO92 had acute inflammation (inset) with

lymphoid depletion but no bacteria were present in the section shown. All sections were stained with H&E except for Panel C as noted. The bar in the photographs (unless otherwise noted) represents 200  $\mu\text{m}$ .

The liver of animals infected with the parental *Y. pestis* KIM/D27 strain showed parenchyma with widespread, poorly formed granulomas composed of activated macrophages, scattered lymphocytes and occasional neutrophils. Sinusoids also revealed increased numbers of inflammatory cells. Under high power magnification, liver granulomas showed macrophages with prominent eosinophilic cytoplasm and nuclei with vesicular chromatin. Likewise, the red pulp in the spleens displayed lymphoid hyperplasia and extensive necrosis with karyorrhectic nuclei (data not shown).

On the contrary, animals infected with the  $\Delta lpp$  mutant of KIM/D27 showed occasional, poorly formed granulomas in the liver. The spleens of  $\Delta lpp$  mutant-infected mice exhibited parenchyma with prominent hematopoiesis, lymphoid hyperplasia, and some infiltration of red pulp by macrophages, but there was a complete absence of necrosis (data not shown). Taken together, these data indicated that the  $\Delta lpp$  mutant of KIM/D27 induced less tissue damage, compared to its corresponding WT bacterium.

### ***IN VIVO* CYTOKINE ANALYSIS**

The rationale for these studies was to assess the role of proinflammatory mediators in host tissue damage after infection with either WT *Y. pestis* CO92 or its  $\Delta lpp$  mutant by the i.n. route at the 5 LD<sub>50</sub> dose. The blood was drawn at various time points (24, 48, 72, and 96 h) after infection and analyzed for cytokine and chemokine production. A key to cytokine



and chemokine abbreviations and acronyms can be found in Table 2.3. When we compared at 24 h p.i., the findings in uninfected controls (given levofloxacin) to infected mice from either group (WT or  $\Delta lpp$  mutant), we saw no significant changes in the levels of cytokines or chemokines (data not shown). At 48 h following infection, elevated levels of TNF- $\alpha$ , IL- $\beta$ , IL-1 $\alpha$ , MCP-1, KC, IL-6 and G-CSF were detected in the WT-infected mice, and these continued to rise until the 96 h time point, except in the case of TNF- $\alpha$  which peaked within the first 48 h and then declined (Table 3.3). The MIP-1 $\beta$  levels remained unchanged until 96 h p.i. (Table 3.3).

In the  $\Delta lpp$  mutant-infected group, considerably lower cytokine and chemokine levels were detected when compared to those in the corresponding WT-infected group. This trend was most obvious at 96 h p.i. (Table 3.3). However, slightly higher levels (although not statistically significant) of KC, G-CSF, and IL-6 were observed in the  $\Delta lpp$  mutant-infected group of mice 48 h p.i. compared to those in WT-infected animals. These levels dropped to lower than those in the WT-infected group at the later time points (72 and 96 h) (Table 3.3). Compared to uninfected control mice, only MCP-1 and G-CSF in the  $\Delta lpp$  mutant-infected group maintained higher levels during the course of infection, while the other tested cytokines and chemokines either increased only at the early time point (48 h p.i.) (e.g., IL-1 $\beta$ , TNF- $\alpha$ , KC, and IL-6) or remained unchanged (MIP-1 $\beta$  and IL-6) up to 96 h p.i. (Table 3.3). These data typified the host response to the more virulent WT *Y. pestis* CO92 strain and generally correlated with host inflammatory responses, resulting in better animal survival following infection with the mutant strain. The other 15 tested cytokines (e.g., IL-10, RANTES, IL-12 p70, GM-CSF among others) were not significantly altered in WT- versus

*Δlpp* mutant-infected mice.

We also measured cytokine/chemokine responses using ELISA in the sera of mice infected *via* the i.p. route with the parental strain of *Y. pestis* KIM/D27 and its *Δlpp* mutant ( $1 \times 10^7$  cfu) on days 1 and 3 after infection. Our data indicated that the levels of IL-6, KC (equivalent of IL-8 in humans), and MCP-1 were much reduced in the sera of animals infected with the *Δlpp* mutant compared to those infected with parental bacterium. Likewise, murine RAW 264.7 macrophages infected with the parental strain of *Y. pestis* KIM/D27 at an MOI of 10 for 6 h, produced much higher levels of TNF- $\alpha$ , IL-1 $\beta$ , IL-6, IL-10, MCP-1, GM-CSF, and G-CSF compared to those in host cells infected with the *Δlpp* mutant as measured by Bio-RAD's Bio-Plex assay (data not shown).

#### **COLONIZATION AND DISSEMINATION OF WT AND $\Delta LPP$ MUTANT OF *Y. PESTIS* CO92 IN MOUSE TISSUES AFTER INTRANASAL CHALLENGE IN THE ABSENCE AND PRESENCE OF LEVOFLOXACIN**

To further investigate *Y. pestis* infection in the context of pneumonic plague, we monitored the growth of both WT *Y. pestis* CO92 and its *Δlpp* mutant in the lungs of infected mice and evaluated the ability of the bacteria to disseminate to the bloodstream and the distal organs (e.g. spleen and liver).

As shown in Table 3.4, *Yersinia* bacilli (both WT and *Δlpp* mutant) were mainly localized at the site of infection (lung tissue) at early time points (1-24 h p.i.), and the number of bacteria recovered from the lungs (1 h p.i. and reported as cfu/g of tissue) was similar to that of bacteria initially used to dose the animals ( $5 \times 10^4$  -  $8 \times 10^4$  cfu). These numbers

Hours post infection	IL-1 $\beta$ *		TNF- $\alpha$ *		IL-1 $\alpha$ *		MIP-1 $\beta$ *	
	WT	$\Delta lpp$	WT	$\Delta lpp$	WT	$\Delta lpp$	WT	$\Delta lpp$
0		BDL <sup>^</sup>	451.6 $\pm$ 149.5		BDL <sup>^</sup>		26.7 $\pm$ 13.6	
48	42.5 $\pm$ 4.9	39.6 $\pm$ 14.7	4288.2 $\pm$ 2462.8 <sup>a</sup>	882.7 $\pm$ 309.1 <sup>a</sup>	61.5 $\pm$ 90.1	BDL <sup>^</sup>	36.7 $\pm$ 24.4	28.8 $\pm$ 5.7
72	BDL <sup>^</sup>	BDL <sup>^</sup>	471.0 $\pm$ 298.4	406.6 $\pm$ 241.3	889.0 $\pm$ 574.3 <sup>b</sup>	9.2 $\pm$ 7.5 <sup>b</sup>	30.7 $\pm$ 10.2	14.9 $\pm$ 7.7
96	178.3 $\pm$ 31.0 <sup>a</sup>	5.6 $\pm$ 9.6 <sup>a</sup>	702.9 $\pm$ 517.5	493.6 $\pm$ 187.4	2658.6 $\pm$ 1197.8 <sup>a</sup>	5.0 $\pm$ 7.1 <sup>a</sup>	191.3 $\pm$ 25.1 <sup>a</sup>	17.8 $\pm$ 9.0 <sup>a</sup>
Hours post infection	MCP-1*		KC*		IL-6*		G-CSF*	
	WT	$\Delta lpp$	WT	$\Delta lpp$	WT	$\Delta lpp$	WT	$\Delta lpp$
0		446.8 $\pm$ 33.7	2.9 $\pm$ 0.5		11.9 $\pm$ 9.4		17.8 $\pm$ 2.8	
48	715.9 $\pm$ 443.0	782.4 $\pm$ 337.1	26.1 $\pm$ 19.6	78.9 $\pm$ 58.3	98.6 $\pm$ 36.8	134 $\pm$ 79.4	796.2 $\pm$ 440.5	1442.5 $\pm$ 41.8
72	769.5 $\pm$ 177.4	533.2 $\pm$ 292.8	34.8 $\pm$ 32.9	5.9 $\pm$ 4.0	170.6 $\pm$ 70.7	26.8 $\pm$ 12.9	5444.9 $\pm$ 1531.9 <sup>a</sup>	128.0 $\pm$ 101.3 <sup>a</sup>
96	7944.8 $\pm$ 700.5 <sup>a</sup>	666.5 $\pm$ 206.0 <sup>a</sup>	1447.6 $\pm$ 689.1 <sup>a</sup>	3.6 $\pm$ 2.0 <sup>a</sup>	1752.0 $\pm$ 590.5 <sup>a</sup>	15.6 $\pm$ 8.8 <sup>a</sup>	9515.8 <sup>**</sup>	78.9 $\pm$ 54.9

\*cytokine and chemokine levels are in pg/mL.

<sup>a, b</sup> denotes  $p < 0.001$ <sup>a</sup> or  $p < 0.01$ <sup>b</sup> (Bonferroni test). Comparisons were made between WT and  $\Delta lpp$  mutant strains of *Y. pestis*.

\*\*standard deviation was not calculated because the second value was out of higher range of the analysis.

<sup>^</sup>BDL: below detectable limit of the assay.

Table 3.3: Changes in the levels of cytokines and chemokines in the sera of mice infected with WT or the  $\Delta lpp$  mutant of *Y. pestis* CO92 intranasally.

decreased by 1 log 24 h p.i. in WT-infected mice, but remained stable in  $\Delta lpp$  mutant-infected mice. At 48 h p.i. no significant bacterial multiplication was noted in the lungs in both the WT- and  $\Delta lpp$ -mutant infected mice; however, the bacilli (both WT and  $\Delta lpp$  mutant) started to spread to the livers, but not to the spleens. Interestingly, bacilli were detected in the bloodstreams of mice infected only with WT *Y. pestis* CO92, but not with its  $\Delta lpp$  mutant strain (Table 3.4). At 72 h p.i., the number of bacteria observed in lungs increased by 1 log in both the WT- and  $\Delta lpp$  mutant-infected groups, compared to the levels seen at early time points (1-24 h p.i.) (Table 3.4). All of the livers from infected mice (both the WT and  $\Delta lpp$  mutant groups) were infiltrated with a substantial number of bacteria. In the WT-infected group, bacilli were also detected in spleens and the bloodstream. However, there were no detectable bacteria in the blood or spleen of  $\Delta lpp$  mutant-infected mice (Table 3.4). These data, thus, indicated an impaired ability of the  $\Delta lpp$  mutant for broad dissemination in the mice.

We also noted the overall bacterial replication and dissemination to be very similar between the levofloxacin-treated groups of mice and those left untreated with levofloxacin. Moreover, the  $\Delta lpp$  mutant of *Y. pestis* CO92 multiplied in a manner similar to that of its WT bacterium in mice that were given the sub-inhibitory dose of levofloxacin (Table 3.4). These data suggested a similar antibiotic susceptibility of both the WT and its  $\Delta lpp$  mutant of *Y. pestis* CO92 *in vivo* and agreed with our *in vitro* levofloxacin susceptibility data, as evaluated by using the E-Test, in which both WT *Y. pestis* CO92 and its  $\Delta lpp$  mutant exhibited a similar MIC of 0.032  $\mu\text{g/ml}$ .

Hours post infection	Treatment Group <sup>b</sup> (No Levofloxacin)	Plate Count cfu/g of Tissue or cfu/ml of Blood <sup>a</sup>			
		Lung	Liver	Spleen	Blood
1	WT <i>Y. pestis</i> CO92	2.7 x 10 <sup>5</sup> (2.3 x 10 <sup>5</sup> - 3.2 x 10 <sup>5</sup> )	ND	ND	ND
	$\Delta$ <i>lpp</i> <i>Y. pestis</i> CO92	2.3 x 10 <sup>5</sup> (2.1 x 10 <sup>5</sup> - 2.6 x 10 <sup>5</sup> )			
24	WT <i>Y. pestis</i> CO92	2.4 x 10 <sup>4</sup> (2.0 x 10 <sup>4</sup> - 3.8 x 10 <sup>4</sup> )	Undetected	Undetected	Undetected
	$\Delta$ <i>lpp</i> <i>Y. pestis</i> CO92	3.1 x 10 <sup>5</sup> (1.7 x 10 <sup>5</sup> - 5.0 x 10 <sup>5</sup> )	3.1 x 10 <sup>4</sup> (2/3)** (1.4 x 10 <sup>4</sup> - 4.8 x 10 <sup>4</sup> )		
48	WT <i>Y. pestis</i> CO92	2.7 x 10 <sup>5</sup> * (1.8 x 10 <sup>4</sup> - 5.2 x 10 <sup>5</sup> )	1.0 x 10 <sup>4</sup> * (2/3)** (1.8 x 10 <sup>3</sup> - 1.8 x 10 <sup>4</sup> )	Undetected	4.3 x 10 <sup>3</sup> (2/3)** (1.0 x 10 <sup>3</sup> - 7.5 x 10 <sup>3</sup> )
	$\Delta$ <i>lpp</i> <i>Y. pestis</i> CO92	4.1 x 10 <sup>4</sup> * (1.3 x 10 <sup>4</sup> - 8.7 x 10 <sup>4</sup> )	3.1 x 10 <sup>3</sup> * (1.2 x 10 <sup>3</sup> - 4.5 x 10 <sup>3</sup> )	Undetected	Undetected
72	WT <i>Y. pestis</i> CO92	2.3 x 10 <sup>6</sup> * (7.1 x 10 <sup>5</sup> - 4.2 x 10 <sup>6</sup> )	7.8 x 10 <sup>5</sup> * (9.7 x 10 <sup>4</sup> - 2.1 x 10 <sup>6</sup> )	4.6 x 10 <sup>5</sup> (6.3 x 10 <sup>3</sup> - 1.3 x 10 <sup>6</sup> )	2.1 x 10 <sup>6</sup> (2/3)** (1.0 x 10 <sup>5</sup> - 4.0 x 10 <sup>6</sup> )
	$\Delta$ <i>lpp</i> <i>Y. pestis</i> CO92	3.2 x 10 <sup>6</sup> * (2.4 x 10 <sup>4</sup> - 7.4 x 10 <sup>6</sup> )	2.8 x 10 <sup>5</sup> * (5.0 x 10 <sup>3</sup> - 6.6 x 10 <sup>5</sup> )	Undetected	Undetected
Hours post infection	Treatment Group <sup>b</sup> (Levofloxacin, 0.3-0.5 mg/kg/day)	Lung	Liver	Spleen	Blood
		Lung	Liver	Spleen	Blood
48	WT <i>Y. pestis</i> CO92	1.4 x 10 <sup>4</sup> * (6.1 x 10 <sup>3</sup> - 2.1 x 10 <sup>4</sup> )	6.4 x 10 <sup>3</sup> * (1.1 x 10 <sup>3</sup> - 1.2 x 10 <sup>4</sup> )	Undetected	1.3 x 10 <sup>3</sup> (2/3)** (1.0 x 10 <sup>3</sup> - 1.5 x 10 <sup>3</sup> )
	$\Delta$ <i>lpp</i> <i>Y. pestis</i> CO92	2.3 x 10 <sup>5</sup> * (6.1 x 10 <sup>4</sup> - 3.2 x 10 <sup>5</sup> )	1.3 x 10 <sup>3</sup> * (1.2 x 10 <sup>3</sup> - 1.3 x 10 <sup>3</sup> )	Undetected	Undetected
72	WT <i>Y. pestis</i> CO92	2.3 x 10 <sup>6</sup> * (1.9 x 10 <sup>4</sup> - 5.0 x 10 <sup>6</sup> )	1.2 x 10 <sup>5</sup> * (2.0 x 10 <sup>4</sup> - 1.6 x 10 <sup>5</sup> )	3.4 x 10 <sup>3</sup> (2/3)** (1.0 x 10 <sup>3</sup> - 5.9 x 10 <sup>3</sup> )	2.0 x 10 <sup>2</sup> (1/3)**
	$\Delta$ <i>lpp</i> <i>Y. pestis</i> CO92	2.3 x 10 <sup>5</sup> * (1.7 x 10 <sup>3</sup> - 6.7 x 10 <sup>5</sup> )	4.0 x 10 <sup>5</sup> * (7.1 x 10 <sup>2</sup> - 1.2 x 10 <sup>6</sup> )	Undetected	Undetected

<sup>a</sup>3 mice per treatment group were dosed *via* the i.n. route with 5 x 10<sup>4</sup> cfu of *Y. pestis* CO92 (WT or  $\Delta$ *lpp* mutant). Plate counts are reported as averages with ranges in parentheses.

<sup>b</sup>Treatment group indicates whether mice were given WT or  $\Delta$ *lpp* mutant bacteria and if a sub-inhibitory dose of levofloxacin (0.3-0.5 mg/kg/day) was administered beginning 24 h p.i..

ND: At 1 h p.i., bacterial counts were not determined in any tissue other than the lungs.

\*Statistically similar averages between WT and  $\Delta$ *lpp* treatment groups at individual time points as determined by student's *t*-test (*p* > 0.05).

\*\*The range of bacterial counts represents data from all 3 mice unless otherwise indicated. In such cases, the remaining animals were negative for bacterial counts.

Table 3.4: Quantitative analysis of selected organs for bacterial counts from mice infected with WT or  $\Delta$ *lpp* mutant of *Y. pestis* CO92.

## INTRACELLULAR SURVIVAL OF WT *Y. PESTIS* CO92 AS COMPARED TO ITS $\Delta LPP$ MUTANT *IN VITRO*

In the initial experiment, the bacteria were grown at 28°C prior to infection of macrophages. We observed occurrence in macrophages of nearly a 100% rate of invasion/phagocytosis of both WT bacteria and its  $\Delta lpp$  mutant (42). From 0 to 4 h p.i., the number of WT bacteria within the macrophages increased slightly from  $3.0 \times 10^6$  to  $3.6 \times 10^6$  cfu (Fig. 3.13). On the contrary, the number of  $\Delta lpp$  mutant bacteria within the macrophages decreased from  $3.5 \times 10^6$  to  $1.8 \times 10^6$  cfu/ml ( $p < 0.05$ ) at this time point. At 8 h p.i., the host cells were still viable as assessed by light microscopy, and there was no obvious change in the numbers of viable bacteria (WT or its  $lpp$  mutant) measured in the macrophages. The difference between the number of WT ( $3.1 \times 10^6$  cfu/ml) and  $\Delta lpp$  mutant bacteria ( $1.7 \times 10^6$  cfu/ml) measured, however, was statistically significant at this time point ( $p < 0.05$ ).

By 24 h p.i., the host cells still seemed healthy and adhered to the wells of the tissue culture plate. However, the number of viable  $\Delta lpp$  mutant bacteria decreased by a log to  $2.8 \times 10^5$  cfu/ml between 8 and 24 h p.i., in comparison to the numbers of WT bacteria, which were  $2.2 \times 10^6$  cfu/ml ( $p < 0.01$ ) and decreased only marginally between the 8 and 24 h time points. These data indicated that, although both the WT and mutant bacteria were phagocytosed equally, the intracellular viability of bacteria was significantly affected, with the  $\Delta lpp$  mutant dying off rapidly compared to its WT counterpart. This is not surprising because Lpp is a protein that functions in the stability of the bacterial outer membrane. Its deletion does not affect its stability under stressful growth conditions such as low pH and in the presence of detergents. Instead, the deletion of Lpp may be more important in how resilient the bacterium is against the host defenses. Importantly, neither the WT nor its  $\Delta lpp$

mutant increased in number under the tested conditions in macrophages. Essentially, a similar trend was seen when the bacteria were grown overnight at 37°C (data not shown) instead of at 28°C before infection of macrophages. Because the production of the antiphagocytic capsule and Yops was induced at 37 °C, the percentage of phagocytosis by macrophages decreased to 20% for both the WT and its  $\Delta lpp$  mutant. Finally, we also showed that the intracellular survival of the *Y. pestis* KIM/D27  $\Delta lpp$  mutant was reduced by 50% when compared to the WT bacterium in macrophages 4 h p.i.. Importantly, we could fully complement the survival defect in macrophages when the corresponding gene was supplied to the  $\Delta lpp$  mutant *in trans* (data not shown). For this experiment, various bacterial strains were grown at 28°C and the infection of macrophages occurred at 37°C.

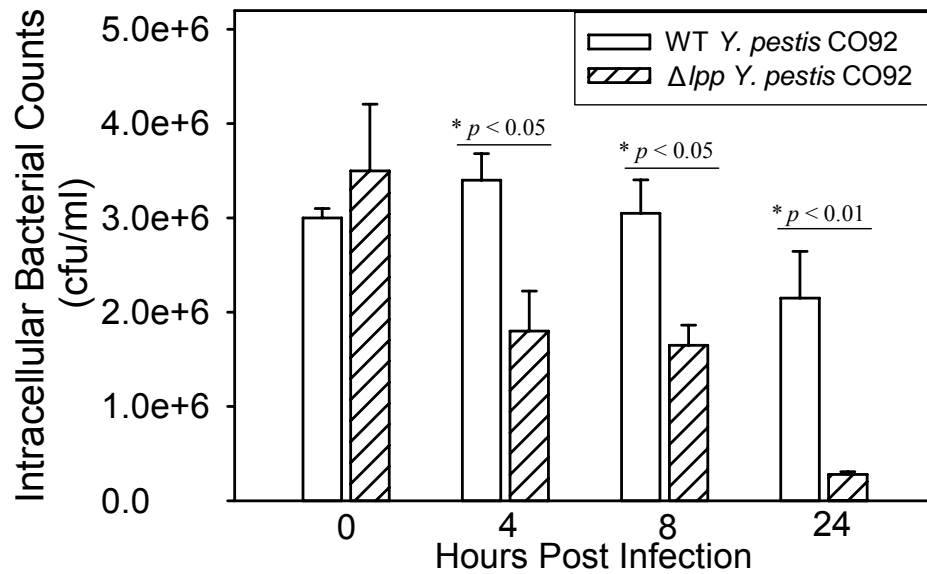


Figure 3.13: Comparison of the survival of the WT or the  $\Delta lpp$  mutant of *Y. pestis* CO92 in murine macrophages. Intracellular survival of 28°C-grown WT and the  $\Delta lpp$

mutant for *Y. pestis* CO92 were assessed at various times by infecting RAW 264.7 murine macrophages for 30 min, followed by gentamicin treatment for 1 h to kill the extracellular bacteria. The decline in the numbers of WT bacteria was gradual over a 24-h period, whereas the decrease in the numbers of  $\Delta lpp$  mutant bacteria was significantly greater, as determined by ANOVA with Bonferroni correction. \*denotes statistically significant differences in the survival of WT bacteria over  $\Delta lpp$  mutant bacteria. The actual *p*-values are shown on the figure.

### ***Discussion***

Currently, pathogenic mechanisms underlying the development of plague are understudied, and the host's response to the infection is largely unexplored. We have provided here, for the first time, detailed analyses of the blood chemistries and blood cell counts during the course of the development of pneumonic plague in mice with *Y. pestis* CO92 strain. Increases in WBC, RBC, Hb, and Hct indicated overwhelming bacterial infection, the loss of fluid following organ failure, and a breach in blood vessel integrity. Furthermore, alterations in platelets and MPV suggested abnormal blood coagulation that would eventually lead to disseminated intravascular coagulation and extensive hemorrhage, which are hallmarks of severe bacterial infection (145). Changes in tissue histopathology were also observed in multiple organs of mice infected *via* the i.n. route, and the lungs were the first and most severely affected tissue. Respiratory failure, as a result of severe congestion and edema in the lungs, was believed to be the main cause of death in mice with pneumonic plague. However, multi-organ failure would occur if animals survive long



enough, as bacteria could be seen in the liver, spleen and in the bloodstream.

It has been reported that mice with pneumonic plague develop a striking biphasic syndrome in which the infection begins with an anti-inflammatory state in the first 24-36 h that rapidly progresses to a highly proinflammatory state by 48 h and death by 3 days (36, 109). Our observations are in agreement with these earlier findings. The asymptomatic state of infection in the first 24-36 h was thought to be likely because of the potent anti-inflammatory activity of the pCD1-based T3SS (109, 126). However in our studies and in those of others, IL-10 (an anti-inflammatory cytokine) levels were not elevated in *Y. pestis*-infected mice (109), and the most recent study has shown that *Y. pestis* LcrV does not efficiently activate TLR-2 signaling. Therefore, the TLR-mediated immunomodulation is unlikely to play a significant role in plague (139).

In searching for new virulence factors and virulence-associated mechanisms in yersiniae, we focused on a 6.3-kDa Lpp (61, 62, 159). We noted that the membrane integrity and T3SS in the yersiniae  $\Delta lpp$  mutants were not affected, and virulence plasmids in the yersiniae  $\Delta lpp$  mutants were normally maintained. Compared to WT *Y. pseudotuberculosis*, we observed that its  $\Delta lpp$  mutant had reduced motility and was significantly less virulent in a mouse model of infection. We obtained similar results with the *S. Typhimurium*  $\Delta lpp$  mutants (159). It has been reported that the non-motile *Salmonella* (i.e., the flagellar mutants) were less virulent in mice (34), while the pathogenicity of *Y. enterocolitica* was not affected in a flagellar mutant ( $\Delta fliA$ ) (97). Therefore, the exact mechanism(s) by which the  $\Delta lpp$  mutant of *Y. pseudotuberculosis* was attenuated needs to be further explored.

In *Y. pestis*, deletion of the *lpp* gene from the KIM/D27 background strain further attenuated its virulence, but surprisingly no obvious difference in the pathogenicity was

observed between the WT and  $\Delta lpp$  mutant strains of CO92 in a pneumonic plague mouse model. Interestingly, when groups of mice infected with either WT CO92 or its  $\Delta lpp$  mutant were given a sub-inhibitory dose of levofloxacin, we observed a significantly higher survival rate, less severe histopathological changes, and reduced cytokine and chemokine levels in the  $\Delta lpp$  mutant-infected group, compared to these parameters in the WT-infected mice. These above-mentioned differences were not due to variation in the susceptibility of WT and the  $\Delta lpp$  mutant to the antibiotic, as we observed similar bacterial loads in the lungs and liver at 48 and 72 h p.i. in both groups. Furthermore, our *in vitro* susceptibility assessment also revealed no detectable differences to the effect of levofloxacin between the WT and its  $\Delta lpp$  mutant.

The mechanism of attenuation elicited by the  $\Delta lpp$  mutant under levofloxacin treatment in *Y. pestis* CO92 is not clear. However, levofloxacin is a fluoroquinolone antibiotic that inhibits bacterial DNA replication and transcription. Therefore with the sub-inhibitory dose of the antibiotic, we might have reduced the number of bacteria to a critical threshold level that would allow us to better discern the contribution of Lpp to bacterial virulence. It has also been reported that the sub-inhibitory dose of fluoroquinolones inhibits the adherence of uropathogenic *E. coli* strains *in vitro* (15). Therefore, it is possible that *Y. pestis*, under the treatment of levofloxacin, might have a similar post-antibiotic effect in that the virulence of both the WT and its  $\Delta lpp$  mutant was reduced.

Importantly, in the bubonic plague mouse model, we clearly demonstrated attenuation of the  $\Delta lpp$  mutant of *Y. pestis* CO92. In fact, the histopathological data indicated that the mutant bacteria cleared from the system, resulting in less severe pathology in the tissue and

better survival of the animals. In contrast, the WT bacteria persisted in the tissues longer, resulting in severe pathology and in animals succumbing to infection.

Interestingly, in the pneumonic plague model, we observed that WT *Y. pestis* CO92 appeared in the bloodstream of infected mice 48 h p.i. and in the spleen and blood 72 h p.i.. However, the  $\Delta lpp$  mutant could not be detected in the spleens or the bloodstream, indicating that the ability of the  $\Delta lpp$  mutant to disseminate was impaired. In addition, although the number of mutant bacteria increased in the lungs 72 h p.i., the tissues appeared normal, indicating an important role of Lpp in inducing histopathological changes. In corroboration with these data, we also demonstrated reduced cytokine/chemokine responses in the sera of mice infected with the  $\Delta lpp$  mutant of both *Y. pestis* CO92 and KIM/D27, compared to that in the WT/parental strain-infected mice.

Additionally, we found that the liver was the most susceptible organ for the colonization of *Y. pestis* when given by the i.n. route as bacteria were detected in the liver between 24-48 h p.i. in both WT- and  $\Delta lpp$  mutant-infected groups of mice. The susceptibility of the liver may be due to its relatively larger physical size and anatomic position; however, the existence of receptor(s) on liver cells that preferentially recruit the bacilli cannot be ruled out. Unlike the liver, the colonization of *Y. pestis* in the spleen only happened at later stages of infection (72 h p.i.) in the WT-infected group of mice. This differs from a recent report stating that *Yersinia* bacilli were detected in the spleen as early as the 36 h p.i. (109), but this divergence may be due to the amounts of the challenge dose, the use of a different strain of mouse (out-bred Swiss-Webster versus in-bred C57BL/6), or by differences in growth conditions during preparation of the inoculum (e.g., 26°C versus 37°C) (102).

Much reduced tissue pathology, decreases in cytokine and chemokine levels, and limited dissemination of the  $\Delta lpp$  mutant, compared to the WT *Y. pestis* CO92, led us to investigate the ability of these mutants to survive *in vitro* in the intracellular environment of murine macrophages. Although it is clear that most yersiniae replication occurs extracellularly, there is evidence suggesting that all three pathogenic *Yersinia* species survive and multiply in macrophages (38, 48, 141, 142). The ability of yersiniae to proliferate in macrophages not only provides a replicative niche for the bacteria, while they are protected from neutrophils, but also allows *Yersinia* to avoid antigen presentation and, therefore, delays the development of a specific immune response. Finally, macrophages may provide the bacterium with a vehicle for safe transport from the initial site of infection to deeper lymph tissues (142).

Based on our data, significantly fewer numbers of  $\Delta lpp$  mutant bacteria were present within macrophages 24 h p.i. when compared to the number of WT bacteria. This correlated well with our bacterial dissemination data, in which the  $\Delta lpp$  mutant displayed an impaired ability to disseminate to the bloodstream and spleens of infected mice. Therefore, the mechanism of attenuation of the *Y. pestis*  $\Delta lpp$  mutant may be due to its inability to survive within the hostile macrophage environment. Data presented in our study indicated that the  $\Delta lpp$  mutant had no obvious defect in T3SS function but such mutants exhibited a defect in intracellular survival in macrophages. These results correlated with a previous study that indicated that the T3SS played no significant role in this niche (141).

Finally, the primary difference between *Y. pestis* KIM/D27 and CO92 strains is the presence of an additional iron transport system (yersiniabactin system) in CO92. Since the  $\Delta lpp$  mutant of KIM/D27 showed a significant defect in virulence compared to that of its

parental strain, while the virulence of the CO92  $\Delta lpp$  mutant *via* the intranasal route was essentially identical to that of the WT CO92 strain, it seems possible that the  $\Delta lpp$  mutant may affect iron transport in some manner and this possibility will be explored further.

We did not observe an increased number of viable bacteria during the course of infection, even in the WT-infected macrophages, unlike in other studies (42, 98, 170, 171). This discrepancy may be due to the fact that yersiniae, when growing intracellularly, form tight aggregates that are not easily dispersed, resulting in an underestimation of bacterial numbers (141, 142). The exact mechanism by which Lpp affects the survival of *Y. pestis* in the macrophages is not clear; however, earlier studies indicated that PhoP, a response regulator of the two-component PhoP/PhoQ sensory transduction system, is involved in regulating one or more genes important for the intracellular survival of *Y. pestis* in macrophages (60, 80, 129). Therefore, it is possible that the expression of the *lpp* gene in *Y. pestis* is under the control of PhoP or vice-versa. Our future studies will focus on investigating the mechanism of preferential intracellular killing of the  $\Delta lpp$  mutant compared to the WT bacteria in macrophages.

Although *Y. pestis* and *Y. pseudotuberculosis* are genetically related bacilli, the diseases they cause are different. We showed that deletion of the *lpp* gene from either the *Y. pseudotuberculosis* YPIII or the *Y. pestis* strains attenuated their virulence. However, *Y. pseudotuberculosis* YPIII is a *phoP* mutant strain and hence is unable to grow in macrophages (76) unlike *Y. pestis*. Therefore, Lpp might be attenuating these species of yersiniae by different mechanism(s) and this possibility needs further study.

In comparison to plasmid-encoded virulence determinants (i.e., the T3SS), the contribution of the chromosomally encoded Lpp in the virulence of yersiniae is subtle;

however, it provides an interesting insight into the complex mechanism of *Yersinia* pathogenesis. To our knowledge, this is the first systematic study illustrating the role of Lpp in the pathogenesis of yersiniae infections. Currently, there is no vaccine licensed in the United States against plague. Although recent studies have indicated that the subunit vaccines containing *Y. pestis* antigens (e.g. LcrV and F1) have immunogenic properties in mice and macaques (50, 183, 190) and appear very promising, the effectiveness of these subunit vaccines against human pneumonic plague transmission has not yet been determined (135).

Until 1999, a formaldehyde-killed, whole cell vaccine, prepared using a highly virulent *Y. pestis* strain 195/P, was used for military personnel, but its production was halted because of severe side effects and of its short-lived protection in humans (151). In addition, the above-mentioned vaccine provided protection against bubonic, but not against pneumonic plague. Although the use of a live attenuated plague vaccine is not approved in the U.S. and many other countries because of safety reasons (172), a *pgm* locus-minus mutant of *Y. pestis* strain EV76 has been used in the countries of the former Soviet Union (173). This vaccine was found to be effective against both bubonic and pneumonic plague (64, 152). However, most of these EV76 derivatives can cause severe local and systemic reactions and gross tissue changes independent of their route of inoculation, thus limiting their use worldwide (173).

In an effort to further attenuate *Y. pestis* EV76, the *lpxM* gene (encoding lipid A myristoyl transferase) was deleted, and the generated  $\Delta lpxM$  mutant synthesized a less toxic penta-acylated LPS, compared to the more toxic hexa-acylated LPS in the parental strain (64). More importantly, the overall virulence potential of  $\Delta lpxM$  mutant of *Y. pestis* EV76

was reduced, and the mutant strain even provided a better level of immunity in immunized hosts (64). Lpp has a synergistic effect with LPS in bacterial virulence, and we have shown that deletion of the *lpp* gene from *Y pestis* KIM/D27 further attenuates this strain, while retaining its immunogenicity. Therefore, our current study not only provides an additional target for yersiniae attenuation, but also indicates that deletion of both *lpp* and the biosynthetic genes for LPS might further attenuate the virulence of yersiniae. Such mutants could be excellent candidates for possible live vaccine development. Indeed our recent study indicated that deletion of *lpp* and *msbB* (a homolog of *lpxM*) genes from *S. Typhimurium* resulted in the generation of superior cell-mediated and humoral immune responses in mice, compared to those in animals infected with the WT bacterium (117).

Since live vaccine strains are potentially released into the environment by vaccinated individuals, safety issues concerning the medical, as well as environmental, aspects must be considered (70). These concerns include a reversion in virulence by acquisition of complementation genes and exchange of genetic information with other vaccine or WT strains of the carrier organism (70). These safety issues must be thoroughly evaluated, especially the safety of such vaccines in immunocompromised hosts (70).

## Chapter 4<sup>†</sup>

### ***Deletion of Chromosomal Braun Lipoprotein Gene (*lpp*) and Curing of Plasminogen Activating Protease (*Pla*)-Encoding Plasmid Dramatically Alter the Virulence of *Yersinia pestis* CO92 in a Pneumonic Mouse Model***

We recently published a detailed characterization of how deletion of the chromosomally encoded murein (Braun) lipoprotein gene, *lpp*, attenuated *Y. pestis* CO92 in the intranasal mouse model of infection and how tissue damage, dissemination, and cytokine production were decreased in mice infected with the  $\Delta lpp$  mutant of *Y. pestis* CO92 compared to those infected with WT bacterium (158). In light of the previous studies describing the attenuation of pPCP1<sup>-</sup> and  $\Delta pla$  mutants of *Y. pestis* (29, 153, 168, 179, 181) and recent research characterizing the importance of Pla in establishing pneumonic infection in mice (110), we undertook studies to delineate how absence of pPCP1 plasmid would attenuate our  $\Delta lpp$  mutant of *Y. pestis* CO92. In this chapter, we characterized the WT and  $\Delta lpp$  mutant strains of *Y. pestis* CO92 from which the pPCP1 plasmid was cured (pPCP<sup>-</sup> and pPCP<sup>-</sup>/ $\Delta lpp$ , respectively) in our mouse model of pneumonic infection.

---

<sup>†</sup> The data presented in this chapter have been submitted for publication to the journal *Microbiology* (3).



## Results

### *Y. PESTIS* $pPCP^-/\Delta LPP$ MUTANT CO92 STRAIN WAS LESS LETHAL THAN WAS WT *Y. PESTIS* OR ITS SINGLE $pPCP1^-$ AND $\Delta LPP$ MUTANTS

Mice were inoculated intranasally with various doses of WT,  $\Delta lpp$ ,  $pPCP^-$ , or  $pPCP^-/\Delta lpp$  *Y. pestis* CO92 and monitored for morbidity and mortality (Fig. 4.1). Mice infected with a 250 LD<sub>50</sub> dose [1 LD<sub>50</sub> was calculated to be 340 bacteria (158)] of either WT or the  $\Delta lpp$  mutant of *Y. pestis* died by days 3 and 5, respectively.

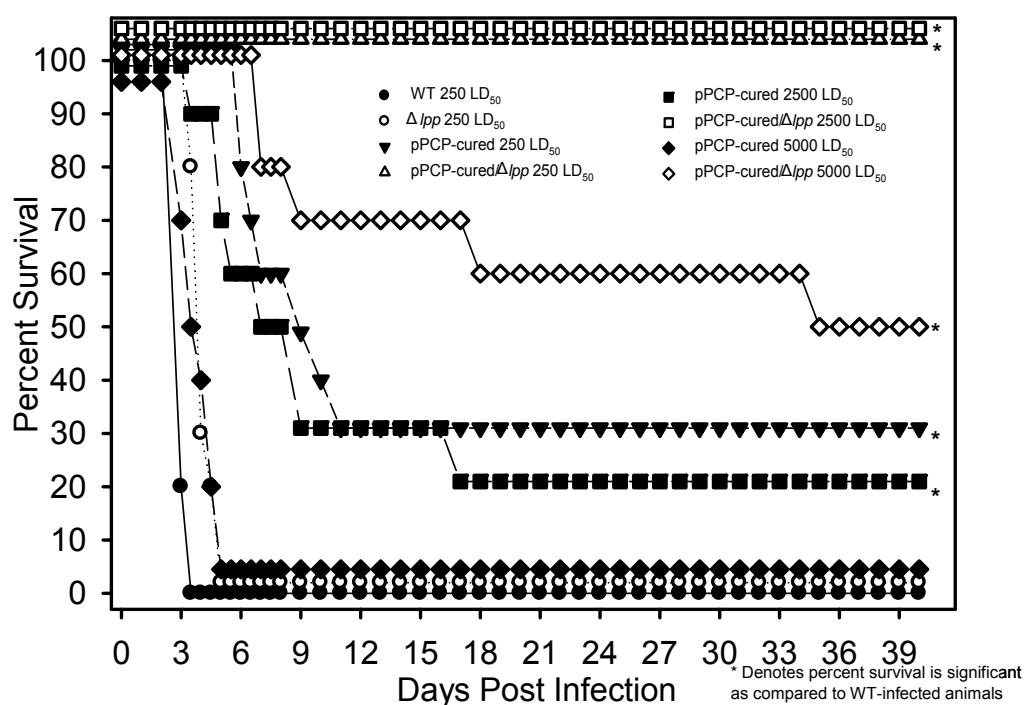


Figure 4.1: Survival analysis of mice infected with WT and mutant *Y. pestis* CO92 strains. Following i.n. inoculation with various doses of WT,  $\Delta lpp$ ,  $pPCP^-$ , and  $pPCP^-/\Delta lpp$  mutants of *Y. pestis*, mice were monitored for morbidity and mortality.

Those infected with a 250 LD<sub>50</sub> dose of either WT (●) or  $\Delta lpp$  (○) *Y. pestis* died by days 3 and 5, respectively. However, mice infected either a 250 LD<sub>50</sub> (Δ) or 2500 LD<sub>50</sub> (□) dose of the pPCP<sup>-</sup>/ $\Delta lpp$  strain showed a 100% survival rate, while those infected with the pPCP<sup>-</sup> strain showed 30% (▼) and 20% (■) survival rates, respectively. At the highest dose tested, 5000 LD<sub>50</sub>, 50% of the mice infected with the pPCP<sup>-</sup>/ $\Delta lpp$  strain survived (◇), while no mice infected with the pPCP<sup>-</sup> strain survived (◆). By Kaplan Meier analysis, only the group infected with a 5000 LD<sub>50</sub> dose of the pPCP<sup>-</sup> strain was not significantly different from the WT and  $\Delta lpp$ -infected groups. All other treatment groups were significantly different ( $p < 0.001$ ).

As expected, the mean time to death was increased in mice infected with the  $\Delta lpp$  mutant of *Y. pestis* CO92 (3, 158). In contrast, mice infected with the pPCP<sup>-</sup>/ $\Delta lpp$  mutant strain showed much higher survival rates at all doses tested than did those animals infected with the pPCP<sup>-</sup> mutant strain alone at the same tested doses. For example, at the lowest tested dose, those mice infected with a 250 LD<sub>50</sub> dose of the pPCP<sup>-</sup>/ $\Delta lpp$  mutant strain showed 100% survival, while those infected with a 250 LD<sub>50</sub> dose of the pPCP<sup>-</sup> mutant strain exhibited only a 30% survival rate. In the 2500 LD<sub>50</sub> dose group, 100% of the mice infected with the pPCP<sup>-</sup>/ $\Delta lpp$  mutant strain survived, while 20% of mice infected with the pPCP<sup>-</sup> mutant strain survived. Finally, at the highest dose of 5000 LD<sub>50</sub>, 50% of the mice infected with the pPCP<sup>-</sup>/ $\Delta lpp$  mutant strain survived. All mice infected with the pPCP<sup>-</sup> mutant strain at this dose died by day 5 p.i.. This indicated to us that curing of the pPCP1 plasmid and deleting the *lpp* gene synergistically attenuated the virulent *Y. pestis* CO92 strain.

***Y. PESTIS* PPCP<sup>-</sup>,  $\Delta$ LPP, AND PPCP<sup>-</sup>/ $\Delta$ LPP MUTANT STRAINS WERE AS CYTOTOXIC AS THE WT *Y. PESTIS* CO92 STRAIN**

The T3SS is encoded on virulence plasmid pCD1 and its expression is thought to cause the cytotoxic effects seen in host cell monolayers (120). We infected HeLa cells with WT and mutant *Y. pestis* strains at an MOI of 10 (Fig. 4.2) and monitored the monolayers using light microscopy. After a 2-h incubation at 37°C, mutant strains  $\Delta$ lpp (Panel C), pPCP<sup>-</sup> (Panel D) and pPCP<sup>-</sup>/ $\Delta$ lpp (Panel E) showed similar cytotoxicity levels when these were compared to the WT *Y. pestis* CO92 strain (Panel B). Panel A shows uninfected HeLa cells. Similar data were observed when HeLa cells were infected with WT versus mutant bacteria at lower MOIs of 1-5 (data not shown). These results indicated that there was proper translocation of T3SS effectors in the mutant strains of *Y. pestis* used in this study.

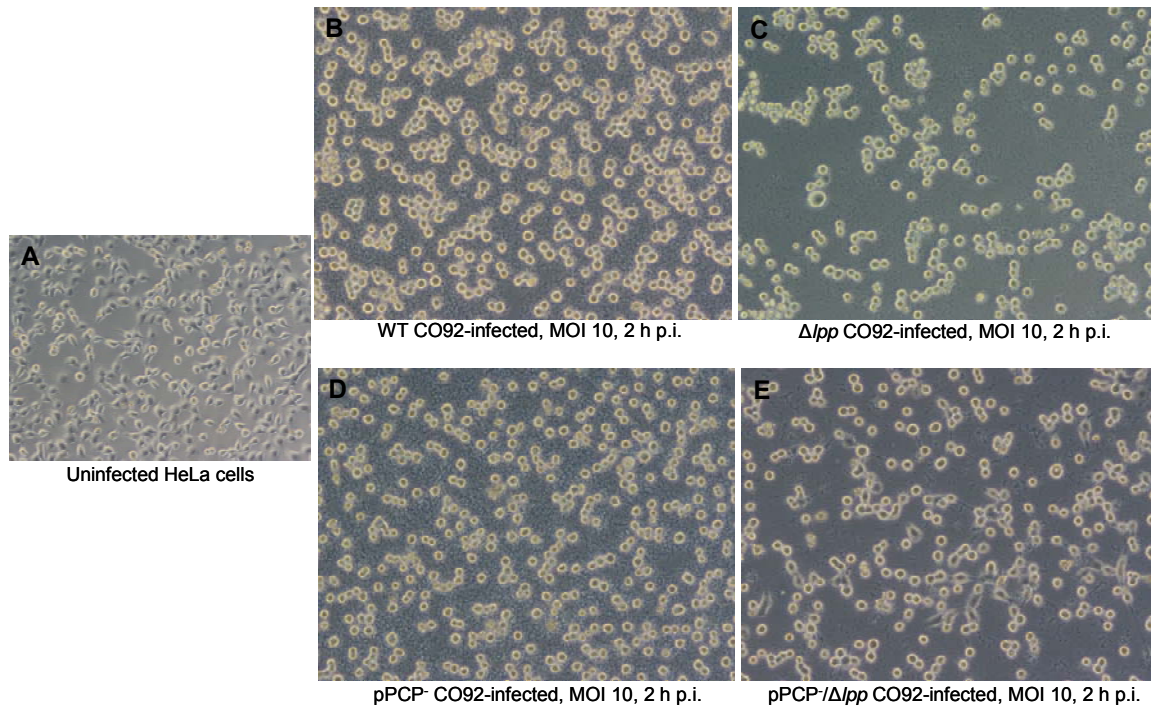


Figure 4.2: Type 3 secretion system-associated cytotoxicity in HeLa cells infected with WT

and mutant *Y. pestis* strains. HeLa cells were infected with an MOI of 10 of WT (Panel B) and mutant *Y. pestis* strains (Panel C, *Y. pestis*  $\Delta lpp$ ; Panel D, *Y. pestis* pPCP<sup>-</sup>; Panel E, pPCP<sup>-</sup>/ $\Delta lpp$ ) and monitored for cytotoxicity. All mutant strains showed an equal level of cytotoxicity within a 2-h time frame as compared to levels in WT-infected cells (Panel B) and in contrast those in uninfected HeLa cells (Panel A). HeLa cell cytotoxicity is defined as a rounding up and detachment of the cell monolayer from tissue culture flasks.

#### **WT *Y. PESTIS* CO92-INFECTED MICE HAD MORE SEVERE TISSUE INJURY THAN DID MICE INFECTED WITH THE MUTANT STRAINS**

Groups of 5 mice were infected with a 250 LD<sub>50</sub> ( $8.5 \times 10^4$  cfu) dose of WT *Y. pestis*, or the  $\Delta lpp$ , pPCP<sup>-</sup>, or pPCP<sup>-</sup>/ $\Delta lpp$  mutant strains. Mice were euthanized and organs harvested at 1 h and 48 h p.i.. Based on the data presented in Fig. 4.1, we chose a timepoint of 48 h for collection of tissues and blood for our subsequent analyses, as by day 3 all of the animals infected with the WT bacterium died due to the high lethal dose (250 LD<sub>50</sub>) of WT *Y. pestis* used in this study. However, we used timepoints of 72 h and 96 h in our previous studies following infection with a 5 LD<sub>50</sub> dose of *Y. pestis* CO92 (4, 5, 158). Portions of the mouse tissues were processed and stained with H&E to assess the level of tissue damage associated with the bacterial infection (Fig. 4.3). At 1 h p.i., no significant tissue damage was noted in the lungs (a), livers (b), spleens (c), or hearts (d) of mice infected with WT (Panel A),  $\Delta lpp$  (Panel B), pPCP<sup>-</sup> (Panel C), or pPCP<sup>-</sup>/ $\Delta lpp$  (Panel D) mutant strains of *Y. pestis* CO92. These sections exhibited histopathology similar to those sections from uninfected mice (anesthetized and given PBS) serving as controls.

At 48 h p.i., the lungs (Fig. 4.3a) of WT-infected mice (Panels E and I) showed mild alveolar edema (asterisks), as well as mild neutrophilic inflammation. Bacteria (arrows) were present in the alveoli of all mice and in the perivascular region in 2 out of 5 mice. The livers (Fig. 4.3b) of 2 of the 5 WT-infected mice (Panels E and I) showed small areas of necrosis (arrowhead) and minimal neutrophilic inflammation in the hepatic sinusoids, which also contained occasional bacteria (arrows) and fibrin. Four out of 5 of the spleens (Fig. 4.3c) of the WT-infected mice group (Panels E and I) had bacteria (arrows) and fibrin in the red pulp, while 1 mouse had lymphoid depletion in the white pulp. One WT-infected mouse had intravascular bacteria in the heart (Fig. 4.3d) at 48 h p.i. (Panel E, arrow). Otherwise, lesions were not observed in the heart. The inflammatory lesions and bacteria seen in the WT-infected mouse organs were consistent with *Y. pestis* infection. In general, lesions tended to diminish in occurrence, severity, and/or the amount of bacteria present in the mice infected with the  $\Delta lpp$ , pPCP<sup>-</sup>, and pPCP<sup>-</sup>/ $\Delta lpp$  mutants in this order (see below) as compared to the WT-infected mice.

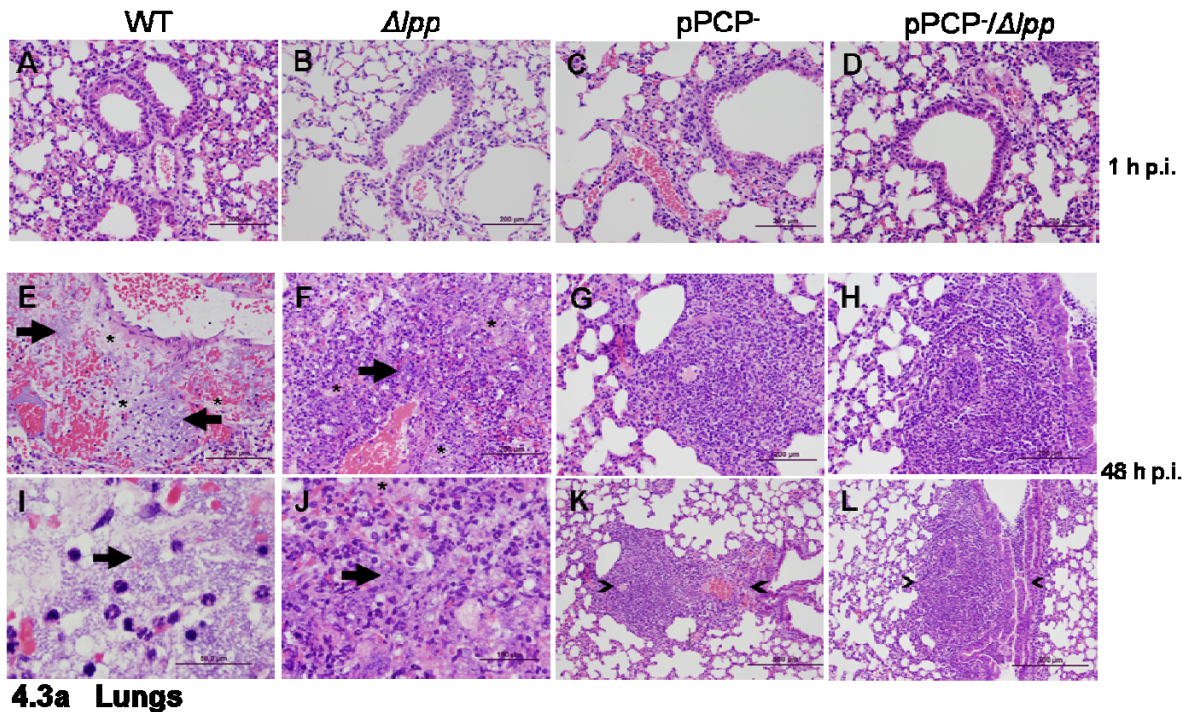
At 48 h p.i., the lungs (Fig. 4.3a) of all 5  $\Delta lpp$ -infected mice (Panels F and J) showed moderate edema (asterisks) and mild neutrophilic inflammation in the alveoli. Bacteria (arrows) were present in most alveoli associated with fibrin. The interstitium had small areas of necrosis in 2 of the 5 mice, and 1 mouse had multiple areas of moderate perivascular edema with mild perivascular fibrin. Two of the 5 mice had minimal neutrophilic inflammation in the sinusoids of the liver (Fig. 4.3b, Panels F and J), while 1 mouse had bacteria (arrows) in the sinusoids. One of 5 mice had bacteria (arrows) and fibrin in the red pulp and moderate lymphoid depletion in the white pulp of the spleen (Fig. 4.3c, Panels F and J). No mice infected with the *Y. pestis*  $\Delta lpp$  mutant had any lesions in the heart (Fig.

4.3d) at 48 h p.i. (Panel F). The pathology seen in various organs of mice infected with the WT and the  $\Delta lpp$  mutant strain of *Y. pestis* appeared similar. This was not surprising, as the bacterial dose given to the mice was very high (250 LD<sub>50</sub>) and animals infected with both the WT and the mutant died by day 5 (Fig. 4.1). However, we noted that in the organs of mice infected with the  $\Delta lpp$  mutant there were less severe changes when compared to those tissues from WT-infected mice at 48 h p.i., which coincided with a longer mean time to death for the  $\Delta lpp$  mutant (Fig. 4.1).

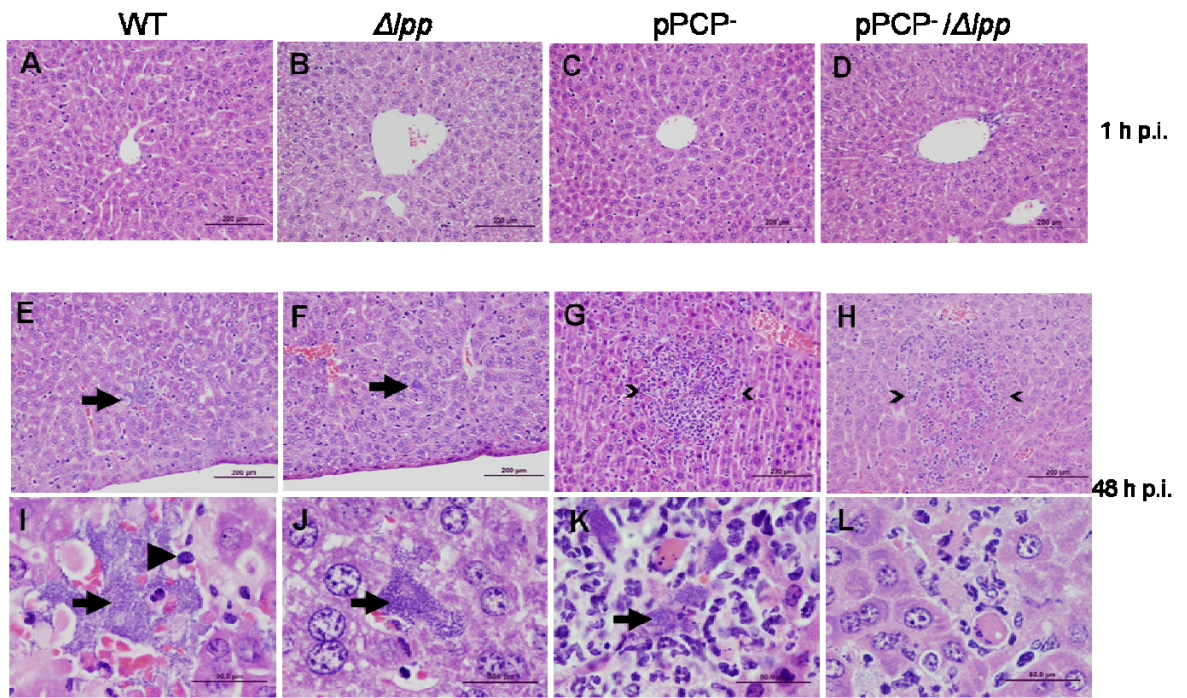
At 48 h p.i., the lungs (Fig. 4.3a) of mice infected with the pPCP<sup>-</sup> mutant strain (Panels G and K) showed mild neutrophilic inflammation (outlined by chevrons) in both the alveolar and perivascular regions. Three of 5 mice had mild alveolar fibrin, 1 of 5 mice had alveolar edema, and 1 of 5 had mild hemorrhaging. Bacteria were not present in any of the lung tissue samples, while 1 of 5 mice infected with the pPCP<sup>-</sup> mutant strain had bacteria in the liver sinusoids (Fig. 4.3b, Panels G and K, arrow). Two of 5 mice had minimal and mild neutrophilic liver inflammation (outlined by chevrons). No mice infected with the *Y. pestis* pPCP<sup>-</sup> mutant strain exhibited any lesions in the spleen (Fig. 4.3c, Panels G and K) or heart (Fig. 4.3d, Panel G). These histopathology data corresponded with gradual and reduced mortality in mice infected with the pPCP<sup>-</sup> mutant strain compared to that found in the WT- and  $\Delta lpp$ - mutant strains of *Y. pestis* CO92 (Fig. 4.1).

At 48 h p.i., the lungs (Fig. 4.3a) of all 5 mice infected with the pPCP<sup>-</sup>/ $\Delta lpp$  mutant (Panels H and L) had perivascular neutrophilic inflammation, while only 3 had perivascular edema. Two of 5 mice had mild peribronchiolar inflammation (outlined by chevrons), and 1 mouse had mild neutrophilic inflammation in the bronchioles. In the liver (Fig. 4.3b) at 48 h p.i., 3 of 5 mice infected with the pPCP<sup>-</sup>/ $\Delta lpp$  mutant (Panels H and L) had mild neutrophilic

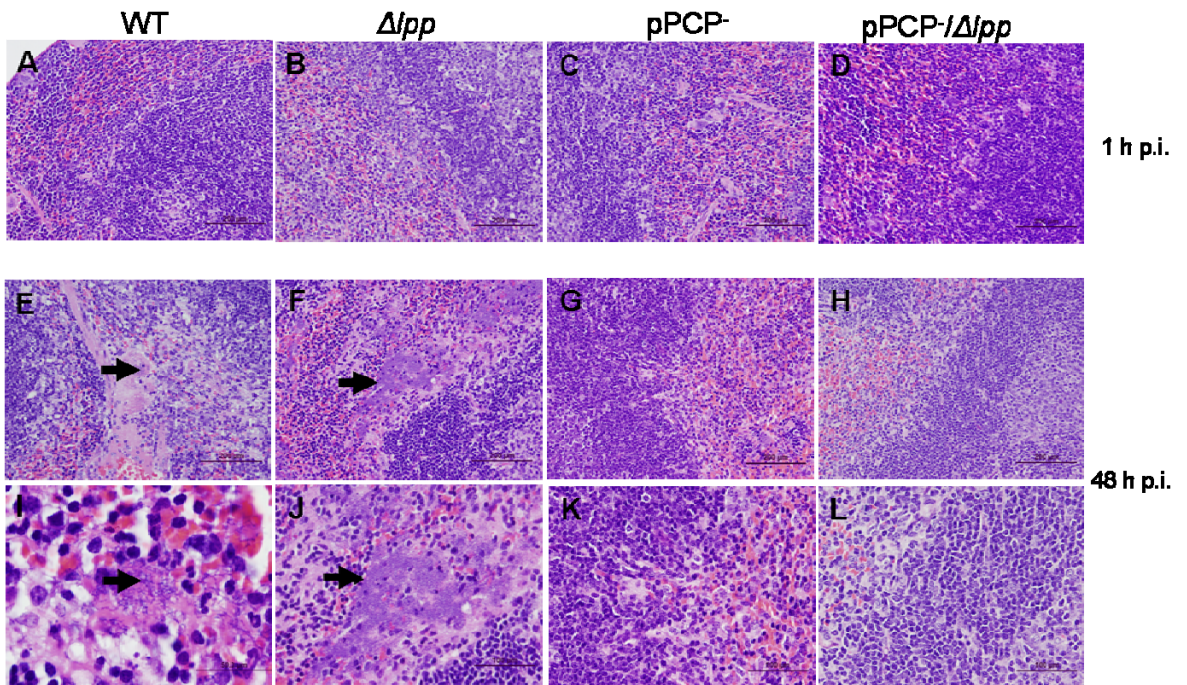
inflammation (outlined by chevrons), and one of these had a small area of necrosis in the sinusoids. The livers of the other 2 mice in this group were within normal limits. Additionally, the spleens (Fig. 4.3c, Panels H and L) and hearts (Fig. 4.3d, Panel H) of all of the mice infected with the pPCP<sup>-</sup>/Δ*lpp* mutant were within normal limits. Bacteria were not present in any of the tissue sections from these mice. Overall, the changes seen in different organs of mice infected with the pPCP<sup>-</sup>/Δ*lpp* mutant strain were minimal compared to changes in WT- and other mutant-infected mice.







**4.3b Liver**



**4.3c Spleen**



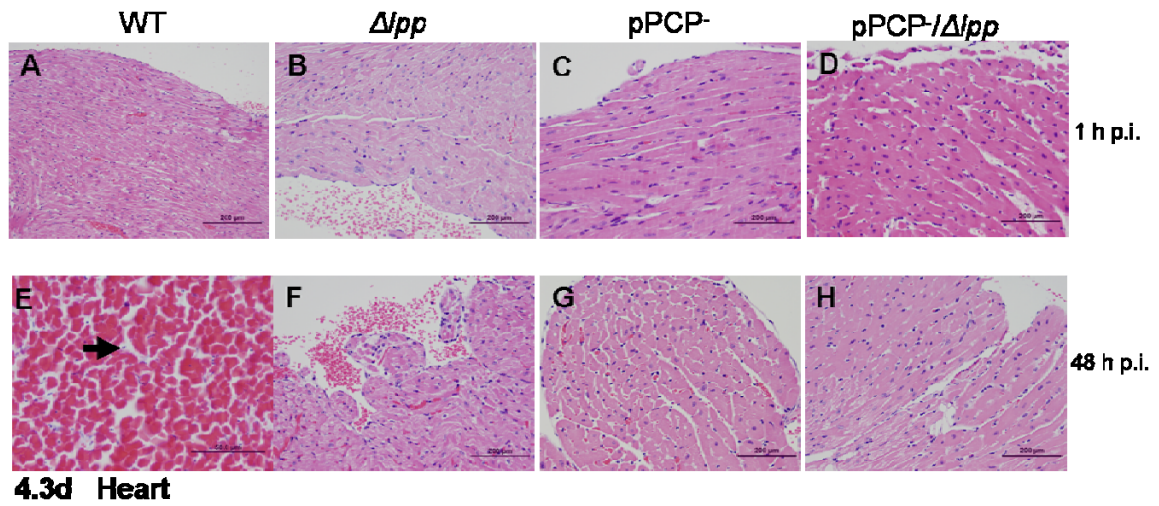


Figure 4.3: Histopathology of mouse tissues following infection with WT and mutant *Y. pestis* strains. Groups of 5 mice were infected with 250 LD<sub>50</sub> ( $8.5 \times 10^4$  cfu) of WT *Y. pestis*, or  $\Delta lpp$ , pPCP<sup>-</sup>, or pPCP<sup>-</sup>/ $\Delta lpp$  mutant strains. Mice were euthanized, and the lungs (a), livers (b), spleens (c), or hearts (d) were harvested at 1 h and 48 h p.i.. No significant tissue damage was noted in mice infected with WT (Panel A),  $\Delta lpp$  (Panel B), pPCP<sup>-</sup> (Panel C), or pPCP<sup>-</sup>/ $\Delta lpp$  (Panel D) mutant strains of *Y. pestis* CO92 at 1 h p.i. (controls). Tissue sections of WT-infected mice at 48 h p.i. are shown in Panels E and I,  $\Delta lpp$  – infected mice are shown in Panels F and J, pPCP<sup>-</sup>-infected mice are shown in Panels G and K, and pPCP<sup>-</sup>/ $\Delta lpp$  –infected mice are shown in Panels H and L. Bacteria in these sections are indicated by an arrow, edema is indicated by an asterisk, inflammation is outlined by chevrons, and necrosis is indicated with an arrowhead. All sections were stained with H&E and size bars are indicated on each picture.

***Y. PESTIS* CO92 CURED FOR THE pPCP1 PLASMID OR DELETED FOR THE *LPP* GENE EXHIBITED DIFFERENTIAL SURVIVABILITY IN PERIPHERAL ORGANS COMPARED TO THAT IN WT-INFECTED MICE AT 48 H P.I.**

Organs retrieved for histopathologic analysis were also homogenized and cultured to assess the survivability of the 2 pPCP mutant strains (pPCP<sup>-</sup> and pPCP<sup>-</sup>/ $\Delta$ *lpp*) as compared to the WT and  $\Delta$ *lpp* mutant strains in the peripheral organs of the mice. The organs of 5 mice infected with each of the 4 bacterial strains were homogenized at 1 h and 48 h p.i. and cultured on SBA plates. Colonies were counted and data were plotted on a log scale to easily visualize the increases and decreases in bacterial numbers. Importantly, the numbers of bacteria in the lungs (Fig. 4.4a) of WT- and  $\Delta$ *lpp* mutant-infected mice increased by 1-2 logs at 48 h p.i. when compared to 1 h p.i. control lung tissues. However, the number of bacteria cultured from WT- and  $\Delta$ *lpp* mutant-infected mice were not statistically different at 48 h p.i. Conversely, in mice infected with either the pPCP<sup>-</sup> or pPCP<sup>-</sup>/ $\Delta$ *lpp* mutant, the levels of bacteria present in the lungs at 48 h p.i. dropped when compared to the levels in the lungs at 1 h p.i.. This drop was significant ( $p < 0.05$ ) when we compared the findings with those in the WT-infected mice, but not when compared to the levels in the  $\Delta$ *lpp* mutant-infected mice at 48 h p.i.. This indicated an inability of these mutant bacteria (pPCP<sup>-</sup> or pPCP<sup>-</sup>/ $\Delta$ *lpp* mutant) to survive within the lung.

Bacteria recovered from the livers of mice (Fig. 4.4b) infected with either the WT or its  $\Delta$ *lpp* mutant strain increased by 4-5 logs from 1 h p.i. to 48 h p.i.. These increases in the numbers of bacteria recovered from the livers of  $\Delta$ *lpp*-infected mice were similar to what we previously reported (158). However, only 1 of 5 mice in both the pPCP<sup>-</sup>- or pPCP<sup>-</sup>/ $\Delta$ *lpp* mutant-infected groups had an appreciable number of bacteria in the liver. In the remaining 4

mice, no detectable numbers of bacteria were noted in the livers of animals infected with either the pPCP<sup>-</sup> or pPCP<sup>-</sup>/ $\Delta$ lpp mutant strain when compared to those findings in the WT-infected mice. The limit of detection of bacteria in various organs in mice was approximately 80 cfu.

On the other hand, in the spleen (Fig. 4.4c), there was no significant differences between the numbers of bacteria that disseminated in WT-infected mice compared to findings in the  $\Delta$ lpp<sup>-</sup>, pPCP<sup>-</sup>, or pPCP<sup>-</sup>/ $\Delta$ lpp mutant-infected mice at 48 h p.i.. The trend, however, indicated an inability of  $\Delta$ lpp mutant bacteria (only 1 out of 5 mice having an appreciable number of bacteria) to survive within spleen cells, as we previously reported (158). Interestingly, in 3 and 2 of 5 mice, respectively, appreciable numbers of the pPCP<sup>-</sup> and pPCP<sup>-</sup>/ $\Delta$ lpp mutant bacteria were noted in the spleen. These data were in contrast to what was observed in the lungs and livers of mice infected with the pPCP<sup>-</sup> and pPCP<sup>-</sup>/ $\Delta$ lpp mutant strains, as they did not survive in these tissues after 48 h p.i. (Fig. 4.4a and b). These data suggested to us that both of these mutants could disseminate to the liver and spleen but were possibly differentially killed in these two organs.

No pPCP<sup>-</sup> or pPCP<sup>-</sup>/ $\Delta$ lpp mutant bacteria were detected in the hearts of mice (Fig. 4.4d) infected with these strains, whereas significantly ( $p < 0.05$ ) higher levels of WT and  $\Delta$ lpp strains were detected in heart at 48 h p.i.. Likewise, WT bacteria were detected in the blood of mice (Fig. 4.4e) at 48 h p.i.. Only 1 out of 5 mice showed appreciable numbers of  $\Delta$ lpp mutant bacteria in the blood. Although no pPCP<sup>-</sup>/ $\Delta$ lpp mutant was detected in the blood at 48 h p.i., 3 of 5 mice had low levels of the pPCP<sup>-</sup> mutant in the blood.

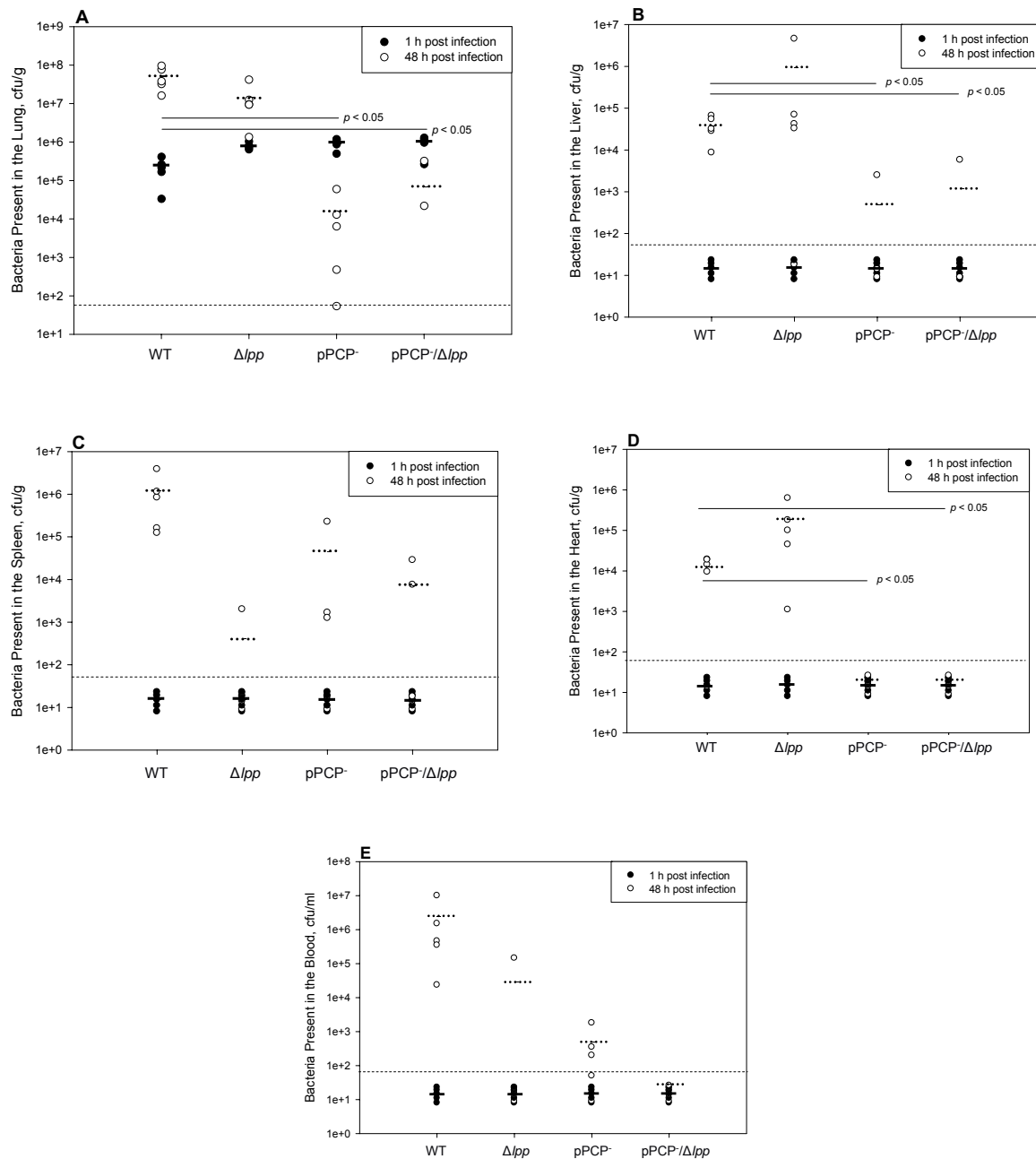


Figure 4.4: Survival of WT and mutant *Y. pestis* strains 1 h and 48 h p.i. in peripheral organs of mice. Groups of 5 animals were infected with a 250 LD<sub>50</sub> dose of WT and mutant *Y. pestis* strains. At 1 and 48 h p.i., mice were euthanized, blood was drawn and organs harvested, homogenized, serially diluted and cultured on

SBA plates. Bacterial counts per g of lung (a), liver (b), spleen (c), heart (d) and per ml of blood (e) were determined for 1 h p.i. (●) and 48 h p.i. (○). Solid bars indicate the average value at 1 h p.i., while hashed bars indicate the average value at 48 h p.i.. The dotted line parallel to the x-axis is the limit of bacterial detection. Significant differences (Student's *t*-test) between groups are noted.

**MICE INFECTED WITH *Y. PESTIS* CO92 STRAINS CURED OF THE PPCP1 PLASMID CONTAINING THE *PLA* GENE SHOWED LOWER LEVELS OF CYTOKINES AND CHEMOKINES BY 48 H P.I. COMPARED TO THE LEVELS IN WT BACTERIA-INFECTED MICE**

In parallel with the histopathology and dissemination experiments, blood was drawn *via* cardiac puncture from mice at 1 h and 48 h after i.n. inoculation with either WT *Y. pestis* CO92 or one of the mutant strains. The sera from uninfected mice were used as controls. The levels of 32 cytokines and chemokines were evaluated by using Millipore's Milliplex assay. A maximum of 23 of these cytokines/chemokines showed a response. A key to the abbreviations and acronyms used for the cytokines and chemokines can be found in Table 2.3.

In the lungs (Table 4.1), WT-infected mice had an overwhelming inflammatory response at 48 h p.i.. Of the 32 cytokines and chemokines tested, 21 were significantly higher ( $p < 0.05$ ) than in the control samples (marked with \*\*) and 2 were higher but lacked statistical significance. In mice infected with the  $\Delta lpp$  mutant, the levels of cytokines and chemokines were generally similar to those in WT-infected mice at 48 h p.i.. This is not surprising given the high dose, 250 LD<sub>50</sub>, used for this study. The levels of

cytokines/chemokines in mice infected with the pPCP<sup>-</sup> mutant strain, however, dropped by 48 h p.i. when we compared them with the levels in WT-infected mice. Of interest, G-CSF, IP-10, KC, MCP-1, M-CSF, RANTES, and VEGF were significantly lower than the levels noted in WT-infected mice ( $p < 0.05$ , indicated by \*). Additionally, levels of IL-6, IL-12p70, LIF, and TNF- $\alpha$ , when compared to the levels in WT-infected mice, were also significantly lower ( $p < 0.05$ , indicated by \*) in mice infected with the pPCP<sup>-</sup> mutant strain. We noted a significant drop ( $p < 0.05$ , indicated by \*) in the levels of 20 cytokines and chemokines in the lung homogenates of mice infected with the pPCP<sup>-</sup>/ $\Delta lpp$  mutant strain by 48 h p.i.. For most of these cytokines and chemokines, the decrease was substantially greater than in mice infected with either of the single mutants. This indicated to us that a potential synergistic effect occurred attributable to deletion of the *lpp* gene and curing of the pPCP1 plasmid in the mouse model of infection. In fact, 16 of these cytokines and chemokines decreased between 90% and 100% as compared to those levels from the WT-infected mice, and 5 more decreased between 50% and 89% at 48 h p.i.. Eotaxin levels decreased by 17%, when compared to the levels in WT-infected mice, while IL-10 levels decreased by 32%.

In the livers of infected mice (Table 4.2), changes were noted in the levels of 19 cytokines and chemokines. Of these, 14 were significantly increased ( $p < 0.05$ , indicated by \*\*) in the livers of WT-infected mice when compared to the levels in control mice at 48 h p.i.. Significant decreases ( $p < 0.05$ , indicated by \*\*) were noted in the levels of MIG and MIP-2 in the livers of  $\Delta lpp$ -infected mice by 48 h p.i.. In mice infected with the pPCP<sup>-</sup> mutant strain at 48 h p.i., significant decreases were noted in the levels of G-CSF, IL-1 $\alpha$ , KC, LIF, M-CSF, MIP-2, and TNF- $\alpha$  as compared to those levels in WT-infected mice. Only Eotaxin was significantly increased over those levels noted in WT-infected mice.

	Control Lung pg/ml	Lung WT 48 h pi pg/ml	Lung Δ/pp 48 h pi pg/ml	Lung pPCP- 48 h pi pg/ml	Lung pPCP-/Δ/pp 48 h pi pg/ml	Decrease in pPCP-/Δ/pp as compared to WT
<b>Eotaxin</b>	53.7 ± 9.5	208.9 ± 47.4**	166.4 ± 66.3	185.6 ± 145.9	173.4 ± 36.1	17%
<b>G-CSF</b>	3.9 ± 7.7	109349.6 ± 18765.1**	123550.2 ± 6680.5	30269.9 ± 27584.9*	1540.3 ± 2736.3*	99%
<b>GM-CSF</b>	8.6 ± 11.1	606.7 ± 445.9**	1858.9 ± 1096.0*	121.5 ± 182.1	9.0 ± 9.3*	99%
<b>IFN-γ</b>	0.00	8611.5 ± 8873.8**	1946.9 ± 1897.9	2277.2 ± 2177.7	70.0 ± 54.8	99%
<b>IL-1α</b>	29.3 ± 14.8	7602.6 ± 5424.4**	13499.2 ± 3410.0	1730.6 ± 2811.7	1226.4 ± 210.4*	84%
<b>IL-1β</b>	80.8 ± 27.5	1116.5 ± 455.7**	2007.1 ± 432.6	451.3 ± 567.8	69.3 ± 11.9*	94%
<b>IL-6</b>	4.4 ± 1.9	77587.5 ± 31991.9**	67325.8 ± 30834.6	20104.6 ± 19519.5*	204.2 ± 102.3*	100%
<b>IL-10</b>	14.2 ± 2.0	19.2 ± 3.2**	17.2 ± 1.9	12.3 ± 6.0	13.0 ± 2.6*	32%
<b>IL-12p70</b>	14.0 ± 6.2	137.9 ± 23.0**	145.9 ± 34.0	72.2 ± 29.9*	12.3 ± 7.3*	91%
<b>IL-17</b>	0.9 ± 1.9	374.0 ± 191.9**	505.9 ± 185.8	131.0 ± 130.5	7.4 ± 13.3*	98%
<b>IP-10</b>	34.7 ± 6.5	5943.4 ± 990.1**	4598.3 ± 1572.3	3448.4 ± 678.1*	439.6 ± 413.5*	93%
<b>KC (IL-8)</b>	44.1 ± 10.5	19490.0 ± 6928.2**	20693.6 ± 7488.5	6444.9 ± 3598.0*	1695.7 ± 1777.1*	91%
<b>LIF</b>	0.1 ± 0.2	1013.6 ± 664.8**	784.6 ± 228.2	184.8 ± 338.9*	2.1 ± 1.7*	100%
<b>LIX</b>	68.1 ± 12.6	798.4 ± 231.7**	1154.9 ± 284.3	434.6 ± 292.6	318.4 ± 286.3*	60%
<b>MCP-1</b>	22.0 ± 4.7	6730.5 ± 4184.6**	4830.6 ± 3264.0	1262.9 ± 833.4*	219.3 ± 187.9*	97%
<b>M-CSF</b>	20.4 ± 6.7	402.8 ± 141.1**	286.7 ± 31.4	123.8 ± 113.7*	72.4 ± 11.4*	82%
<b>MIG</b>	746.0 ± 436.6	110005.6 ± 101342.5	79025.8 ± 50104.8	70950.3 ± 29665.6	5112.9 ± 4621.8	95%
<b>MIP-1α</b>	43.5 ± 29.2	1915.7 ± 767.9**	3147.8 ± 1208.2	1401.9 ± 1637.1	161.8 ± 72.8*	92%
<b>MIP-1β</b>	9.2 ± 18.4	2097.3 ± 1137.7**	4025.7 ± 1156.1	2204.8 ± 3383.11	145.2 ± 62.3*	93%
<b>MIP-2</b>	1.1 ± 2.1	16499.4 ± 9576.0**	25247.1 ± 10156.5	4800.7 ± 8574.5	127.7 ± 100.5*	99%
<b>RANTES</b>	37.7 ± 13.1	215.1 ± 16.3**	123.4 ± 28.9	90.9 ± 56.7*	61.5 ± 14.9*	71%
<b>TNF-α</b>	2.2 ± 1.7	285.2 ± 109.3**	434.1 ± 145.9	61.3 ± 73.9*	4.3 ± 2.5*	98%
<b>VEGF</b>	121.2 ± 52.5	203.7 ± 83.6	163.6 ± 57.0	72.4 ± 20.9*	90.5 ± 21.1*	56%

\*Denotes significant changes as compared to WT-infected mice (Student's *t* test, *p* < 0.05).

\*\*Denotes a significant difference in WT-infected groups as compared to control group (Student's *t* test, *p* < 0.05).

Table 4.1: Cytokine and chemokine levels (pg/ml) in the lung homogenates of mice 48 h after intranasal infection with WT or mutant *Y. pestis* strains.

In mice infected with the pPCP<sup>-</sup>/Δ*lpp* mutant strain, significant decreases ( $p < 0.05$ , indicated by \*) were noted in the levels of 14 cytokines and chemokines in the liver, with G-CSF, IFN- $\gamma$ , IL-1 $\alpha$ , KC, LIF, MCP-1, M-CSF, and MIP-2 dropping between 90% and 100%, when compared to the levels in WT-infected mice. IL-1 $\beta$ , IL-6, MIG, MIP-1 $\alpha$ , and TNF- $\alpha$  levels decreased between 50% and 90%, while LIX decreased by only 16% compared to those in the livers of WT-infected mice at 48 h p.i. The levels of Eotaxin and IL-12p70 increased compared to those in WT at 48 h p.i., while neither the IL-10 nor MIP-1 $\beta$  levels changed at 48 h p.i. in the livers of mice infected with the pPCP<sup>-</sup>/Δ*lpp* mutant strain. We again noted a synergistic effect in the decrease of many of the cytokine and chemokine levels in the livers of mice infected with the pPCP<sup>-</sup>/Δ*lpp* mutant as compared to mice infected with either single mutant strain by 48 h p.i..

In the spleen (Table 4.3) at 48 h p.i., we noted changes in the levels of 19 cytokines and chemokines with significant increases ( $p < 0.05$ , indicated by \*\*) in 10 of these in WT-infected mice as compared to control mice. The levels of Eotaxin, IP-10, and MIG significantly decreased ( $p < 0.05$ , indicated by \*\*) in Δ*lpp*-infected mice when compared with their levels in WT-infected mice. The levels of Eotaxin, G-CSF, IP-10, KC, LIF, MCP-1, and MIP-1 $\alpha$  were significantly decreased ( $p < 0.05$ , indicated by \*) in the spleens of mice infected with pPCP<sup>-</sup> mutant bacteria when compared to levels in WT-infected mice. In mice infected with the pPCP<sup>-</sup>/Δ*lpp* mutant strain, the levels of 17 cytokines and chemokines decreased significantly ( $p < 0.05$ , indicated by \*) compared to the levels in WT-infected mice, with 13 of these decreased between 90% and 100%, 3 between 50% and 89%, and 1 with a 21% decrease. Many of these showed a synergistic decrease when compared to mice infected with the single mutants. Only RANTES increased significantly ( $p < 0.05$ , indicated



	Control Liver pg/ml	Liver WT 48 h pi pg/ml	Liver $\Delta pp$ 48 h pi pg/ml	Liver pPCP- 48 h pi pg/ml	Liver pPCP- $\Delta pp$ 48 h pi pg/ml	Decrease in pPCP- $\Delta pp$ as compared to WT
<b>Eotaxin</b>	108.2 $\pm$ 11.3	37.4 $\pm$ 23.7**	68.7 $\pm$ 57.6	115.3 $\pm$ 34.6*	91.7 $\pm$ 46.4*	increase
<b>G-CSF</b>	56.1 $\pm$ 22.7	53606.5 $\pm$ 34665.9**	42096.1 $\pm$ 24141.3	7165.1 $\pm$ 9232.0*	208.6 $\pm$ 204.4*	100%
<b>IFN-<math>\gamma</math></b>	20.7 $\pm$ 10.4	382.1 $\pm$ 347.9	95.4 $\pm$ 123.3	112.7 $\pm$ 136.9	7.7 $\pm$ 10.4*	98%
<b>IL-1<math>\alpha</math></b>	354.1 $\pm$ 38.3	1691.2 $\pm$ 1049.8**	2629.2 $\pm$ 4368.1	486.4 $\pm$ 381.1*	145.6 $\pm$ 57.5*	91%
<b>IL-1<math>\beta</math></b>	72.4 $\pm$ 20.1	186.4 $\pm$ 103.24	185.3 $\pm$ 320.7	100.6 $\pm$ 105.2	70.1 $\pm$ 41.9*	62%
<b>IL-6</b>	33.7 $\pm$ 9.9	292.7 $\pm$ 153.9**	346.8 $\pm$ 391.4	102.7 $\pm$ 65.7	74.1 $\pm$ 29.1*	75%
<b>IL-10</b>	16.6 $\pm$ 3.7	39.9 $\pm$ 26.0	44.1 $\pm$ 17.3	32.9 $\pm$ 20.8	54.5 $\pm$ 20.5	unchanged
<b>IL-12p70</b>	48.9 $\pm$ 10.8	39.3 $\pm$ 19.5	47.0 $\pm$ 34.0	72.2 $\pm$ 41.8	115.0 $\pm$ 66.9*	increase
<b>IP-10</b>	101.9 $\pm$ 34.6	1490.6 $\pm$ 1625.6	680.5 $\pm$ 1124.1	2682.0 $\pm$ 2085.4	169.3 $\pm$ 114.4	89%
<b>KC (IL-8)</b>	50.2 $\pm$ 5.5	10496.2 $\pm$ 3263.9**	13914.2 $\pm$ 11605.6	3547.5 $\pm$ 1421.6*	882.6 $\pm$ 1003.7*	92%
<b>LIF</b>	0.00	21.8 $\pm$ 16.0**	20.5 $\pm$ 12.8	2.0 $\pm$ 2.1*	0.1 $\pm$ 0.3*	100%
<b>LIX</b>	61.1 $\pm$ 12.0	303.9 $\pm$ 43.3**	282.5 $\pm$ 147.7	190.5 $\pm$ 119.5	255.5 $\pm$ 88.8*	16%
<b>MCP-1</b>	130.3 $\pm$ 31.1	1590.7 $\pm$ 1110.7**	1095.1 $\pm$ 1505.7	635.9 $\pm$ 492.9	136.3 $\pm$ 83.4*	91%
<b>M-CSF</b>	63.5 $\pm$ 23.0	378.3 $\pm$ 191.5**	412.9 $\pm$ 284.3	68.7 $\pm$ 41.3*	39.5 $\pm$ 21.5*	90%
<b>MIG</b>	1808.4 $\pm$ 2169.1	115125.3 $\pm$ 63867.1**	31435.7 $\pm$ 32203.3*	79936.0 $\pm$ 50072.7	33656.2 $\pm$ 45248.2*	71%
<b>MIP-1<math>\alpha</math></b>	75.4 $\pm$ 20.9	168.4 $\pm$ 66.4**	201.1 $\pm$ 251.2	133.7 $\pm$ 55.5	79.6 $\pm$ 45.4*	53%
<b>MIP-1<math>\beta</math></b>	148.5 $\pm$ 46.0	48.9 $\pm$ 52.6**	127.2 $\pm$ 208.9	72.2 $\pm$ 72.7	63.9 $\pm$ 70.9	unchanged
<b>MIP-2</b>	379.2 $\pm$ 90.6	3481.1 $\pm$ 1817.3**	880.5 $\pm$ 1504.4*	133.9 $\pm$ 31.1*	146 $\pm$ 101.6*	96%
<b>TNF-<math>\alpha</math></b>	10.7 $\pm$ 3.5	41.2 $\pm$ 18.1**	29.2 $\pm$ 45.1	12.7 $\pm$ 9.2*	6.6 $\pm$ 3.0*	84%

\*Denotes significant changes as compared to WT-infected mice (Student's *t* test, *p* < 0.05).

\*\*Denotes a significant difference in WT-infected groups as compared to control group (Student's *t* test, *p* < 0.05).

Table 4.2: Cytokine and chemokine levels (pg/ml) in the liver homogenates of mice 48 h after intranasal infection with WT or mutant *Y. pestis* strains.

by \*) in mice infected with the pPCP<sup>-</sup>/Δ*lpp* mutant strain, compared to RANTES levels found in WT-infected mice at 48 h p.i..

We noted changes in 13 cytokines and chemokines in the heart homogenates (Table 4.4) of mice at 48 h p.i.. Levels of G-CSF, IL-6, IL-9, KC, and M-CSF were significantly higher ( $p < 0.05$ , indicated by \*\*) in WT-infected mice compared to control mice. In Δ*lpp* mutant-infected mice, G-CSF was significantly higher ( $p < 0.05$ , indicated by \*) compared to G-CSF levels in WT-infected mice, while IL-9 and MIG were significantly lower ( $p < 0.05$ , indicated by \*). In mice infected with the pPCP<sup>-</sup> mutant strain, IL-9 and MIG were also significantly lower ( $p < 0.05$ , indicated by \*) in the heart compared to the levels in WT-infected mice. In mice infected with the pPCP<sup>-</sup>/Δ*lpp* mutant strain, however, levels of G-CSF, IL-1α, IL-6, IL-9, IL-12p70, KC, MCP-1, and TNF-α were all significantly lower than the levels noted in the hearts of WT-infected mice at 48 h p.i.. Levels of five of these cytokines and chemokines were synergistically lower than the levels seen in either of the single mutant-infected mice (pPCP<sup>-</sup> or Δ*lpp*). The levels of LIX and M-CSF remained unchanged in the hearts of pPCP<sup>-</sup>/Δ*lpp* mutant-infected mice.

In the sera (Table 4.5) at 48 h p.i., changes were noted in the levels of 21 cytokines and chemokines in infected mice. Increases were noted in all of these in WT-infected mice when compared to findings in the control mice, with 12 of these increased significantly ( $p < 0.05$ , indicated by \*\*). G-CSF was significantly higher ( $p < 0.05$ , indicated by \*) in Δ*lpp*-infected mice than in WT-infected mice, but no other significant changes were noted in this group. In mice infected with the pPCP<sup>-</sup> mutant strain, all 21 cytokines and chemokines decreased, but Eotaxin, G-CSF, IL-1α, IL-10, MIP-1β, RANTES, and TNF-α were significantly ( $p < 0.05$ , indicated by \*) decreased compared to their levels in the sera of WT-

	Control Spleen pg/ml	Spleen WT 48 h pi pg/ml	Spleen $\Delta/pp$ 48 h pi pg/ml	Spleen pPCP- 48 h pi pg/ml	Spleen pPCP- $\Delta/pp$ 48 h pi pg/ml	Decrease in pPCP- $\Delta/pp$ as compared to WT
<b>Eotaxin</b>	35.3 $\pm$ 15.5	260.9 $\pm$ 146.6**	68.9 $\pm$ 38.0*	59.3 $\pm$ 22.2*	44.4 $\pm$ 7.7*	83%
<b>G-CSF</b>	0.00	10479.6 $\pm$ 4902.4**	11308.6 $\pm$ 11251.0	1858.3 $\pm$ 3040.9*	85.7 $\pm$ 50.0*	99%
<b>IFN-<math>\gamma</math></b>	7.1 $\pm$ 5.3	764.8 $\pm$ 1040.2	80.2 $\pm$ 179.4	1341.5 $\pm$ 2795.8	2.0 $\pm$ 4.0	100%
<b>IL-1<math>\alpha</math></b>	34.3 $\pm$ 7.2	297.7 $\pm$ 72.8**	282.1 $\pm$ 386.6	130.5 $\pm$ 149.2	12.9 $\pm$ 26.7*	96%
<b>IL-1<math>\beta</math></b>	73.6 $\pm$ 5.1	51.0 $\pm$ 33.3	33.7 $\pm$ 69.9	31.1 $\pm$ 28.3	24.5 $\pm$ 9.0*	52%
<b>IL-6</b>	0.1 $\pm$ 0.2	480.9 $\pm$ 501.5	1083.2 $\pm$ 2404.5	34.2 $\pm$ 38.1	0.00	100%
<b>IL-10</b>	24.0 $\pm$ 4.4	20.3 $\pm$ 5.7	17.8 $\pm$ 6.4	16.9 $\pm$ 6.1	9.5 $\pm$ 4.7*	53%
<b>IL-12p70</b>	9.3 $\pm$ 4.0	14.8 $\pm$ 5.7	8.4 $\pm$ 11.1	8.7 $\pm$ 4.6	0.9 $\pm$ 1.3*	94%
<b>IP-10</b>	191.6 $\pm$ 38.4	5690.3 $\pm$ 2084.2**	643.4 $\pm$ 805.5*	1482.3 $\pm$ 1571.3*	159.8 $\pm$ 55.6*	97%
<b>KC (IL-8)</b>	19.5 $\pm$ 6.0	11519.0 $\pm$ 3906.6**	5848.9 $\pm$ 4951.5	3753.4 $\pm$ 1309.4*	251.0 $\pm$ 156.9*	98%
<b>LIF</b>	0.00	5.9 $\pm$ 4.3**	3.9 $\pm$ 7.4	0.7 $\pm$ 0.6*	0.00*	100%
<b>MCP-1</b>	0.00	1080.2 $\pm$ 411.5**	376.3 $\pm$ 338.3	345.7 $\pm$ 246.2*	29.3 $\pm$ 26.0*	97%
<b>M-CSF</b>	10.8 $\pm$ 3.6	58.6 $\pm$ 57.2	30.3 $\pm$ 27.6	33.6 $\pm$ 20.7	46.4 $\pm$ 20.4*	21%
<b>MIG</b>	5979.1 $\pm$ 492.2	103722.9 $\pm$ 69002.8	12724.8 $\pm$ 8270.8*	57997.8 $\pm$ 67578.4	9048.2 $\pm$ 3431.4*	91%
<b>MIP-1<math>\alpha</math></b>	27.8 $\pm$ 23.8	210.8 $\pm$ 101.8**	210.9 $\pm$ 434.9	58.6 $\pm$ 80.2*	12.4 $\pm$ 17.2*	94%
<b>MIP-1<math>\beta</math></b>	164.0 $\pm$ 71.0	533.6 $\pm$ 270.0**	726.2 $\pm$ 1176.8	256.2 $\pm$ 145.1	163.0 $\pm$ 94.8*	69%
<b>MIP-2</b>	0.00	483.1 $\pm$ 462.6	91.3 $\pm$ 123.9	42.4 $\pm$ 39.4	0.00*	100%
<b>RANTES</b>	133.8 $\pm$ 63.6	96.8 $\pm$ 24.1	67.2 $\pm$ 19.7	108.3 $\pm$ 40.7	135.3 $\pm$ 22.0*	increase
<b>TNF-<math>\alpha</math></b>	2.7 $\pm$ 1.0	13.0 $\pm$ 5.4**	12.3 $\pm$ 23.0	8.0 $\pm$ 8.6	1.3 $\pm$ 1.7*	90%

\*Denotes significant changes as compared to WT-infected mice (Student's *t* test, *p* < 0.05).

\*\*Denotes a significant difference in WT-infected groups as compared to control group (Student's *t* test, *p* < 0.05).

Table 4.3: Cytokine and chemokine levels (pg/ml) in the spleen homogenates of mice 48 h after intranasal infection with WT or mutant *Y. pestis* strains.

	Control Heart pg/ml	Heart WT 48 h pi pg/ml	Heart $\Delta pp$ 48 h pi pg/ml	Heart pPCP- 48 h pi pg/ml	Heart pPCP- $\Delta pp$ 48 h pi pg/ml	Decrease in pPCP- $\Delta pp$ as compared to WT
<b>G-CSF</b>	0.00	13834.7 $\pm$ 6060.7**	17371.1 $\pm$ 10839.4*	3773.8 $\pm$ 4863.4	102.7 $\pm$ 69.2*	99%
<b>IFN-<math>\gamma</math></b>	1.1 $\pm$ 1.8	42.5 $\pm$ 82.5	4.6 $\pm$ 10.2	3.5 $\pm$ 7.8	0.7 $\pm$ 1.4	98%
<b>IL-1<math>\alpha</math></b>	22.0 $\pm$ 6.5	59.4 $\pm$ 38.8	76.9 $\pm$ 52.5	18.2 $\pm$ 22.3	4.5 $\pm$ 7.3*	92%
<b>IL-6</b>	5.6 $\pm$ 1.4	517.7 $\pm$ 407.6**	1363.7 $\pm$ 2396.2	185.9 $\pm$ 259.6	3.1 $\pm$ 5.9*	99%
<b>IL-9</b>	377.0 $\pm$ 51.2	246.7 $\pm$ 29.2**	205.1 $\pm$ 54.2*	231.8 $\pm$ 58.0*	92.2 $\pm$ 71.3*	63%
<b>IL-12p70</b>	4.9 $\pm$ 2.3	5.0 $\pm$ 3.2	7.7 $\pm$ 7.6	2.2 $\pm$ 2.5	0.00*	100%
<b>IP-10</b>	0.8 $\pm$ 1.3	68.1 $\pm$ 69.4	37.8 $\pm$ 43.8	31.6 $\pm$ 28.1	20.3 $\pm$ 17.8	70%
<b>KC (IL-8)</b>	5.3 $\pm$ 3.1	381.3 $\pm$ 152.6**	1060.3 $\pm$ 1825.6	91.1 $\pm$ 85.4	55.3 $\pm$ 25.1*	85%
<b>LIX</b>	0.00	29.4 $\pm$ 25.6	50.0 $\pm$ 50.2	17.4 $\pm$ 25.4	44.0 $\pm$ 42.0	unchanged
<b>MCP-1</b>	1.3 $\pm$ 2.6	276.3 $\pm$ 234.7	251.7 $\pm$ 315.6	52.5 $\pm$ 42.7	27.7 $\pm$ 16.2*	90%
<b>M-CSF</b>	1.4 $\pm$ 1.0	5.5 $\pm$ 3.2**	6.5 $\pm$ 5.9	2.6 $\pm$ 2.3	21.9 $\pm$ 15.9	unchanged
<b>MIG</b>	12.7 $\pm$ 7.0	1151.4 $\pm$ 1350.4	188.6 $\pm$ 67.1*	297.4 $\pm$ 174.4*	225.2 $\pm$ 121.8	80%
<b>TNF-<math>\alpha</math></b>	0.1 $\pm$ 0.3	1.3 $\pm$ 1.2	2.8 $\pm$ 4.0	0.1 $\pm$ 0.2	0.00*	100%

\*Denotes significant changes as compared to WT-infected mice (Student's *t* test, *p* < 0.05).

\*\*Denotes a significant difference in WT-infected groups as compared to control group (Student's *t* test, *p* < 0.05).

Table 4.4: Cytokine and chemokine levels (pg/ml) in the heart homogenates of mice 48 h after intranasal infection with WT or mutant *Y. pestis* strains.

	Control Serum pg/ml	Serum WT 48 h pi pg/ml	Serum $\Delta$ lpp 48 h pi pg/ml	Serum pPCP- 48 h pi pg/ml	Serum pPCP- $\Delta$ lpp 48 h pi pg/ml	Decrease in pPCP- $\Delta$ lpp as compared to WT
<b>Eotaxin</b>	171.18 $\pm$ 7.41	839.6 $\pm$ 524.8**	999.7 $\pm$ 543.4	275.9 $\pm$ 39.1*	277.5 $\pm$ 115.6*	67%
<b>G-CSF</b>	31.6 $\pm$ 13.5	147789.2 $\pm$ 14893.4**	191055.6 $\pm$ 41153.5*	67493.4 $\pm$ 57595.5*	4038.0 $\pm$ 4734.4*	97%
<b>GM-CSF</b>	0.00	52.1 $\pm$ 11.5**	61.0 $\pm$ 9.2	26.4 $\pm$ 22.7	1.3 $\pm$ 2.9*	98%
<b>IFN-<math>\gamma</math></b>	0.00	7499.3 $\pm$ 13412.7	654.2 $\pm$ 1141.6	343.8 $\pm$ 514.7	17.1 $\pm$ 32.8	100%
<b>IL-1<math>\alpha</math></b>	16.2 $\pm$ 11.5	275.1 $\pm$ 133.3**	285.2 $\pm$ 154.8	117.4 $\pm$ 71.7*	46.9 $\pm$ 55.4*	83%
<b>IL-1<math>\beta</math></b>	0.00	137.6 $\pm$ 150.5	191.0 $\pm$ 190.4	21.2 $\pm$ 25.8	0.00	100%
<b>IL-6</b>	2.3 $\pm$ 0.6	29832.5 $\pm$ 12846.8**	57595.9 $\pm$ 45622.0	11745.5 $\pm$ 12186.2	393.1 $\pm$ 466.2*	99%
<b>IL-9</b>	4.9 $\pm$ 6.6	82.4 $\pm$ 19.2	76.7 $\pm$ 17.0	28.6 $\pm$ 21.2	5.4 $\pm$ 5.7*	93%
<b>IL-10</b>	3.5 $\pm$ 1.0	10.6 $\pm$ 4.5**	13.4 $\pm$ 4.9	4.5 $\pm$ 2.2*	2.8 $\pm$ 0.5*	74%
<b>IL-12p70</b>	1.6 $\pm$ 1.8	113.7 $\pm$ 82.4**	89.4 $\pm$ 21.5	37.5 $\pm$ 31.2	20.1 $\pm$ 30.4*	82%
<b>IL-17</b>	0.9 $\pm$ 1.8	432.8 $\pm$ 498.9	652.4 $\pm$ 582.55	123.2 $\pm$ 164.3	1.9 $\pm$ 2.8	100%
<b>IP-10</b>	73.2 $\pm$ 19.4	4434.8 $\pm$ 2834.0**	3178.3 $\pm$ 1542.2	2318.6 $\pm$ 1859.9	177.6 $\pm$ 91.4*	96%
<b>KC (IL-8)</b>	23.8 $\pm$ 6.1	26499.7 $\pm$ 25849.2	30148.6 $\pm$ 33508.6	3287.5 $\pm$ 3158.8	132.8 $\pm$ 61.5	99%
<b>MCP-1</b>	2.2 $\pm$ 4.4	13143.9 $\pm$ 13258.1	11476.6 $\pm$ 16279.1	622.4 $\pm$ 448.3	49.1 $\pm$ 49.2	100%
<b>M-CSF</b>	0.00	9.4 $\pm$ 7.1**	8.6 $\pm$ 5.8	3.8 $\pm$ 2.9	0.4 $\pm$ 0.5	96%
<b>MIG</b>	137.9 $\pm$ 121.8	42713.7 $\pm$ 63895.0	1169.3 $\pm$ 1020.7	1062.8 $\pm$ 843.4	258.2 $\pm$ 211.0	99%
<b>MIP-1<math>\alpha</math></b>	0.00	296.9 $\pm$ 45.5**	568.3 $\pm$ 367.5	198.0 $\pm$ 125.1	58.3 $\pm$ 48.7*	80%
<b>MIP-1<math>\beta</math></b>	0.00	392.5 $\pm$ 178.8**	2071.6 $\pm$ 2613.7	97.9 $\pm$ 112.0*	0.00*	100%
<b>MIP-2</b>	36.4 $\pm$ 18.4	4721.9 $\pm$ 9749.3	4980.3 $\pm$ 10603.9	33.0 $\pm$ 24.0	16.1 $\pm$ 18.1	100%
<b>RANTES</b>	4.3 $\pm$ 1.8	91.2 $\pm$ 52.9	66.1 $\pm$ 47.5	21.3 $\pm$ 16.2*	8.5 $\pm$ 6.1*	91%
<b>TNF-<math>\alpha</math></b>	0.3 $\pm$ 0.5	42.0 $\pm$ 17.7**	58.6 $\pm$ 51.6	5.9 $\pm$ 6.1*	0.1 $\pm$ 0.2*	100%

\*Denotes significant changes as compared to WT-infected mice (Student's *t* test, *p* < 0.05).

\*\*Denotes a significant difference in WT-infected groups as compared to control group (Student's *t* test, *p* < 0.05).

Table 4.5: Cytokine and chemokine levels (pg/ml) in the sera of mice 48 h after intranasal infection with WT or mutant *Y. pestis* strains.

infected mice. In mice infected with the pPCP<sup>-</sup>/Δ*lpp* mutant strain, a similar pattern was noted, but levels of G-CSF, GM-CSF, IL-1α, IL-6, IL-9, IL-12p70, IP-10, MIP-1α, MIP-1β, RANTES, and TNF-α all were significantly decreased ( $p < 0.05$ , indicated by \*) by 80%-100% compared those in WT-infected mice. Many of these were also synergistically lower than the levels seen in the sera of single mutant-infected mice groups. Eotaxin levels decreased by 67%, and no cytokine or chemokine levels increased in the sera of mice infected with the pPCP<sup>-</sup>/Δ*lpp* mutant compared to those in WT-infected mice.

#### **LACK OF SURVIVABILITY OF *Y. PESTIS* CO92 MUTANTS IN MURINE MACROPHAGES WAS MORE DEPENDENT UPON THE *LPP* GENE THAN THE PPCP1 PLASMID**

RAW 264.7 murine macrophages were infected at an MOI of 1 with each of the *Yersinia* strains grown overnight at 28°C. Infected macrophages were harvested after a 1-h gentamicin treatment (0-h time point), and at 4, 8, and 24 h post treatment. Gentamicin treatment of macrophages after infection (100 μg/ml) and throughout the time course (10 μg/ml) was used to kill any extracellular bacteria. At each time point, macrophages were lysed and cultured on SBA plates to determine the percentage of intracellular survival of *Y. pestis* strains (Fig. 4.5). Data were normalized to the 0-h time points, and we observed nearly 100% phagocytosis for all strains. At 4 h p.i., the numbers of WT cells recovered from macrophages decreased slightly, compared to those at the 0-h time point, while the numbers of mutant bacteria recovered from macrophages were significantly decreased ( $p < 0.001$ ) compared to WT-infected cells. The numbers of the pPCP<sup>-</sup>/Δ*lpp* mutant strain recovered from macrophages decreased the most, however, to a level significantly different ( $p < 0.001$ ) from that of the pPCP<sup>-</sup> mutant strain, while maintaining a level of survival similar to that of

the  $\Delta lpp$  mutant strain. At 4 h p.i., the absence of Lpp appears to be the determining factor for the intracellular survival of these *Y. pestis* strains within macrophages.

At 8 h p.i., the number of WT *Y. pestis* bacteria that survived within the macrophages decreased only slightly from the 4-h time point and again showed a significantly higher ( $p < 0.001$ ) level of survivability when compared to findings in the other 3 mutant strains. A similar pattern with the mutant strains emerged at this time point except that the number of  $\Delta lpp$  mutant bacteria that survived decreased to a level significantly ( $p < 0.001$ ) below that of the pPCP<sup>-</sup> or pPCP<sup>-</sup>/ $\Delta lpp$  mutant strains recovered from macrophages.

At 24 h p.i., the number of WT bacteria that survived inside the macrophages did not change compared to their numbers at the 8-h time point. Although the number of pPCP<sup>-</sup> mutant bacteria increased from the 8-h time point, the numbers of bacteria retrieved from macrophages was significantly ( $p < 0.001$ ) lower than that of the WT bacteria. The survivability of the  $\Delta lpp$  and pPCP<sup>-</sup>/ $\Delta lpp$  mutant strains dropped dramatically compared to the survivability of either the WT or pPCP<sup>-</sup> mutant strains and were not significantly different from each other at 24 h p.i.. Taken together, these data indicated that the lack of survivability of bacteria within macrophages seemed to be more dependent on the presence of Lpp rather than pPCP1 in these *Y. pestis* strains.

## ***Discussion***

We recently showed that deletion of the *lpp* gene from *Y. pestis* CO92 affected the virulence of the organism in the pneumonic plague mouse model (158). Other investigators also reported attenuation in *Y. pestis* strains lacking either the pPCP1 plasmid or the *pla* gene

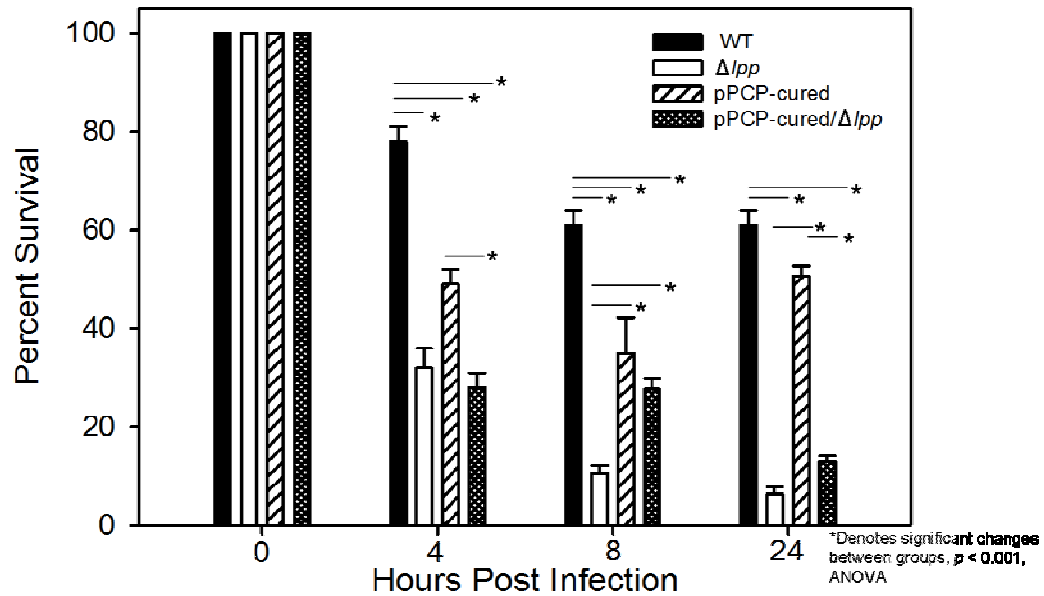


Figure 4.5: Survival of WT and mutant *Y. pestis* strains *in vitro*. Murine RAW 264.7 macrophages were infected at an MOI of 1 with WT and mutant *Y. pestis* strains for 30 min. Monolayers were treated with 100  $\mu$ g/ml gentamicin for 1 h, and, at the indicated time points (post gentamicin), macrophages were lysed. Lysates were serially diluted and cultured on SBA plates. Colonies were counted and data were normalized to the 0-h time point. Significant differences (ANOVA,  $p < 0.001$ ) between groups are noted.



when administered in mice by the subcutaneous (29, 153, 168, 179, 181), aerosol (179, 181), and intranasal (110) routes. In fact, Lathem et al concluded that Pla was responsible for establishing infection in the lung when bacteria were administered intranasally but was not necessary for *Y. pestis* to disseminate from the lungs to peripheral organs, e.g., spleen (110). In this report, we showed that *Y. pestis* strains lacking both the *lpp* gene and the pPCP1 plasmid were highly attenuated in the pneumonic plague mouse model, when compared to the single *lpp* gene deletion or pPCP1-cured strains of *Y. pestis* CO92. Further, such strains exhibited drastically reduced tissue injury and a muted cytokine and chemokine induction in tissue homogenates and sera when compared to equivalent findings in WT-,  $\Delta lpp$ -, and pPCP1<sup>-</sup> mutant strains. We opted to cure the pPCP1 plasmid from WT and  $\Delta lpp$  *Y. pestis* CO92 strains over selectively deleting the *pla* gene, as pesticin and pesticin-immunity protein do not contribute to the virulence of *Y. pestis* in the animal model (9).

We used a much higher dose (250 LD<sub>50</sub>) of bacteria in the current study with similar results (158). Based on our previous study at a dose of 5 LD<sub>50</sub>, WT-infected mice began to die between 60 h and 72 h p.i., and we noted appropriate cytokine and chemokine responses and definitive pathology by 48 h p.i. (4, 5, 158). Additionally, multiple survival/mortality experiments using the pPCP<sup>-</sup> and pPCP<sup>-</sup>/ $\Delta lpp$  mutant strains indicated that we needed very high doses to determine the LD<sub>50</sub> of these two mutant strains. Therefore, in order to use WT and  $\Delta lpp$ -infected mice as a comparison to the two pPCP1 mutant strains with such a large amount of bacteria, we chose the latest time point as 48 h p.i.. As expected, all WT and  $\Delta lpp$ -infected mice died between 3 and 5 days p.i..

In terms of dissemination and survivability of WT *Y. pestis* CO92 and its various mutants in a mouse model, we concluded that the  $\Delta lpp$  mutant could leave the confines of the

lungs to replicate within the liver and the heart, but was unable to do so in the spleen or blood and hence cleared from these organs by 48 h p.i.. This confirmed our previous findings in which we demonstrated a high bacterial ( $\Delta lpp$ ) load in the lungs and liver of mice but not in the spleen and blood at 48 h p.i. (158). The inability to recover mutant bacteria from the spleen could be explained by the uptake and subsequent killing of the mutant by splenic cells or by the migration of immune cells from the spleen following uptake of the mutant bacteria (120). In the lungs, the ability of  $\Delta lpp$  mutant bacteria to replicate indicated either the alveolar macrophages were unable to kill the mutant efficiently or the bacteria were also taken up by lung epithelial cells where they survive effectively and replicated. It is also possible, as was noted above, that these bacteria in the lungs resisted phagocytosis and efficiently grew extracellularly within the lung.

The  $pPCP^-$  and  $pPCP^-/\Delta lpp$  mutant strains were not able to survive in the lung, unlike the WT and  $\Delta lpp$ -mutant strains, and those bacteria that left the lung showed either a tropism for the spleen over the liver, heart, or blood or were cleared by the latter three organs by 48 h. This was confirmed by our histopathology data, with  $pPCP^-$  and  $pPCP^-/\Delta lpp$  mutant strains completely clearing from the tissues 48 h p.i.. Clearly, Pla was required to establish an infection in the lungs of mice and possibly dissemination of bacteria from the lungs to other organs. However, the presence of  $pPCP1^-$  and  $pPCP^-/\Delta lpp$  mutant bacteria at 48 h p.i. in the spleens of 40-60% of the mice indicated that these mutant bacteria did disseminate, albeit in lower numbers or that these mutant bacteria were efficiently killed in the lungs, liver, heart, and blood, but not in the spleen. Alternatively, the  $pPCP1^-$  mutant might have a tropism for the spleen, while the  $\Delta lpp$  mutant migrated mostly to the liver. These data are very provocative and require further studies.

These data corroborated with the cytokine and chemokine induction data from the tissue homogenates and the sera. WT-infected mice showed overwhelming proinflammatory cytokine and chemokine responses by 48 h p.i. in all tissue homogenates and in the sera. Mice infected with the  $\Delta lpp$  mutant had significantly lower levels of MIG and MIP-2 in the liver homogenates, IP-10 and MIG in the spleen homogenates, and IL-9 and MIG in the heart homogenates when compared to WT-infected mice. However the levels of the above-mentioned cytokines and chemokines were lower in those mice infected with either of the two pPCP1 mutants (pPCP1- and pPCP1-/ $\Delta lpp$ ) when compared to the levels in the  $\Delta lpp$  mutant-infected mice. Interestingly, MIG and IP-10 are induced by IFN- $\gamma$  (25), the cytokine with immunoregulatory functions important in the host's response to infection. In the case of the WT and  $\Delta lpp$ -infected mice, however, the overwhelming induction of cytokines and chemokines in our Milliplex panel led to their demise. Mice infected with either pPCP1 mutant, on the other hand, showed lower cytokine and chemokine responses, and evidence of tissue repair by 48 h p.i., which indicated to us that by this time point the mice had resolved the infection. In fact, a previous study by Lathem et al showed that mice infected with a *pla* isogenic mutant had little elevation in the quantities of cytokine transcripts (IL-10, IL-1 $\alpha$ , IL-17, IL-6, MIP-2, and TNF- $\alpha$ ) at 24 h p.i. (110), which indicated that these mice and those in our study avoided the massive proinflammatory response that more than likely contributed to the demise of our WT- and  $\Delta lpp$ -infected mice. Taken together, these data suggested to us that Lpp and Pla contributed to bacterial virulence by different mechanisms, but synergistically resulted in a more efficient clearance of the bacteria from mice and hence their higher survival rate.

These *in vivo* data corroborated with our *in vitro* studies in which we infected murine

RAW 264.7 macrophages with various mutant strains. As noted, the  $\Delta lpp$  mutant bacteria died rapidly within the macrophages, and minimal numbers of this mutant was recovered from the host cells at 24 h p.i. when compared to that in macrophages infected with the WT or the pPCP1-cured mutant strain of *Y. pestis* CO92. A similar survival pattern as that noted for the  $\Delta lpp$  mutant bacteria was observed for the pPCP<sup>-</sup>/ $\Delta lpp$  mutant strain, indicating that Lpp and not Pla contributed to bacterial survival in macrophages. In contrast, in the liver, both WT and the  $\Delta lpp$  mutant bacteria could efficiently survive. *Y. pestis* produces an antiphagocytic capsule and Yops at 37°C and, as a result, efficiently grows extracellularly (38, 142, 176). Another alternative is that the WT and  $\Delta lpp$  mutant bacteria escaped killing by resisting phagocytosis and grew extracellularly in the liver.

It appeared that the genes (e.g., *pla*) encoded by the pPCP1 plasmid did not influence survivability of the bacteria within macrophages, as the number of pPCP1<sup>-</sup> mutant bacteria that survived were similar to the number of WT bacteria in macrophages. This supported an earlier study which showed neither the pCD1 nor pPCP1 virulence plasmids were required in *Yersinia* to efficiently grow within macrophages (170).

Importantly, deletion of Lpp and Pla resulted in a greater ability of mice to recover from infection following high doses (250-2500 LD<sub>50</sub>), as compared to the single mutant strains, and this effect was synergistic. Because of the absence of Pla, chemotaxis of inflammatory cells was not impeded and complement C3 not inactivated resulting in a vigorous-enough immune response for the mice to survive infection (168). The cytokine and chemokine profiles by 48 h p.i. indicated that the mice infected with the double mutant or the pPCP1-cured strain successfully overcame a substantial bacterial infection, while those infected with either the WT or  $\Delta lpp$  mutant strains succumbed to infection by 48-72 h p.i.. In

fact, for many of these profiles, the decrease in the levels of cytokines and chemokines from the tissue homogenates and the sera was synergistically lower in the double mutant-infected mice than in mice infected with either of the single mutants. The histopathology data concurred with these results. By 48 h p.i., the tissue had already begun to heal in the mice infected with either of the pPCP mutants (pPCP- and pPCP<sup>-</sup>/Δ*lpp*), when compared to tissue in WT- or Δ*lpp*-infected mice. Taken together, these data indicated important roles of Pla and Lpp in the virulence of *Y. pestis* CO92.

## CHAPTER 5‡

### ***Characterization of a Mouse Model of Plague after Aerosolization of Yersinia pestis CO92***

*Y. pestis*, the plague bacterium, has been placed on the list of category A select agents because of its potential use as a biological warfare weapon. The dynamics of pneumonic infection following aerosolization of a highly virulent *Y. pestis* CO92 strain are understudied. Therefore, the purpose of this analysis was to characterize the mouse plague model following aerosolization of *Y. pestis* CO92. We accomplished this by determining the LD<sub>50</sub> dose, bacterial dissemination, cytokine/chemokine production, and tissue damage in Swiss-Webster mice over a 72-h course of infection.

### ***Results***

#### **MURINE MODEL FOR DEVELOPING PNEUMONIC PLAGUE BY AEROSOLIZATION OF *Y. PESTIS* CO92**

Due to the limited number of studies performed on aerosolized *Y. pestis* in the murine model, our first goal was to calculate the precise LD<sub>50</sub> dose of *Y. pestis* using a whole-body aerosol chamber. Four groups of 10 mice each were exposed to *Y. pestis* CO92 prepared as described in Chapter 2, and diluted so that the nebulizer concentrations of bacteria prior to aerosolization were  $1.0 \times 10^7$ ,  $1.0 \times 10^8$ ,  $1.0 \times 10^9$ , and  $1.0 \times 10^{10}$  cfu/ml. Nebulization consistently resulted in an approximately 1-log drop in the number of bacteria introduced

---

‡ Copyright © Society for General Microbiology, *Microbiology*, vol 154, p 1939-1948, 2008. Used with permission.

into the aerosolization chamber. Therefore, the resulting bacterial suspension concentrations ( $C_{neb}$ ), after nebulization, were  $4.0 \times 10^6$ ,  $3.7 \times 10^7$ ,  $4.5 \times 10^8$ , and  $2.0 \times 10^9$  cfu/ml, respectively (Fig 5.1).

The bacterial dose presented (Dp) to the lungs of each animal inside the Madison chamber was based on Guyton's formula for the measurement of respiratory volumes (82), the algorithms for which have been described previously (148). At the highest  $C_{neb}$ , the Dp was calculated to be  $1.3 \times 10^4$  cfu/ml, while the lowest  $C_{neb}$  ( $4.0 \times 10^6$  cfu/ml) resulted in a Dp of 16 cfu/ml. The mice in this study began dying at 60 h p.i., and the majority died between 72 and 96 h p.i., a timeframe similar to that of our previous study using intranasal challenge (158). The Dp LD<sub>50</sub> for *Y. pestis* CO92 in Swiss-Webster mice was calculated to be  $2.1 \times 10^3$  cfu in the whole-body chamber, which was one log less than that previously reported ( $2.0 \times 10^4$  cfu) using either the nose-only exposure system (7) or the whole-body chamber (75) in the same mouse strain. These differences might be explained by variations in the aerosolization procedures or whether the number of bacteria in the nebulizer was calculated before or after aerosolization.

Interestingly, the LD<sub>50</sub> dose we previously calculated for intranasal administration of *Y. pestis* to the same species of mice was 340 cfu (158). These differences in the calculated LD<sub>50</sub> doses between two pneumonic models (intranasal versus aerosol) might be due to the mode and efficiency of bacterial entry into the lungs. Alternatively, the lower LD<sub>50</sub> dose of *Y. pestis* CO92 via the intranasal versus aerosol route may be due to nebulization during aerosolization, which could result in affecting virulence determinant(s) (e.g., pili, toxins, etc.) present on the bacterial surface, which would thereby increase the number of bacteria

necessary to cause infection *via* the aerosol route.

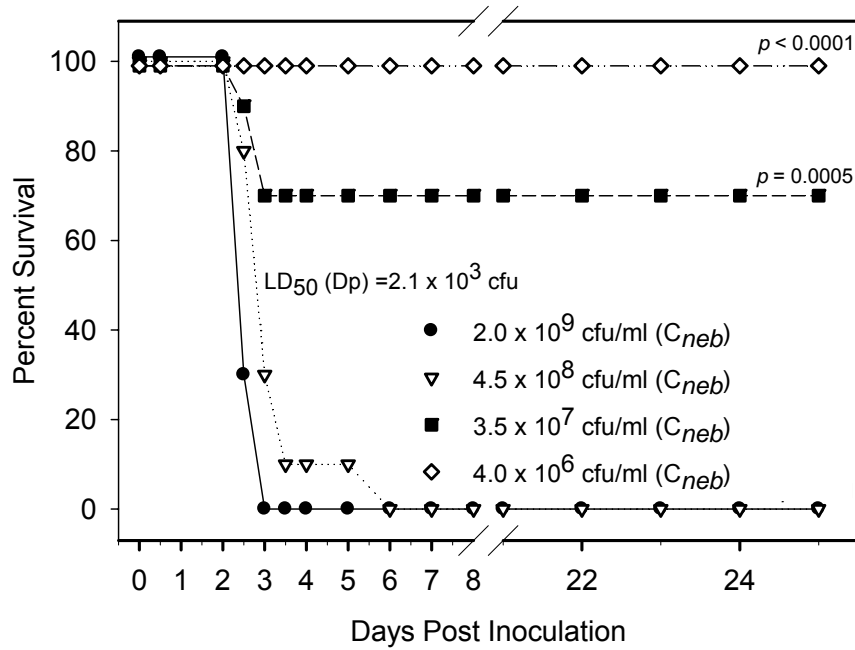


Figure 5.1: Calculation of the LD<sub>50</sub> for aerosolized *Y. pestis* CO92. Groups of 10 female Swiss-Webster mice each were aerosolized with 4 doses (C<sub>neb</sub>) of *Y. pestis*: 4.0 x 10<sup>6</sup>, 3.5 x 10<sup>7</sup>, 4.5 x 10<sup>8</sup>, and 2.0 x 10<sup>9</sup> cfu/ml. The LD<sub>50</sub>, based on the presented dose (Dp), was calculated to be 2.1 x 10<sup>3</sup> cfu. The *p*- values, as compared to the highest challenge dose, are indicated on the graph.



## HISTOPATHOLOGY FOLLOWING AEROSOLIZATION

To assess tissue injury occurring following aerosol-administered *Y. pestis* (Dp of  $1.3 \times 10^4$  cfu/ml) in mice, we euthanized 5 animals at 1, 24, 48, and 72 h p.i., harvested and formalin-fixed the lungs, liver, spleen, and heart. For brevity, only histopathology is shown for control animals (1 h p.i.) and at 72 h p.i. in Fig 5.2. The animal tissues harvested 1 h p.i. served as appropriate negative controls as we noted in our previous aerosol studies (data not shown) that animals 1 h post diluent (no bacteria) exposure showed neither pathology nor alterations in cytokine and chemokine levels compared to uninfected mice that were not subjected to aerosolization of the diluent.

Animals infected and examined at 1 h p.i. had no lesions in the lung, liver, spleen or heart and served as controls (Fig 5.2, Panels A-D). At 24 h p.i., 3 of the mice had acute inflammation in the lungs usually in association with blood vessels. Two of the 5 mice had small areas of minimal acute inflammation and necrosis in the liver. One of these mice had a mild inflammatory cell (neutrophilic) infiltrate in the red pulp of the spleen (data not shown). There were no significant lesions present in the hearts of any of the 5 mice.

At 48 h p.i., 4 of the 5 mice had lung inflammation associated with blood vessels, as in the 24 h p.i. mice. Four of the mice had mild acute inflammation and liver necrosis with occasional bacteria observed in one of the animals. The spleens of 3 of the mice exhibited neutrophilic infiltrates and some necrotic cells in the red pulp (data not shown). There were no significant lesions present in the hearts of any mice at 48 h p.i..

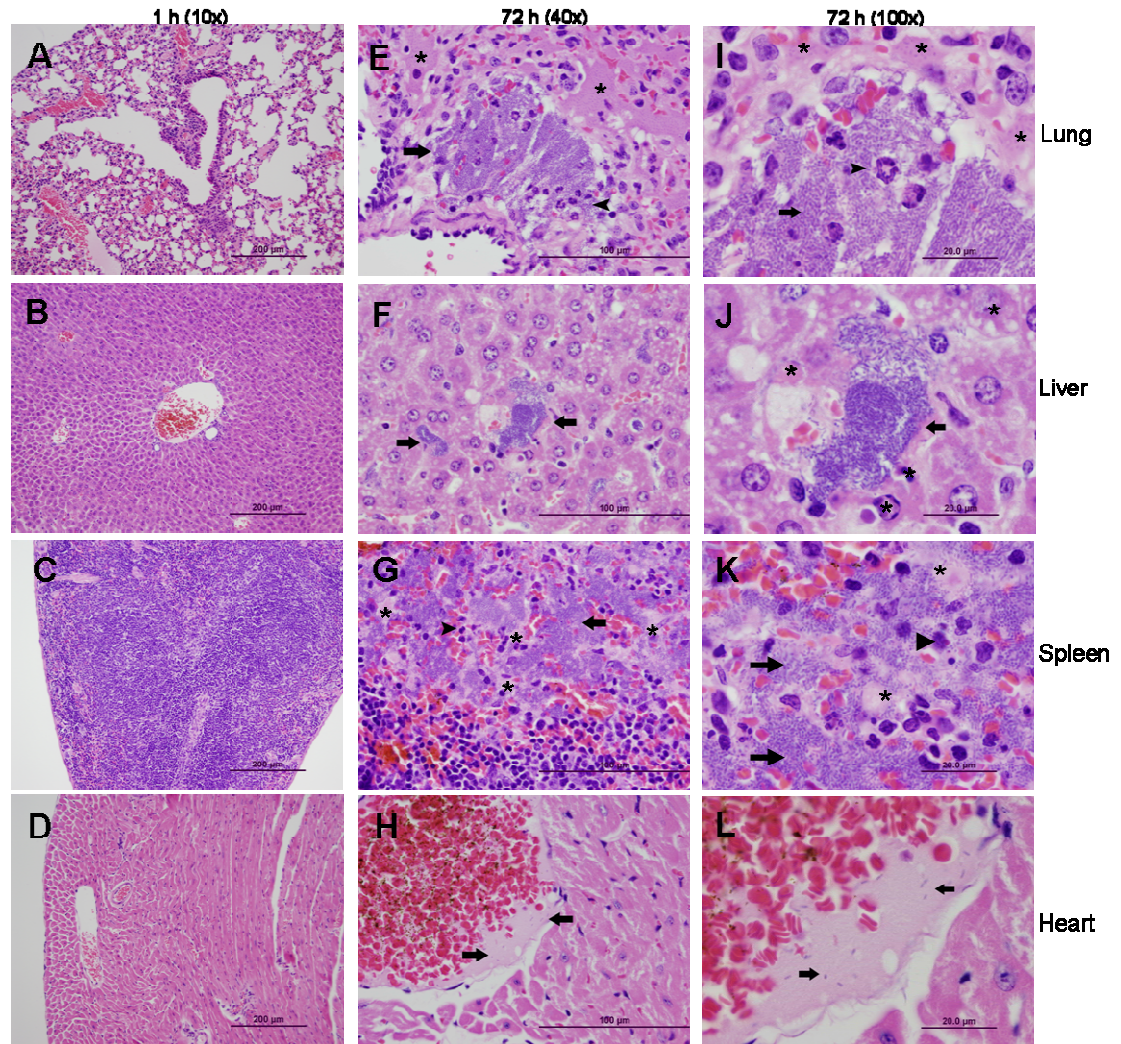


Figure 5.2: Histopathology of mouse tissue 72 h after exposure to aerosolized *Y. pestis*. Panels A-D show tissue samples (lungs, liver, spleen, and heart, respectively) at 1 h following exposure and represent negative controls for this study. At 72 h p.i., the mouse lungs showed large clumps of bacteria (Panels E and I, at arrow) with edema (asterisks) and smaller groups of bacteria. Acute inflammatory cells (at arrowhead) were present within the larger bacterial clump. The livers contained several large clumps of bacteria (Panels F and J,

at arrow) in the parenchyma, and some hepatocytes near the bacteria were necrotic (asterisk). The spleens contained large clumps of bacteria (Panels G and K, at arrow) with edema (asterisks) and necrotic and acute inflammatory cells (at arrowhead). The hearts contained intravascular bacteria (Panels H and L, at arrow) within a blood vessel. In the 10x pictures at 1 h p.i., the bar represents 200  $\mu\text{m}$ . In the 40x pictures at 72 h p.i., the bar represents 100  $\mu\text{m}$  while in the 100x pictures, the bar represents 20  $\mu\text{m}$ . All sections were stained with H&E. Lower magnification data are shown for the control tissues (1 h p.i.) to cover larger areas of the tissues as convincing evidence that there was no pathology seen in these tissues.

At 72 h p.i., the mice exposed to the highest presented dose of bacteria ( $1.3 \times 10^4$  cfu/ml) began to die, and this was reflected in the histopathology of their tissues. The lungs of all mice were inflamed (Fig 5.2, Panels E and I, inflammatory cells at arrowheads) as in the earlier groups, but the reaction was more prominent with edema (see asterisks), and small-to-large groups of bacteria were present (at arrows), characteristics common in pneumonic plague infections (96). All mice had acute inflammatory changes in the liver with necrosis (Panels F and J, at asterisks), the presence of fibrin, and a variable number of rod-shaped bacteria (at arrows). All 5 mice had moderate lymphoid depletion in the white pulp of the spleen and variable numbers of bacteria (Panels G and K, at arrows), with congestion, edema (at asterisks), fibrin and cellular loss in the red pulp. The spleen was also infiltrated with inflammatory cells (at arrowheads). The heart showed occasional intravascular bacteria (Panels H and L, at arrows). We also noted the presence of *Y. pestis* (based on size and morphology) in different organs of infected mice by Giemsa staining.

We noticed a relatively rapid onset of infection, resulting in the death of the animals within 72-96 h p.i after they were exposed to aerosolized *Y. pestis* CO92. This is in agreement with previous studies that indicated the slightest delay of antibiotic (doxycycline, ciprofloxacin, or chloramphenicol) treatment resulted in death from pneumonic plague (77, 96, 109). Our own studies also indicated that if the antibiotic treatment (e.g., levofloxacin) was delayed in mice by 36-48 h after infection with *Y. pestis* CO92 *via* the intranasal route, animals succumbed to infection (data not shown). The histopathology reported herein in this aerosol model was quite similar to that we (158) and others (30, 109) reported, having used the intranasal model, with immediate effects seen in mouse lungs by 24 h p.i., as well as liver and spleen involvement beginning 48 h p.i.. On the contrary, an earlier study that utilized an aerosol model reported no remarkable changes in the livers of infected mice for up to 72 h p.i. (164). These differences between the studies may be due to variations in bacterial strain or dose, mouse strain, or aerosolization conditions (e.g., airflow through the aerosol chamber) (75).

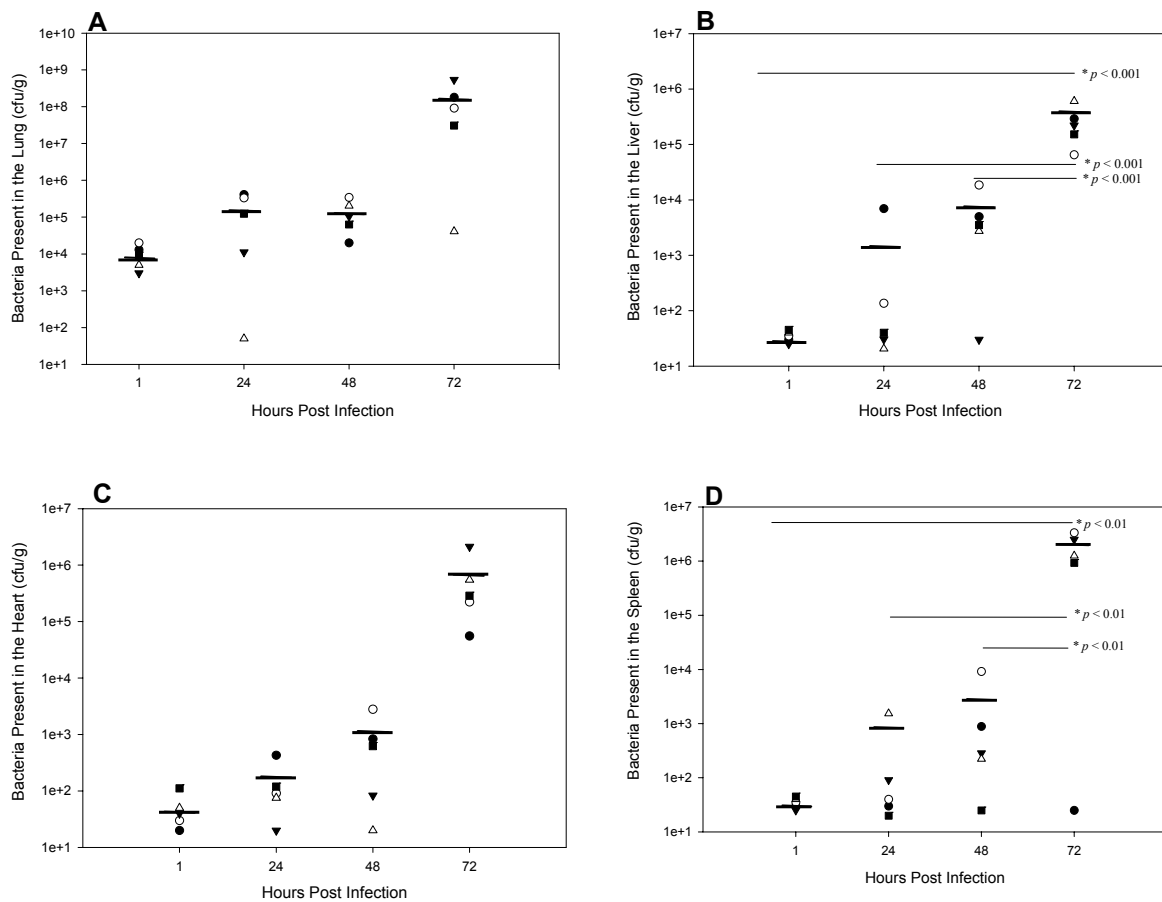
#### **BACTERIAL DISSEMINATION FOLLOWING AEROSOLIZATION OVER A 72-H PERIOD**

At 1, 24, 48, and 72 h p.i. with *Y. pestis* CO92, mice were anesthetized and blood drawn *via* cardiac puncture, after which the animals were euthanized and the organs harvested, homogenized, and cultured on SBA plates, as described in Chapter 2. As expected, a generally upward trend in the number of bacteria was found in different organs, which was indicative of a successful bacterial infection. Bacteria multiplied in the lungs in the first 24 h p.i., having increased in number by 1-2 logs, but the most substantial increase was by 3 logs between 48 h and 72 h p.i. (Fig 5.3A). An increase in the number of bacteria (by

approximately 5 logs) reported at 72 h p.i. was not considered statistically significantly increased compared to bacterial numbers 1-24 h p.i. because of a single mouse in which only a marginal increase in bacterial number was noted when compared to the other 4 mice at 72 h p.i.. Similar changes in bacterial numbers over the course of infection were seen in an earlier aerosol study (165) and in other reports in which mice were infected *via* the intranasal route (30, 109). In contrast, in our most recent intranasal study, we observed an initial drop in the number of bacteria in the lungs of mice by 24 h p.i., but noted similar increases in the numbers of bacteria until 72 h p.i. (158).

A progressive increase in the number of bacteria in other mouse organs, such as the liver (Fig 5.3B), heart (Fig 5.3C), and spleen (Fig 5.3D) was noted over the 72 h infection period, indicating bacterial dissemination throughout the body and multi-organ involvement. The greatest increase in bacterial numbers in these organs was also seen between 48 and 72 h p.i., with statistically significant increases in the liver and spleen between these two timepoints of 48 and 72 h p.i.. As seen in the lungs, a single mouse prevented the increase in bacterial numbers seen in the heart at 72 h p.i. from being statistically significant compared to other earlier time points after infection. Likewise, a significant increase in bacterial numbers cultured from the blood was noted at 72 h p.i. when the latter samples were compared to the 1-h control samples (Fig 5.3E). We believe our inability to culture bacteria from the blood at 24 and 48 h p.i. indicated a rapid dissemination of bacteria to peripheral organs. Alternatively, viable bacteria might be circulating in the bloodstream inside the phagocytic cells, and hence we were unable to detect them at earlier time points of infection. In our future studies, we will compare bacterial growth in serum samples and lysed total leukocytes to validate this hypothesis. However, at 72 h p.i., the infection was overwhelming,

resulting in the detection of a significant number of bacteria in the blood. This multi-organ involvement was noted in previous studies utilizing the intranasal model of pneumonic plague (109, 158) and earlier aerosol models (164, 165).



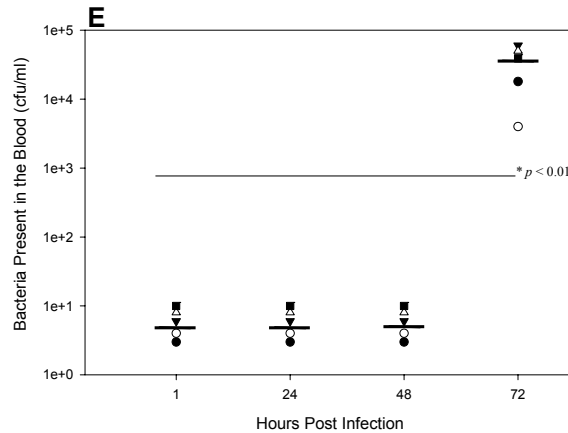


Figure 5.2: Dissemination of *Y. pestis* CO92 through the organs of mice at 1 h and 72 h p.i.. Following aerosolization, 5 mice per group were euthanized at 1, 24, 48, and 72 h p.i. (20 mice total). The lungs (A), liver (B), heart (C), and spleen (D) of each animal were homogenized and the blood (E) collected. All tissues were cultured on SBA plates to assess the kinetics of *Y. pestis* dissemination. Data were plotted on a log scale to allow visualization of all of the data points, however, overlapping at various time points did occur. The detectable limit of bacteria was approximately 80 cfu/g of the tissue. The horizontal bar represents the average number of bacteria present at each time point. The symbols represent different mice at each time point. Significant increases in the number of bacteria over time are indicated with an asterisk, and the  $p$ -values (ANOVA) are indicated in the figure.

### ***IN VIVO* CYTOKINE ANALYSIS**

The organ homogenates and blood from infected mice at 1 and 72 h p.i. were analyzed for cytokine profiles using Bio-Plex, as described in Chapter 2. A key to the

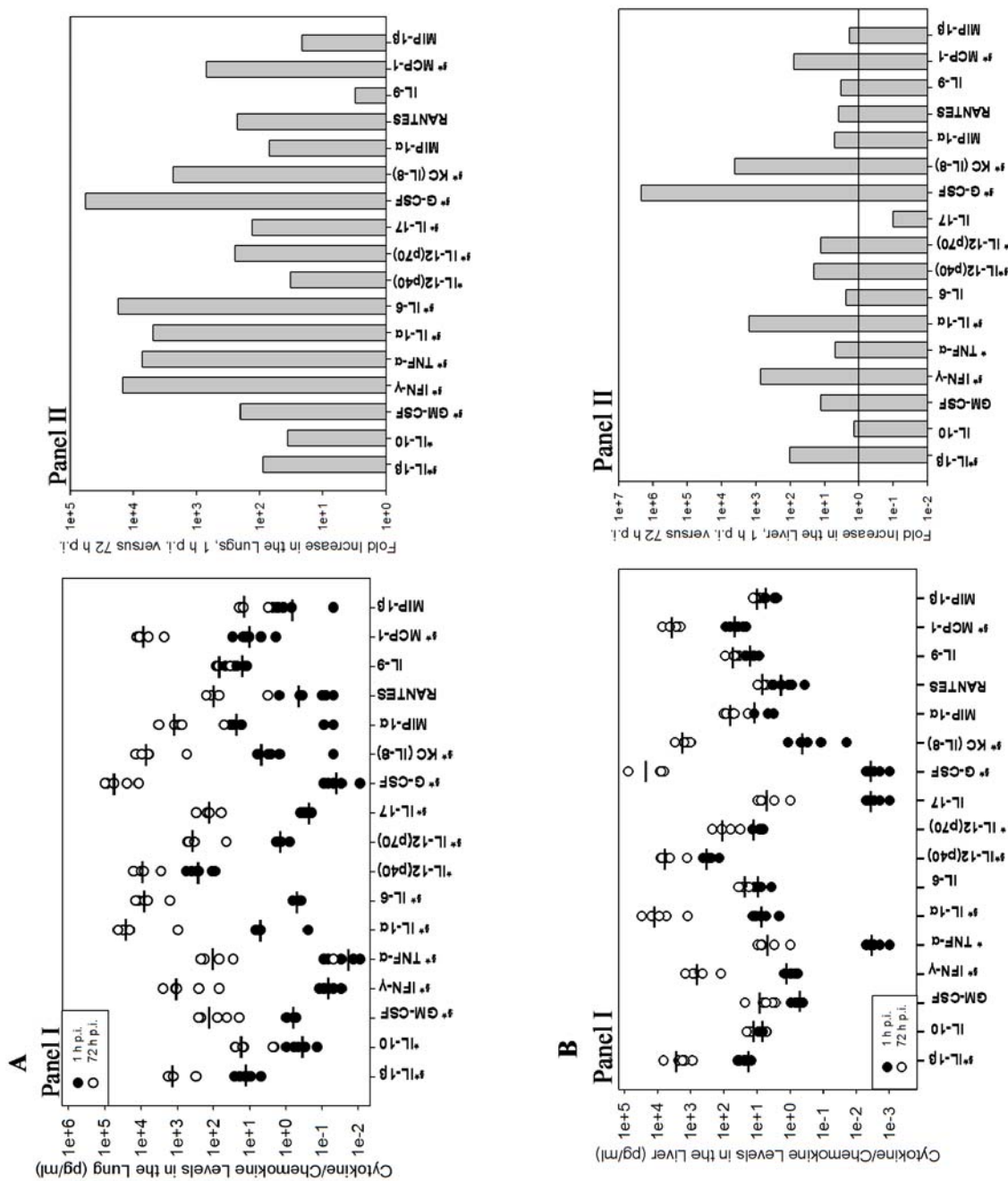
abbreviations and acronyms used for cytokines and chemokines measured in these studies can be found in Table 2.3. We chose to compare the levels of cytokines and chemokines in control animals (1 h p.i.) to 72 h p.i. based on our previous study in which we detected most changes in their levels in the sera at the later time point of 96 h p.i. (158). The sera and tissues from animals 1 h p.i. had similar levels of cytokines and chemokines as noted in the sera and tissues of uninfected (subjected to aerosolization with the diluent alone) control mice. Of the 23 cytokines and chemokines in the Bio-Plex mouse panel, differences were noted in 16 tissue homogenates, as displayed in Fig 5.4. For the remaining 7 cytokines and chemokines on the panel, we noticed either no detectable level at both 1 and 72 h p.i. or the levels were unusually high in the control animals, so these were left out of our analysis. There were statistically significant increases in the concentration of 12 of the cytokines and chemokines detected in the lung homogenates at 72 h p.i. when these samples were compared to a 1-h control sample, while the remaining 4 (MIP-1 $\alpha$ , RANTES, IL-9, and MIP-1 $\beta$ ) showed an increasing trend (Fig 5.4A, Panel I). Cytokines and chemokines that exhibited 100- to 1000-fold or greater increases from 1 h to 72 h p.i. were denoted with the symbol § (Fig 5.4A, Panel II). Specifically of interest were the dramatic increases in proinflammatory cytokines, such as IL-1 $\beta$ , IL-1 $\alpha$ , IFN- $\gamma$ , IL-12p70, TNF- $\alpha$ , and IL-6 at 72 h p.i. compared to their levels in the control. Previous studies utilizing an intranasal model showed similar increases in various cytokines/chemokines (30, 109, 158). Of additional interest were the substantial increases seen in the levels of GM-CSF and G-CSF, which function in the proliferation and survival of monocytes and neutrophils, respectively, as well as of the levels of the chemoattractants MCP-1 (monocytes) and KC, human equivalent of IL-8, (neutrophils).

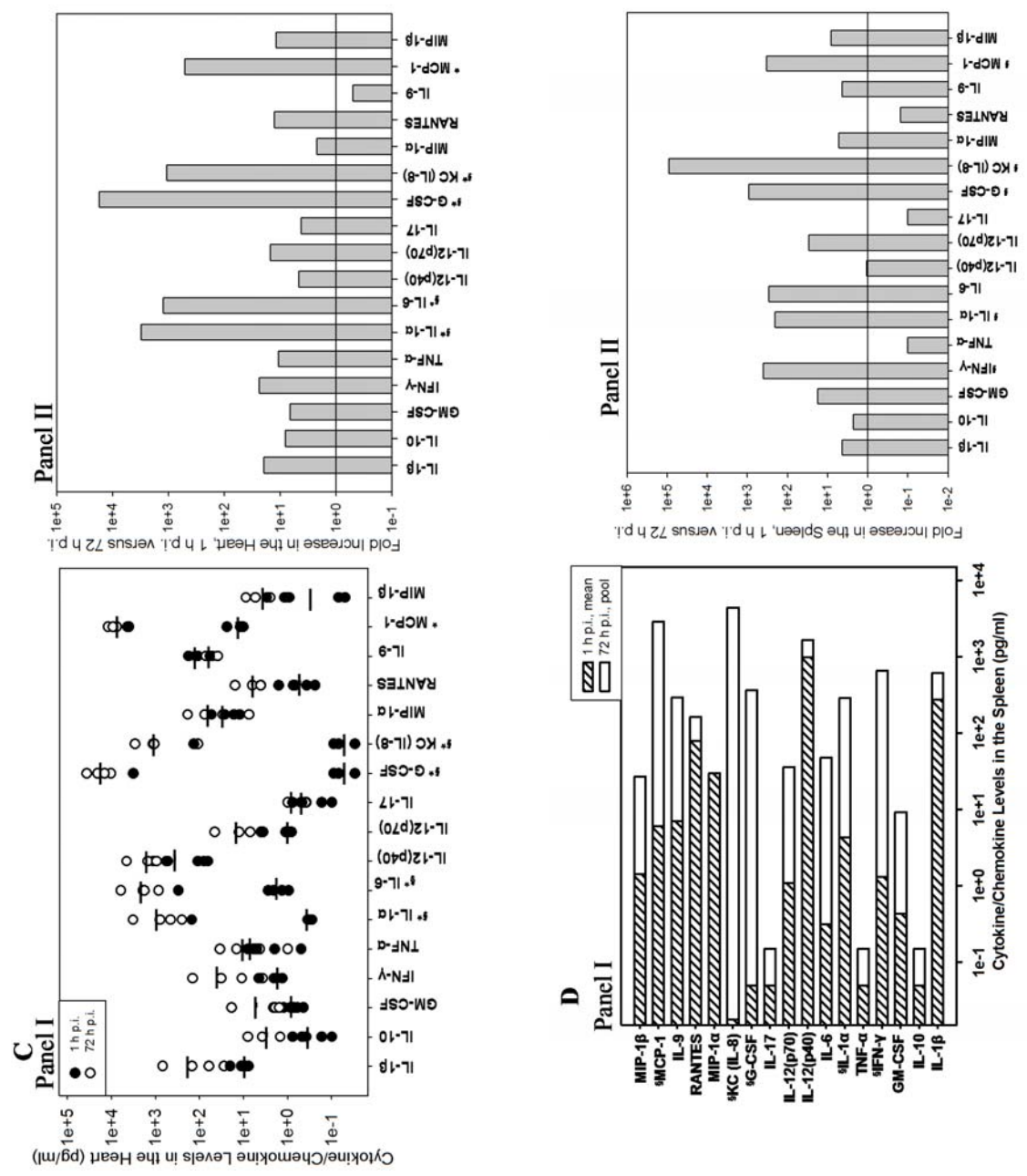


In the liver homogenates (Fig 5.4B, Panel I), we noted significant increases in 7 of the cytokines and chemokines in the panel at 72 h p.i., while most others showed an increasing trend. We observed the most dramatic increases in IL-1 $\beta$ , IL-1 $\alpha$ , IFN- $\gamma$ , IL-12p70, G-CSF and the chemoattractants MCP-1 and KC (100- to 1000-fold or greater, denoted with the symbol §, Fig 5.4B, Panel II). The heart (Fig 5.4C, Panels I and II) also exhibited significant and dramatic increases (100- to 1000-fold or greater, denoted with the symbol §) in the levels of IL-1 $\alpha$ , IL-6, G-CSF, KC, and MCP-1 levels at 72 h p.i. All other cytokine and chemokine levels detected in the heart showed an increasing trend from 1 to 72 h p.i..

The spleen homogenates (Fig 5.4D) and blood samples (Fig 5.4E) of the 5 mice at each time point were pooled, preventing us from statistically analyzing these data. However, we presented typical results from two independent experiments. We had to pool these samples as a result of the thickness of the blood and tissue homogenates due to the development of overwhelming infections, which made it difficult to filter out small samples from each mouse. We noted an upward trend of cytokine/chemokine levels following infection with *Y. pestis* CO92, similar to those seen in the lungs, liver, and heart of mice at 72 h p.i., and which indicated a severe systemic proinflammatory response late in infection. These data were in agreement with our recent studies documenting the effect of *Y. pestis* infection when the bacteria were introduced into mice *via* the intranasal route, as there was an increase in the production of various cytokines/chemokines in the sera (158). Specifically of interest in the spleen were the substantial increases (denoted with the symbol §, and graphed by fold-increase in Figs 5.4D, Panel II and 5.4E, Panel II) in the levels of MCP-1, KC, G-CSF, IL-1 $\alpha$ , and IFN- $\gamma$ , while the blood showed dramatic increases in the levels of the MIP-1 $\beta$ , MIP-1 $\alpha$ , MCP, IL-1 $\beta$ , IL-1 $\alpha$ , IFN- $\gamma$ , IL-12p70, IL-6, KC, and G-CSF at 72 h p.i..

These data indicated that within 72 h after infection, a powerful and systemic recruitment of inflammatory cells and release of proinflammatory cytokines were initiated as a result of infection with aerosolized *Y. pestis*.





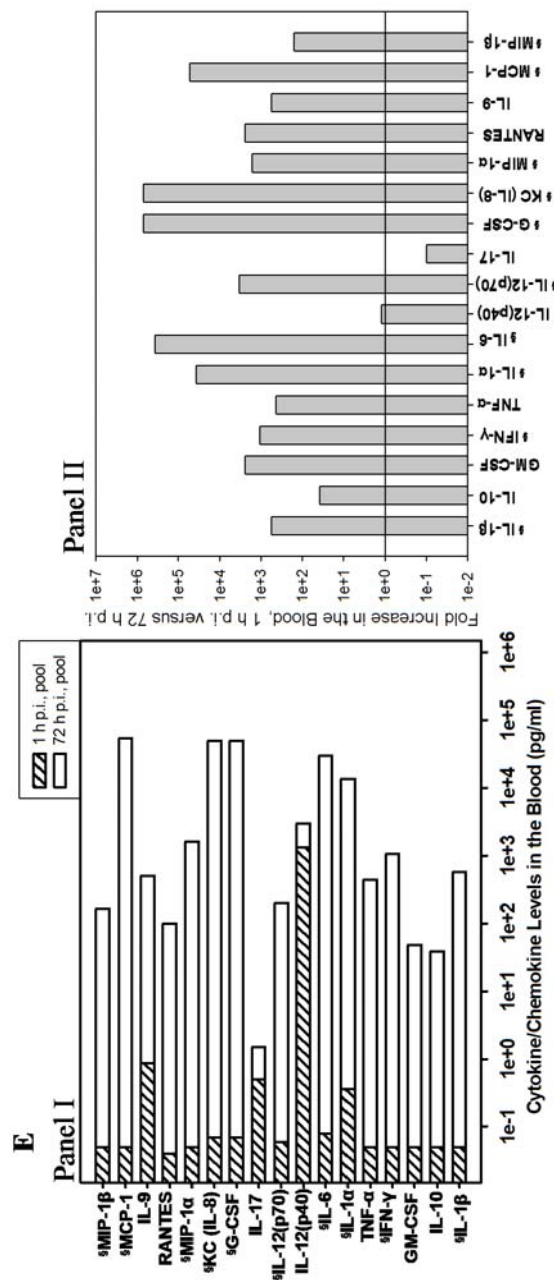


Figure 5.4: Cytokine and chemokine levels in various organ homogenates at 1 h and 72 h p.i.. Following aerosolization, 20 mice were euthanized at 1, 24, 48, and 72 h p.i. (5 mice per group, except where indicated). For cytokine analysis, we examined only tissue homogenates and sera at 1 h and 72 h p.i.. Homogenates of the lungs (A, Panel I), liver (B, Panel I), heart (C, Panel I, 4 mice at 1 h p.i.), and spleen (D, Panel I) and the sera (E, Panel I) of each mouse were analyzed by Bio-Plex for cytokine and chemokine levels. Overlapping of some data points may prevent one from seeing all 5 points (Figs 5.4A-C). The asterisk denotes significant increases in cytokine or chemokine concentration at 72 h p.i. ( $p < 0.05$ , Student's  $t$ -test), and the bar represents the average cytokine or chemokine level at each time point. A

small amount of spleen homogenate at 72 h p.i. required pooling of the samples (Fig 5.4D). Both a lack of sample and moribund mice made it necessary to pool both the 72-h p.i. blood

samples (Fig 5.4E). For consistency, we also pooled the 1-h p.i. samples for this study. Data were plotted on a log scale in order to allow us to visualize all of the data points. The symbol § indicates a 100- to 1000-fold or greater increase in the cytokine/chemokine levels from 1 to 72 h p.i.. Fold-increase of each cytokine and chemokine between these two time points is shown in Fig 5.4A, Panel II through Fig 5.4E, Panel II.

## ***Discussion***

The virulent bacterium *Y. pestis* CO92 causes a severe infection and illness (pneumonia) in humans and animals when given by the inhalation routes. Thus, the present study provided a comprehensive examination of infection kinetics of *Y. pestis* when administered to mice by the aerosol route using whole-body Madison chamber. Tissue damage was evident at 24 h p.i. in the lungs, as assessed by histopathology, and between 48 and 72 h p.i. in peripheral tissues, following both histopathological and proinflammatory cytokine analyses. Bacteria increased in numbers within 24 h p.i. in the lungs and, between 24 and 72 h p.i., disseminated rapidly to the peripheral tissues. These data indicated the model's similarity to the more commonly used intranasal model and the appropriateness of both the inhalational models in studying pneumonic plague. However, to mimic bacterial infection following an intentional release of virulent *Y. pestis* in the environment as a result of bioterrorism, the aerosol model of plague is more suitable for studying progression of the disease. In this report, we have fully characterized the mouse model in terms of bacterial dissemination, histopathology, and cytokine profiling after aerosolization of *Y. pestis* CO92.

## Chapter 6§

### ***Characterization of the Rat Pneumonic Plague Model: Infection Kinetics***

#### ***Following Aerosolization of Yersinia pestis CO92***

*Y. pestis* is spread during natural infection by the fleas of rodents. Historically associated with infected rat fleas, studies on the kinetics of infection in rats are surprisingly few, and these reports have focused mainly on bubonic plague. Although the natural route of primary infection results in bubonic plague in humans, it is commonly thought that aerosolized *Y. pestis* will be utilized during a biowarfare attack. Accordingly, based on our previous characterization of the mouse model of pneumonic plague, we sought to examine the progression of infection in rats exposed in a whole-body Madison chamber to aerosolized *Y. pestis* CO92. The data from this study allowed us to characterize for the first time a rat pneumonic plague model following aerosolization of *Y. pestis*.

### ***Results***

#### **CALCULATION OF THE LD<sub>50</sub> DOSE FOR AEROSOLIZED *Y. PESTIS* CO92 IN THE RAT MODEL**

As this is the first characterization of pneumonic plague in Brown Norway rats, we initially sought to determine the LD<sub>50</sub> of *Y. pestis* CO92 using both intranasal inoculation and aerosol administration, as previously described (5, 133, 158). For intranasal administration, we chose doses ranging from  $1 \times 10^2$  to  $1 \times 10^6$  cfu of *Y. pestis* CO92 and inoculated 10 rats per group. Using these doses and the method published by Reed and Muench (144), we

---

§ Copyright © Elsevier Limited, *Microbes and Infection*, vol 11, p 205-214, 2008. Used with permission.

determined the intranasal LD<sub>50</sub> dose to be approximately 250 cfu in both weight ranges (either 50-75 or 150-175 g) of rats (data not shown), similar to the LD<sub>50</sub> (340 cfu) we reported in Swiss-Webster mice (158).

For aerosol administration, we exposed groups of unanesthetized rats (10 per group and weighing 50-75 g) to 5 different doses of *Y. pestis* CO92 and then monitored them p.i. for mortality (Fig 6-1). We determined after the first experiment that calculation of the LD<sub>50</sub> would rely on 3 of these doses:  $1 \times 10^{10}$ ,  $1 \times 10^9$ , and  $1 \times 10^8$  cfu/ml before aerosolization.

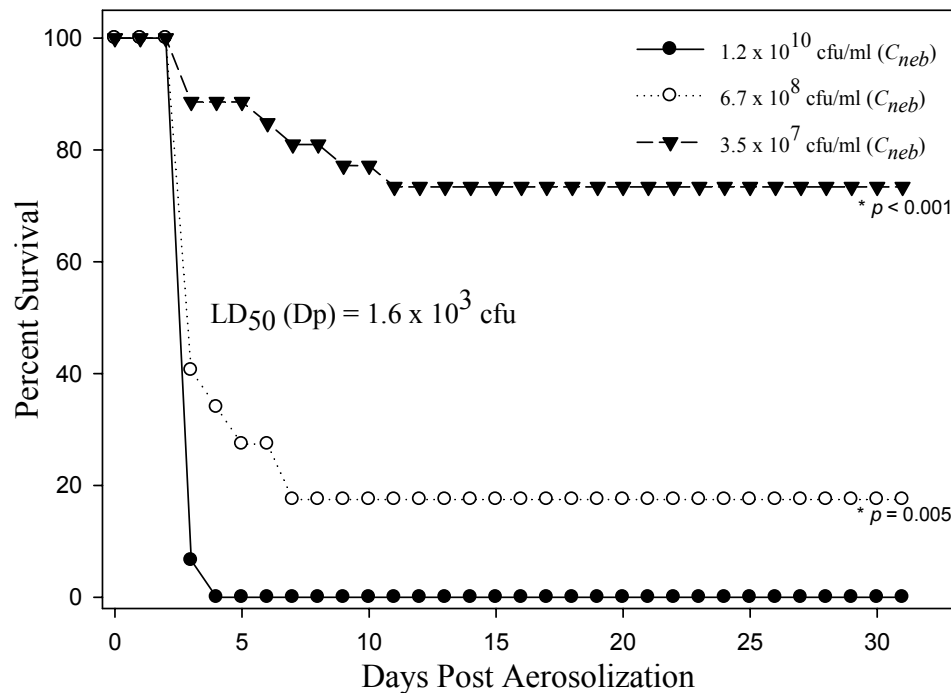


Figure 6.1: Calculating the LD<sub>50</sub> dose in a rat model using aerosolized *Y. pestis* CO92.

Groups of 10 female Brown Norway rats were exposed to different doses of *Y. pestis* ranging from  $1 \times 10^6$  to  $1 \times 10^{10}$  cfu/ml (prior to nebulization) and observed for mortality. The number of bacteria entering the aerosolization

chamber typically dropped by less than 1 log resulting in the indicated concentration after nebulization ( $C_{neb}$ ). Based on the presented dose (Dp), the LD<sub>50</sub> in rats was calculated as  $1.6 \times 10^3$  cfu. The survival rates seen in the  $3.5 \times 10^7$  and  $6.7 \times 10^8$  cfu/ml groups were significant (noted by asterisks) as compared to those in the  $1.2 \times 10^{10}$  cfu/ml group. The  $p$ -values are indicated on the graph.

Data in Fig 6.1 depict the average of 3 experiments using these 3 doses. By culturing the residual suspension after nebulization on SBA plates, we generally observed a loss of less than 1 log in the number of viable bacteria (5), and these doses, called  $C_{neb}$ , were  $1.2 \times 10^{10}$  cfu/ml,  $6.7 \times 10^8$  cfu/ml,  $3.5 \times 10^7$  cfu/ml (averaged from 3 experiments, Fig 6-1). The average presented doses (Dp) of bacteria [3, 12] corresponding to each  $C_{neb}$  were:  $4.4 \times 10^4$ ,  $3.9 \times 10^3$ ,  $2.3 \times 10^2$  cfu, respectively. The calculated LD<sub>50</sub> dose for aerosolized *Y. pestis*, based on the average of the Dp, was  $1.6 \times 10^3$  cfu. Previously, we calculated an LD<sub>50</sub> of  $2.1 \times 10^3$  cfu in mice exposed to aerosolized *Y. pestis* CO92 (5), similar to the dose in rats we noted above. We concluded that a similar number of bacteria were required to achieve pneumonic infection in both mice and rats when bacteria were administered by the aerosol route.

#### **TISSUE INJURY IN RATS RESULTING FROM AEROSOLIZATION OF *Y. PESTIS* CO92**

Brown Norway rats (5 per group) were exposed to an 8.6 LD<sub>50</sub> dose of *Y. pestis* CO92 and sacrificed at 1, 24, 48, and 72 h following aerosolization. The lungs, liver, and spleen were removed, fixed in buffered formalin, and prepared for H & E staining as previously described (5, 158). Uninfected rats (Figs 6.2A through C, Panel A) and animals exposed to



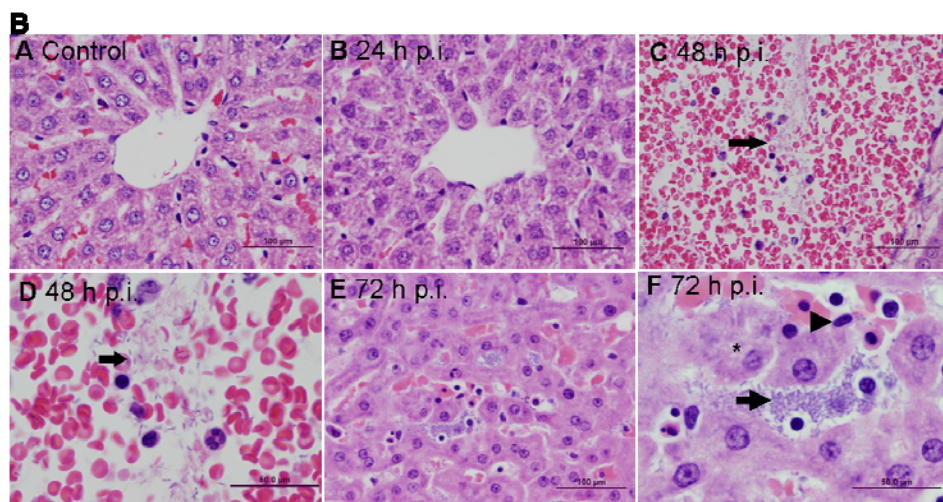
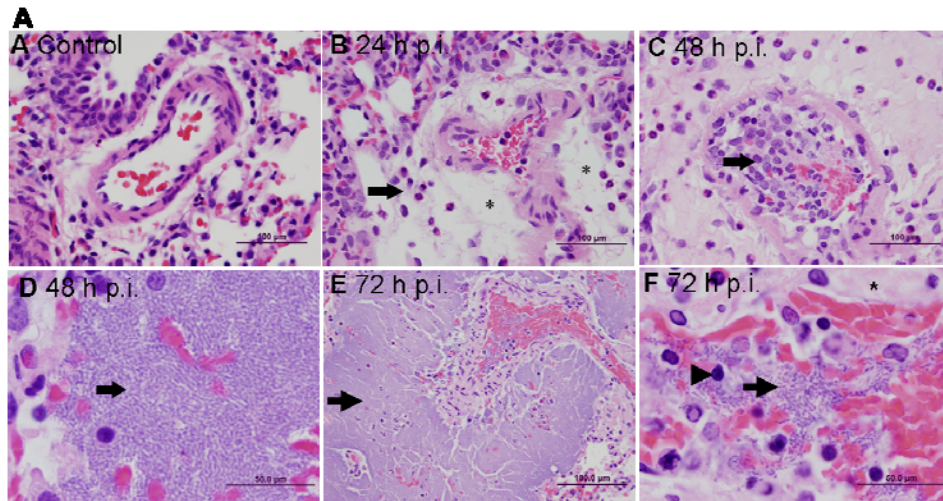
sterile water in the aerosolization chamber (sacrificed at 1 h and 72 h post aerosolization) were used as controls. No difference was found in the histopathology between these three groups of control rats, and, therefore, no alterations in histopathology were attributed to the aerosolization process. At 24 h p.i., all 5 rats showed minimal perivascular edema (Fig 6.2A, Panel B, at asterisk) and acute inflammation (at arrow) in the lungs, and 3 exhibited additional subacute inflammation within the lung parenchyma. Acute inflammation was characterized by the presence of neutrophils while subacute inflammation indicated a mixture of neutrophils and mononuclear cells (e.g., macrophages and lymphocytes). These observations of an influx of neutrophils and mononuclear cells suggest that host lung tissues have initiated an immune response to the bacteria. We noted a similar inflammatory response in the mouse lung following aerosol administration (5), whereas such inflammatory infiltrate was typically not seen before 36 h p.i. following intranasal inoculation of mice (30, 109, 158). No changes were seen in the liver or spleen of rats (Figs 6.2B and C, Panel B) at this time point of 24 h.

The lungs of rats at 48 h p.i. showed a mild-to-moderate perivascular edema and acute inflammation, subacute inflammation in the lung parenchyma, mild leukocytosis (Fig 6.2A, Panel C, at arrow) in blood vessels, a moderate and diffuse bacteremia, and the presence of bacteria in many alveoli (Panel D, at arrow). In 2 of the 5 rats, a mild, multifocal bacteremia was seen in the liver (Fig 6.2B, Panels C and D at arrow). In the spleen at 48 h p.i., all 5 rats had mild-to-moderate numbers of bacteria (Fig 6.2C, Panel D, at arrow), minimal-to-moderate acute inflammation and fibrin (Panels C and D, at asterisks). Bacteria noted were consistent with *Y. pestis*; however, a *Yersinia*-specific staining was not performed. These observations agreed with our recently published report of significant tissue

injury at 48 h following aerosol administration of *Y. pestis* in mice (5). Likewise, subcutaneous inoculation of rats with the virulent *Y. pestis* 195/P strain showed dramatic histopathological changes in spleen after 48 p.i. (155). Significant tissue injury in either lungs (30, 109, 158) or in spleen and liver (158) as well was also noted after intranasal inoculations of mice with *Y. pestis* CO92.

The lungs of rats at 72 h p.i. (Fig 6.2A, Panels E and F) showed mild-to-moderate perivascular and alveolar edema (Panel F, at asterisk), subacute inflammation, mild congestion, leukocytosis in the blood vessels, and mild-to-moderate bacteremia. A degenerate inflammatory cell (at arrowhead) and clumps of bacteria (at arrows) could be seen at the higher magnification in Panel F and at the lower magnification in Panel E. Similar tissue injury was noted in previous reports of mice infected by the aerosol (5) and intranasal (109, 158) routes and is expected given the terminal nature of the animals at this time point of 72 h p.i..

The livers of all of the rats at 72 h p.i. (Fig 6.2B, Panels E and F) showed low bacterial numbers, but clumps of bacteria within sinusoids (Panel F, at arrow), multifocal bacteremia, acute inflammatory cells (degenerate cell at arrowhead), and necrotic hepatocytes (at asterisk). The spleen (Fig 6.2C, Panels E and F) showed evidence of edema (Panel F, at asterisk), acute inflammatory cells (degenerate cell at arrowhead), and moderate numbers of bacteria (at arrow). The histopathology in these rat tissues and in other studies using the mouse as a model system of pneumonic plague 72 h p.i. indicated dissemination of bacteria from the lung to other peripheral organs, such as the spleen and liver (5, 109, 158) and, along with the data from the lung, reflected the terminal nature of these animals at 72 h p.i..



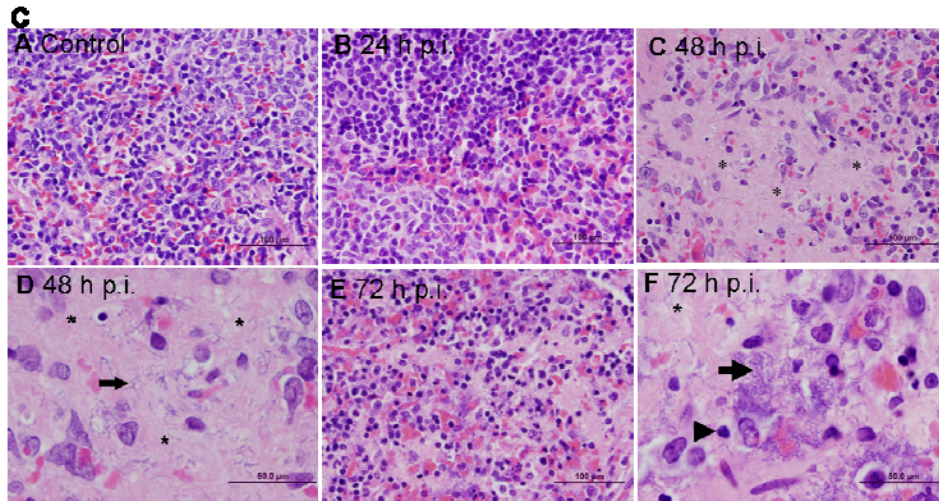


Figure 6.2: Histopathology of rat organs at different time points following aerosolization of *Y. pestis* CO92. Figs 6.2A-C, Panel A, show tissue sections from the lungs, liver, and spleen, respectively, from uninfected animals. The remaining panels represent tissues from infected rats. In the lungs (Fig 6.2A), minimal perivascular edema (Panel B, at asterisk) and acute inflammation (at arrow) were present at 24 h p.i.. At 48 h p.i. (Panels C and D), the lungs showed perivascular edema, acute inflammation, and mild leukocytosis (Panel C, at arrow) in blood vessels, and there were bacteria in many alveoli (Panel D, at arrow). At 72 h p.i. (Panels E and F), the lungs of rats showed clumps of bacteria (at arrows), subacute inflammatory cells (degenerate cell at arrowhead) and edema (at asterisk). In the liver (Fig 6.2B), no changes were seen at 24 h p.i. (Panel B), but 48 h p.i. showed a mild, multifocal bacteremia (Panels C and D at arrow). At 72 h p.i. (Panels E and F), there were clumps of sinusoidal bacteria (Panel F, at arrow), acute inflammatory cells (degenerate cell at arrowhead), and necrotic hepatocytes (at asterisk). In the spleen (Fig

6.2C), no changes were seen at 24 h p.i. (Panel B), but at 48 h p.i. the rats had mild-to-moderate numbers of bacteria (Fig 6.2C, Panel D, at arrow) and fibrin was present (Panels C and D, at asterisks). At 72 h p.i. (Panels E and F), edema was present (Panel F, at asterisk) as were acute inflammatory cells (degenerate cell at arrowhead), and moderate numbers of bacteria in clumps (at arrow). The greatest number of lesions was seen in the lungs, and the spleen had more lesions than did the liver. The bar represents the magnification (50  $\mu$ m – 100  $\mu$ m). All tissue sections were stained with H&E.

#### **DISSEMINATION OF AEROSOLIZED *Y. PESTIS* CO92 IN RAT TISSUES**

To assess the dissemination of *Y. pestis* CO92 to the peripheral organs of the rats, 5 animals per group were sacrificed at 1, 24, 48, and 72 h after aerosolization. The lungs, livers, and spleens were homogenized and dilutions were cultured on SBA plates for 48 h at 28°C to determine the disseminative ability of the bacteria (Fig 6.3).

The average number of bacteria present in the lungs of rats at 1 h p.i. was quite close to the dose of *Y. pestis* presented (8.6 LD<sub>50</sub>) to these animals after aerosolization (Fig 6.3A) indicating the rats received the intended dose of bacteria. We noted approximately a one log increase in bacterial load 24 h p.i. in lungs in the present study. However, between 24 h and 48 h p.i., we noted either a slight decrease or no change in the outgrowth of bacteria in the lungs in our studies of pneumonic plague (either *via* the intranasal or the aerosol route) infection (5, 158). This is in contrast to the findings of other investigators in which bacterial number continued to increase between 24 h and 48 h p.i. (30, 109). Some of these variations could be attributed to different mouse strains and inoculation doses that were used by these investigators (5, 30, 109, 158). By 72 h p.i. (Fig 6.3A), the lungs of rats showed an increase

in the numbers of bacteria by about 2.5 logs. These changes in the lungs of rats over the course of infection were considered statistically significant ( $p < 0.001$ , ANOVA) and complemented the mortality and histopathology data.

Following culturing on SBA plates, no bacteria were detected in the livers of rats at 1 h p.i., but there was at least a 4-log increase in the number of bacteria detected at 24 h p.i. (Fig 6.3B). We also noted dissemination of bacteria from the lungs to the livers of mice 24 h after aerosolization (5), a phenomenon not seen this early in infection following intranasal inoculation of mice (30, 158), suggesting an establishment of severe liver infection earlier using the aerosol model of infection. Bacterial levels in the livers of rats decreased slightly 48 h p.i. in contrast to the increase in levels noted in the mouse model of pneumonic infection (5, 30, 158). Finally by 72 h p.i., bacterial levels in the livers of rats increased substantially (Fig 6.3B). These changes in the livers of rats over the course of infection were considered statistically significant ( $p < 0.05$ , ANOVA).

In the spleens of rats, no bacteria were detected following culture on SBA plates at either the 1 h or 24 h p.i. time points (Fig 6.3C). This is in contrast to the increases in bacterial load we noted in mice 24 h following aerosolization of *Y. pestis* (5). By 48 h p.i., there was a 5-log increase in the number of bacteria detected in the spleens of rats, correlating to the level of tissue injury seen by histological examination at this time. Interestingly, we could detect large increases in bacterial number in the spleens of mice 48 h following aerosol administration (5); however, we were unable to detect bacteria in the spleens of mice 48 h after intranasal inoculation (158). In contrast, other investigators noted increases in bacterial levels in spleens 48 h following intranasal inoculation of mice (30, 109) and subcutaneous inoculation of rats (155) with virulent *Y. pestis*. As mentioned earlier, such

differences could be attributed to different mouse and bacterial strains and animal species used by various investigators (5, 30, 109, 155, 158). By 72 h p.i., the number of bacteria in the spleens of rats increased by another 2.5 logs, and, although not considered statistically significant, there was an upward trend in the number of bacteria as the infection progressed, also correlating to the tissue damage reported based on histopathology at the same time point.

Bacterial dissemination in the blood was also assessed. However, as indicated earlier, the moribund nature of the rats made it difficult to draw blood *via* cardiac puncture at 72 h p.i.. As a result, the latest time point for bacterial dissemination in the blood was 48 h p.i. (Fig 6.3D). No bacteria were detected in the blood in the first 24 h after infection, but the increase in bacterial levels by 48 h p.i. was substantial. The variability in the number of bacteria recovered from individual rats at this time point of 48 h resulted in bacterial number to not be statistically significant in comparison to the levels at 1 h p.i. despite the increase by at least 4 logs between these two timepoints. Overall, these data indicated that animals succumbed to infection either due to pneumonia or subsequent systemic spread of bacteria to different organs or both (158).

It is worth pointing out that *Y. pestis* CO92 is naturally resistant to polymyxin B (36). Consequently, we initially added polymyxin B to tissue homogenate and blood sample dilutions for plating in this dissemination study (Fig 6.3). This approach was followed to obtain more accurate counts of *Y. pestis* away from any potential tissue contaminants, as described in our previous mouse aerosol model study (5). However, we noted that *Y. pestis* CO92 isolated from animal tissues was more susceptible to polymyxin B as measured by the reduced bacterial counts when compared to *Y. pestis*-specific bacteria grown in the absence of this antibiotic. Consequently, bacterial numbers in the tissue homogenates and blood

samples could be under-estimated in the presence of polymyxin B. As a result, we presented the dissemination data in Fig 6.3 in the absence of the antibiotic. As polymyxin B binds to lipopolysaccharide (LPS), the increased susceptibility of *Y. pestis* CO92 *in vivo* to this antibiotic may be due to differential alteration in the structure of LPS and needs to be further explored.

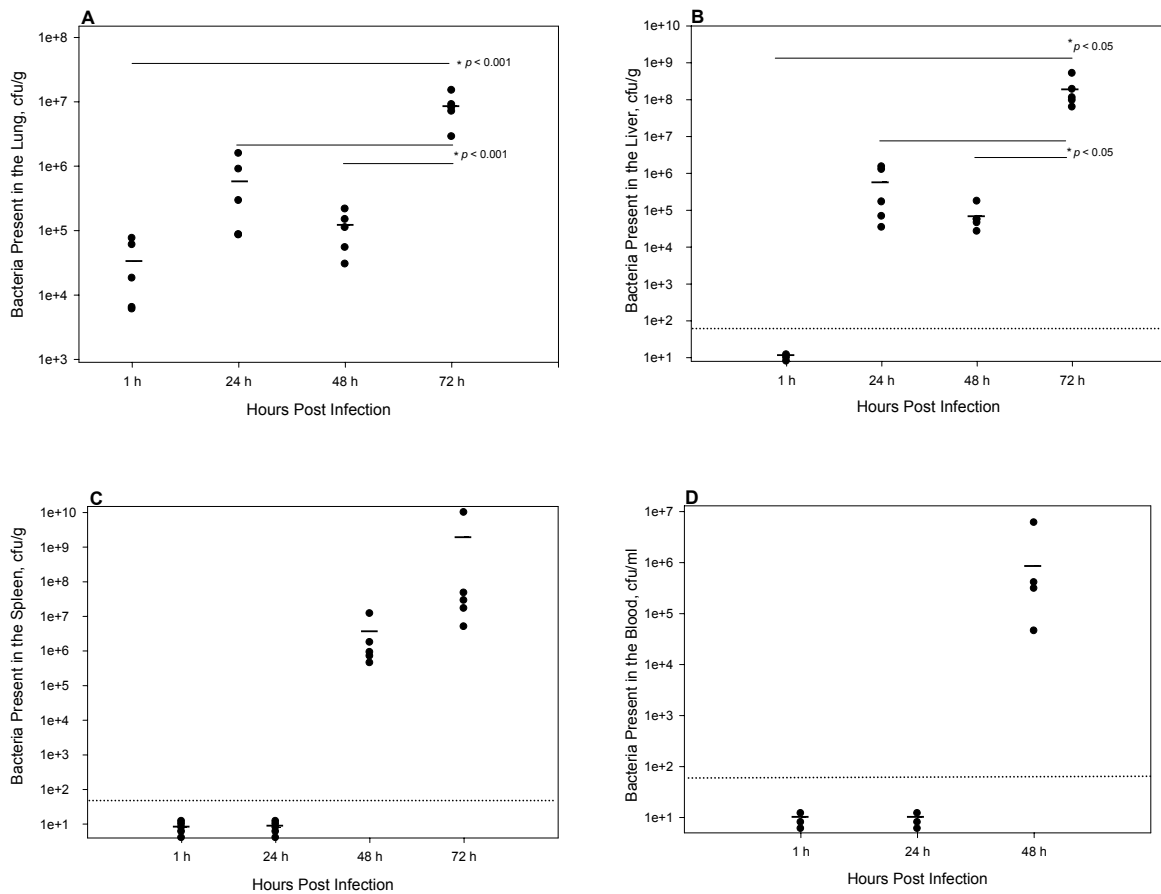


Figure 6.3: Dissemination of bacteria at various time points p.i. with *Y. pestis* CO92 in different organs of rats. At 1, 24, 48, and 72 h after aerosolization, 5 rats were euthanized at each time point, and the lungs (A), liver (B), and spleen (C) of each animal was homogenized. Blood (D) was drawn at 1, 24, and 48 h post



aerosolization. The tissue homogenates and whole blood were cultured on SBA plates, and the numbers of bacterial colonies quantified. Log scale was utilized in assessing the kinetics of infection in order to visualize the data from each of the 5 rats, represented by closed circles at each timepoint. The average number of bacteria in the homogenates at each timepoint is indicated by a horizontal bar. The dotted line in Figs 6.3B-D indicates the limit of detection of bacteria (80-100 cfu) in these samples. An upward trend in bacterial numbers was seen in all of the tissues; however, only data from the lung and liver showed significant increases (ANOVA) over the course of infection. The *p*-values are indicated on the graph.

#### ***IN VIVO* CYTOKINE AND CHEMOKINE ANALYSIS**

In parallel with both the histopathologic and dissemination analyses, tissue homogenates from the rats at 1, 24, 48, and 72 h p.i. were analyzed *via* LINCOplex using a panel of 24 rat cytokines and chemokines as previously described (5, 158). A key to the abbreviations and acronyms for the cytokines and chemokines measured in this study can be found in Table 2.3. Cytokine and chemokine levels from the samples at 1 h p.i. were similar to those from uninfected animals and were used as controls. Between 1 h and 72 h p.i., the most prominent changes occurred in the levels of 10 cytokines and chemokines in the lung, 8 in the liver, and 9 in the sera and spleen (Table 6.1, Fig 6.4). Changes (either increases or decreases) in levels (pg/ml) considered statistically significant (by student's *t*-test) are indicated by an asterisk. The levels of the remaining 14-16 cytokines and chemokines that exhibited little change between time points were not shown in this table.

	Sample	IL-1 $\alpha$	MCP-1	MIP-1 $\alpha$	IL-1 $\beta$	IL-6	IL-9	INF- $\gamma$	IL-17	IL-18	GRO-KC
Lung	1 h p.i.	195.9 $\pm$ 84.0	73.5 $\pm$ 46.0	24.2 $\pm$ 5.6	152.4 $\pm$ 53.6	0.00	47.6 $\pm$ 36.9	0.00	0.00	1599.7 $\pm$ 414.7	342.4 $\pm$ 12.4
	24 h p.i.	102.0 $\pm$ 60.1	1304.2 $\pm$ 1887.8	6.9 $\pm$ 8.3	138.6 $\pm$ 84.3	9.6 $\pm$ 8.2	167.1 $\pm$ 35.84	0.00	0.00	5356.7 $\pm$ 1770.3	643.7 $\pm$ 164.1
	48 h p.i.	1231.8 $\pm$ 731.0	996.2 $\pm$ 885.0	567.2 $\pm$ 136.2	805.2 $\pm$ 45.3	4168.7 $\pm$ 7071.0	254.0 $\pm$ 30.7	2098.4 $\pm$ 1150.3	3.1 $\pm$ 5.0	12281.5 $\pm$ 3828.3	12619.9 $\pm$ 4100.5
	72 h p.i.	2121.8 $\pm$ 1058.7	1301.4 $\pm$ 1048.1	785.4 $\pm$ 268.2	651.1 $\pm$ 56.3	15772.2 $\pm$ 3968.3	179.0 $\pm$ 37.8	1703.9 $\pm$ 506.4	21.7 $\pm$ 20.3	7848.7 $\pm$ 2508.0	17300.2 $\pm$ 1348.2
Liver	1 h p.i.	838.4 $\pm$ 281.2	69.5 $\pm$ 41.9	0.00	94.0 $\pm$ 12.5	177.4 $\pm$ 60.7	77.0 $\pm$ 16.4	74.4 $\pm$ 33.4	0.00	994.2 $\pm$ 75.7	74.3 $\pm$ 7.3
	24 h p.i.	462.0 $\pm$ 150.1	838.0 $\pm$ 829.0	11.5 $\pm$ 4.3	66.4 $\pm$ 16.1	320.2 $\pm$ 167.8	332.8 $\pm$ 58.0	355.6 $\pm$ 136.9	0.00	2746.0 $\pm$ 1212.7	941.6 $\pm$ 183.9
	48 h p.i.	679.7 $\pm$ 193.7	1471.7 $\pm$ 1247.2	83.6 $\pm$ 18.9	253.7 $\pm$ 27.8	309.4 $\pm$ 129.7	435.4 $\pm$ 46.7	1284.8 $\pm$ 278.9	0.00	1223.3 $\pm$ 578.5	2633.0 $\pm$ 482.4
	72 h p.i.	367.5 $\pm$ 176.4	1028.5 $\pm$ 691.6	73.5 $\pm$ 28.9	88.1 $\pm$ 21.5	866.8 $\pm$ 497.1	307.0 $\pm$ 44.0	696.7 $\pm$ 370.7	0.00	673.9 $\pm$ 198.2	3262.8 $\pm$ 775.4
Spleen	1 h p.i.	54.1 $\pm$ 26.3	4.8 $\pm$ 7.0	22.9 $\pm$ 3.3	338.3 $\pm$ 79.1	14.2 $\pm$ 18.5	134.6 $\pm$ 63.6	3.9 $\pm$ 4.7	0.00	2035.6 $\pm$ 520.3	107.2 $\pm$ 9.1
	24 h p.i.	40.1 $\pm$ 14.5	330.9 $\pm$ 487.2	6.4 $\pm$ 4.2	335.4 $\pm$ 111.3	38.2 $\pm$ 12.0	215.1 $\pm$ 51.8	0.00	0.00	8271.1 $\pm$ 2983.6	566.1 $\pm$ 142.6
	48 h p.i.	1772.2 $\pm$ 598.3	836.6 $\pm$ 774.7	311.6 $\pm$ 100.6	812.4 $\pm$ 60.6	209.3 $\pm$ 211.4	263.9 $\pm$ 46.3	8345.5 $\pm$ 1693.6	0.00	12822.6 $\pm$ 4610.1	2935.7 $\pm$ 1161.9
	72 h p.i.	696.9 $\pm$ 355.8	1879.3 $\pm$ 1421.7	397.8 $\pm$ 117.0	240.1 $\pm$ 142.8	567.3 $\pm$ 185.4	43.4 $\pm$ 30.3	1577.4 $\pm$ 1059.1	0.00	2805.3 $\pm$ 3092.7	2370.7 $\pm$ 2343.2

\*Denotes significant changes as compared to 1 h p.i..

Data represent the mean level and standard deviation from 5 rats.

Table 6.1: Cytokine and chemokine levels (pg/ml) in tissues following *Y. pestis* aerosol inoculation.

In the lungs, chemokines such as MIP-1 $\alpha$ , MCP-1, and GRO/KC (similar to KC in mice) were significantly elevated at 48 h p.i. and even more so at 72 h p.i (Table 6.1). These chemokines recruit inflammatory cells to the injured tissue and induce the secretion of proinflammatory cytokines in response to infection. The levels of proinflammatory cytokines such as IL-1 $\alpha$ , IL-6, and IL-17 were all significantly elevated at 72 h p.i.. The lungs were the only tissue in which IL-17 was detected, and, although the level was low with a high standard deviation ( $21.7 \pm 20.3$ ), it was statistically elevated as compared to the level 1 h p.i.. Even though the levels of IL-1 $\beta$ , IL-9, and IFN- $\gamma$  were all significantly elevated above control at 72 h p.i., the peak levels occurred at 48 h p.i..

Interestingly, there was an increase in the level of IL-18 at 24 h p.i. in lungs, with an additional increase at 48 h p.i., followed by a drop at 72 h p.i.. IL-18 plays a role in inducing T cells to produce IFN- $\gamma$ , and the latter facilitates activation of macrophages in response to infection. By 72 h p.i., however, immune systems of the rats were unable to compete with the bacterial infection. Similar drastic increases in most cytokines/chemokines were seen late in infection in the lung homogenates and bronchoalveolar lavage fluid (BALF) of mice inoculated intranasally, and this delay in the proinflammatory response was thought to be controlled by the T3SS effectors encoded by genes located on the virulence plasmid, pCD1 (30, 109).

Similar elevations in cytokines and chemokines late in infection were seen in the liver, spleen, and serum, indicating a delay in the innate immune response that is necessary to successfully fight the bacterial infection. In the liver, MIP-1 $\alpha$  and MCP-1 were significantly elevated at 48 h p.i. and dropped at 72 h p.i., while GRO/KC reached its highest level at 72 h p.i.. Proinflammatory cytokines IL-9 and IFN- $\gamma$  were significantly elevated at 48 h p.i., but

incurred a slight decrease at 72 h p.i. while still maintaining levels significantly above that of the control. The level of IL-6 was statistically the highest at 72 h p.i.. The level of IL-1 $\alpha$  began dropping at 24 h p.i., and, after showing a slight increase at 48 h p.i., dropped to below the control level at 72 h p.i.. Both IL-18 and IL-1 $\beta$  increased above control levels at 24 h or 48 h p.i. and then decreased at 72 h p.i. to a level below control. No IL-17 was detected in the liver.

In the spleen, MIP-1 $\alpha$  and MCP-1 levels were significantly higher than that of the control at 72 h p.i., while GRO/KC reached its peak level 48 h p.i.. Both IFN- $\gamma$  and IL-1 $\alpha$  peaked at 48 h p.i. and, while their levels at 72 h p.i. decreased, they were still above the control levels. Interestingly, IL-1 $\beta$ , IL-9, and IL-18 showed their highest levels at 48 h p.i. and then decreased to either close-to (IL-18) or below (IL-1 $\beta$  and IL-9) control levels at 72 h p.i. IL-6 showed a gradual increase and peaked at 72 h p.i.. No IL-17 was detected in the spleen. While most proinflammatory cytokines increased by 72 h p.i., some decreased compared to the 48-h levels possibly as a result of their rapid degradation.

Additionally, blood was drawn and sera isolated from rats at 1, 24, and 48 h p.i. for analysis of cytokine and chemokine levels. At 24 h p.i., significant increases (by at least one log) in levels above control were seen in IL-1 $\alpha$ , MCP-1, IL-9, and GRO/KC (data not shown) indicating the initiation of cell recruitment, proliferation, and proinflammatory cytokine release that would significantly increase by 48 h p.i.. These cytokines and chemokines in addition to MIP-1 $\alpha$ , IL-1 $\beta$ , IL-6, and IFN- $\gamma$  were all significantly increased by 1.5-2 logs at 48 h p.i. (Fig 6.4), while IL-18 showed an increase above 1-h control that was not considered significant. Substantial increases in IFN- $\gamma$  levels were noted in the sera of rats in this study (Fig 6.4) as well as 48-72 h following subcutaneous inoculation of rats (155).

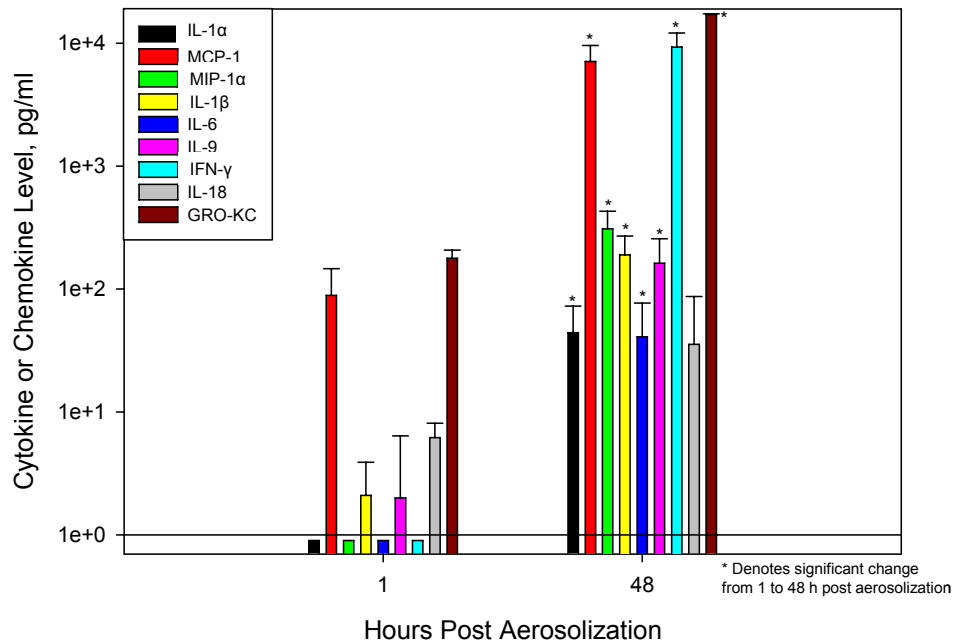


Figure 6.4 LINCOp $lex$  analysis of cytokine and chemokine levels at 1 h and 48 h post aerosolization with *Y. pestis* CO92 in rat sera. In parallel with the bacterial dissemination experiment, blood was drawn at 1 h, 24 h, and 48 h following aerosolization from 5 rats per group, and the sera were analyzed by LINCOp $lex$  for cytokine and chemokine levels. Of the 24 cytokines and chemokines tested, there were increases in 9 of these in the sera of rats. The increases in 8 cytokines and chemokines were considered significant (denoted by an asterisk,  $p < 0.05$ , student's  $t$  –test). The solid line indicates the limit of detection of cytokine and chemokines in these samples. Data were plotted on a log scale to better assess the changes between 1-h and 48-h samples. The data for the 24 h time point are not shown.

Most interestingly, we observed marginal increases in TNF- $\alpha$  in the lung and spleen homogenates of rats unlike the significant changes we observed in the lungs, liver, and sera of mice following aerosolization of *Y. pestis* (5). Likewise, increases in TNF- $\alpha$  were reported in the sera from 4 of 8 rats following subcutaneous inoculation (155) as well as in the BALF and lung homogenates following the intranasal inoculation of mice with *Y. pestis* (30, 109). We were intrigued by this finding because TNF- $\alpha$  is an important indicator of a proinflammatory response to infection. Further studies are needed to confirm these results and to demonstrate the role of TNF- $\alpha$  in *Y. pestis*-associated pneumonic infections in rats.

#### **PASSIVE TRANSMISSION OF *Y. PESTIS***

To assess the transmission of *Y. pestis* between rats, animals were intranasally challenged with 2 doses of WT *Y. pestis* CO92 and housed one uninfected rat to two infected rats per cage (3 cages per challenge dose) immediately following challenge. We chose the intranasal route of infection because aerosol administration leaves droplets of *Y. pestis* on the fur of the animals, which would allow the transmission of the bacteria from infected to uninfected animals to occur by other routes (e.g., grooming). At 72 h p.i., all rats infected with a 2500 LD<sub>50</sub> dose succumbed to infection, while by day 6, the 25 LD<sub>50</sub> challenged group showed 62% mortality in this experiment. At 5 and 9 days after infection, 1 of 3 uninfected rats from each challenge group (the 2500 LD<sub>50</sub> and 25 LD<sub>50</sub> doses of WT *Y. pestis* CO92, respectively) also succumbed to infection. Culturing of liver and lung homogenates on SBA plates and PCR analysis of single colonies from these plates revealed that these rats died as a result of an overwhelming *Y. pestis* infection, indicating that transmission had occurred from infected to uninfected rats. In both cases, bacteria were present in the lungs and the liver

between 6 and 7 logs. Coughing in *Bordetella pertussis*-infected rats has been previously reported (83), and we speculate that transmission of *Y. pestis* in our study may have occurred as a result of rats coughing, although one cannot rule out transmission of infection following grooming or licking of the nasal secretions and/or by biting of uninfected rats by the infected ones. We did not observe any of the above-mentioned behaviors during the course of infection, but the fact that only 2 of the 6 (33%) uninfected rats succumbed to infection by passive transmission may be explained either by previous studies describing the mechanism of coughing in rats (18, 83) or by other mechanisms, e.g., grooming, licking nasal secretions, etc.

It is thought that the source of the cough in rats is laryngeal instead of tracheobronchial (18) suggesting that bacteria in the deepest areas of the lungs may not be mechanically transmitted in this way. Further, it is possible that the rodent nasal turbinate anatomy, unlike that of primates, would significantly reduce generation of aerosolized droplets *via* coughing. Additionally, in a study of the coughing mechanism in *B. pertussis*-infected rats using voice-activated recordings, Hall et al concluded Brown Norway rats cough less frequently than other species of rats (83). Although this report did not discuss potential mechanisms for the transmission of the bacteria, coughing is the most likely scenario for a respiratory pathogen to be transmitted directly between animals. Certainly, more information is needed to better understand the mechanism of transmission of *Y. pestis* from infected to uninfected animals.

## ***Discussion***

This study, a partner to our previous report (5), is the first to document the kinetics of infection following the aerosolization of *Y. pestis* CO92 in a rat model. The rat model of bubonic plague has not been routinely used in *Y. pestis* pathogenesis studies, most likely because there was a general belief that a considerable variation exists in the susceptibility to plague among individual rats (44). However, recent studies showed that the rat bubonic plague model was suitable for characterizing the progression and kinetics of infection, as well as for examining the host immune response to *Y. pestis* (111, 155, 157). We chose to use the Brown Norway rat for our studies because the immunology and genetics of this rat species are well characterized (74).

The LD<sub>50</sub> doses of *Y. pestis* CO92 we calculated for intranasal inoculation and aerosol administration in rats were similar to those we noted in the respective mouse models of pneumonic infection. Furthermore, we noted numbers of bacteria similar to the inoculation dose in the lungs of rats 1 h after aerosolization. Assessment of tissue damage via histopathology and bacterial dissemination analysis indicated a severe inflammatory response and bacterial presence resulting in mortality beginning at 72 h p.i. Interestingly, in both the rat and mouse aerosol (5) models of infection, histopathologic changes were seen in the lungs 24 h p.i.. In contrast, studies in which animals were challenged via the intranasal route, such histopathological changes were noted only after 48 h (30, 109, 158). These data indicated that aerosol administration of bacteria initiates alteration in lung pathology early during infection and could be important in disease progression in humans during bioterrorist attack.



Additionally, in our models of pneumonic infection (aerosol or intranasal), we noted little change in the numbers of bacteria isolated from the lungs of mice [3, 4] and rats until 48 h p.i., while other investigators noted substantial increases in bacterial load in the lungs between 24 and 48 h p.i. (30, 109). Importantly, we noted dissemination of bacteria to the peripheral organs (e.g., liver and spleen) within 24-48 h in mouse and rat aerosol model of pneumonic plague, which was in contrast to their delayed appearance in these tissues when animals were challenged via the intranasal route (30, 109, 158). It is possible that, due to the nature of the intranasal technique, not all of the intended bacteria enter through the nares. Based on this, we speculate that the aerosol inoculation method is a more accurate representation of pneumonic illness.

Cytokine profiling revealed a complementary proinflammatory response later in infection. These animals developed a severe infection and died between 72 h and 96 h after aerosolization due either to pneumonia or multiorgan failure or both. We also noted that a larger number of proinflammatory mediators were induced following aerosol administration of *Y. pestis* in both rats and mice (5) than were noted following the intranasal inoculation of mice (158) after using similar cytokine/chemokine panels. The lag in proinflammatory response we noted early in infection followed by an overwhelming response late during infection was similar, as also reported by other investigators with some variations expected due to differences in animal species, strains of *Y. pestis* used, and modes of inoculation. Taken together, our data from histopathology, bacterial dissemination, and cytokine profiling suggest that aerosol administration of bacteria in animals might represent a better way to study the kinetics of pneumonic disease progression in humans.

Finally, we could demonstrate direct transmission of plague bacteria from infected to uninfected animals housed in the same cage. Rats, unlike mice, do cough and we speculate that transmission of infection occurred via aerosol droplets. Irrespective of the mode of transmission, this experiment is interesting and important because direct transmission of pneumonic plague in rodents, by whatever mechanism, could be important ecologically in natural rodent reservoirs.

In summary of these data, we conclude that the rat, which often has been associated with outbreaks of human urban plague, is a valuable model in which to study microbial pathogenesis, host response, and the efficacy of new medical countermeasures against plague using multiple administration routes (155). Currently, there is no vaccine available against plague. Therefore, for testing new therapeutics and vaccines against this deadly pathogen, well characterized rodent models are needed before new modalities could be tested in non-human primates and humans.

## Chapter 7

### *Future Directions*

Future studies in our laboratory will involve investigating the mechanism by which the  $\Delta lpp$  mutants (both with and without the pPCP1 plasmid) were unable to survive within the hostile macrophage environment. We performed a comparison of the overall gene expression profile between WT and the  $\Delta lpp$  mutant via GeneChip analysis using cDNA from the organs of infected mice. We noted a 2-3 fold decrease in the expression of *gsrA*, a gene responsible for the intracellular response mechanism in *Yersinia* (188, 189), and we are in the process of expressing this gene in *trans* in the  $\Delta lpp$  mutant to demonstrate if intracellular survival is recovered *in vitro*.

Additionally, as *pla* is more important in establishing a disseminating infection in bubonic plague and because we saw a more discernable attenuation of our  $\Delta lpp$  mutant following s.c. administration of the bacteria, testing our *Y. pestis* CO92 pPCP/ $\Delta lpp$  mutant strain in the bubonic mouse and rat models may provide some interesting insight into the pathogenesis of bubonic infection.

### *Concluding Remarks*

The virulent bacterium *Y. pestis* CO92 causes a severe infection and illness (pneumonia) in humans and animals when given by the inhalation routes. Through the course of these studies on the pathogenesis of *Y. pestis* CO92, a new virulence factor (Lpp) was identified, the impact deletion of plasmid pPCP1 and Lpp have on the virulence and dissemination of *Y. pestis* was investigated, and the disease progression following

aerosolization of *Y. pestis* was characterized in two rodent models. In summary of these studies, we conclude that these data have expanded our knowledge base on the pathogenesis of *Y. pestis* infections, most specifically the pneumonic form of the disease.

## Bibliography

1. **Achtman, M., G. Morelli, P. Zhu, T. Wirth, I. Diehl, B. Kusecek, A. J. Vogler, D. M. Wagner, C. J. Allender, W. R. Easterday, V. Chenal-Francisque, P. Worsham, N. R. Thomson, J. Parkhill, L. E. Lindler, E. Carniel, and P. Keim.** 2004. Microevolution and history of the plague bacillus, *Yersinia pestis*. *Proc Natl Acad Sci* **101**:17837-17842.
  
2. **Achtman, M., K. Zurth, G. Morelli, G. Torrea, A. Guiyoule, and E. Carniel.** 1999. *Yersinia pestis*, the cause of plague, is a recently emerged clone of *Yersinia pseudotuberculosis*. *Proc Natl Acad Sci* **96**:14043-14048.
  
3. **Agar, S. L., J. Sha, W. B. Baze, T. Erova, S. M. Foltz, G. Suarez, S. Wang, and A. K. Chopra.** 2009. Deletion of chromosomal Braun lipoprotein gene (lpp) and curing of plasminogen activating protease (Pla)-encoding plasmid dramatically alter the virulence of *Yersinia pestis* CO92 in a pneumonic mouse plague model. *Microbiology* **Submitted**.
  
4. **Agar, S. L., J. Sha, S. M. Foltz, T. E. Erova, K. G. Walberg, W. B. Baze, G. Suarez, J. W. Peterson, and A. K. Chopra.** 2008. Characterization of the rat pneumonic plague model: infection kinetics following aerosolization of *Yersinia pestis* CO92. *Microbes Infect* **11**:205-214.
  
5. **Agar, S. L., J. Sha, S. M. Foltz, T. E. Erova, K. G. Walberg, T. E. Parham, W. B. Baze, G. Suarez, J. W. Peterson, and A. Chopra.** 2008. Characterization of a mouse model of plague after aerosolization of *Yersinia pestis* CO92. *Microbiology* **154**:1939-1948.
  
6. **Aliprantis, A. O., R. B. Yang, M. R. Mark, S. Suggett, B. Devaux, J. D. Radolf, G. R. Klimpel, P. Godowski, and A. Zychlinsky.** 1999. Cell activation and apoptosis by bacterial lipoproteins through toll-like receptor-2. *Science* **285**:736-739.
  
7. **Anderson, G. W., Jr., S. E. Leary, E. D. Williamson, R. W. Titball, S. L. Welkos, P. L. Worsham, and A. M. Friedlander.** 1996. Recombinant V antigen protects mice against pneumonic and bubonic plague caused by F1-capsule-positive and -negative strains of *Yersinia pestis*. *Infect Immun* **64**:4580-4585.
  
8. **Andrews, G. P., D. G. Heath, G. W. Anderson, Jr., S. L. Welkos, and A. M. Friedlander.** 1996. Fraction 1 capsular antigen (F1) purification from *Yersinia pestis* CO92 and from an *Escherichia coli* recombinant strain and efficacy against lethal plague challenge. *Infect Immun* **64**:2180-2187.

9. **Anisimov, A. P., I. V. Bakhteeva, E. A. Panfertsev, T. E. Svetoch, T. B. Kravchenko, M. E. Platonov, G. M. Titareva, T. I. Kombarova, S. A. Ivanov, A. V. Rakin, K. K. Amoako, and S. V. Dentovskaya.** 2009. The subcutaneous inoculation of pH 6 antigen mutants of *Yersinia pestis* does not affect virulence and immune response in mice. *J Med Microbiol* **58**:26-36.
10. **Anisimov, A. P., L. E. Lindler, and G. B. Pier.** 2004. Intraspecific diversity of *Yersinia pestis*. *Clin Microbiol Rev* **17**:434-464.
11. **Anisimov, A. P., R. Z. Shaikhutdinova, L. N. Pan'kina, V. A. Feodorova, E. P. Savostina, O. V. Bystrova, B. Lindner, A. N. Mokrievich, I. V. Bakhteeva, G. M. Titareva, S. V. Dentovskaya, N. A. Kocharova, S. N. Senchenkova, O. Holst, Z. L. Devdariani, Y. A. Popov, G. B. Pier, and Y. A. Knirel.** 2007. Effect of deletion of the *lpxM* gene on virulence and vaccine potential of *Yersinia pestis* in mice. *J Med Microbiol* **56**:443-453.
12. **Bacot, A. W., and C. J. Martin.** 1914. Observation on the mechanism of the transmission of plague by fleas. *J Hyg (Lond) plague suppl* **3**:423-439.
13. **Badger, J. L., and V. L. Miller.** 1995. Role of RpoS in survival of *Yersinia enterocolitica* to a variety of environmental stresses. *J Bacteriol* **177**:5370-5373.
14. **Bahmanyar, M., and D. C. Cavanaugh.** 1976. Plague Manual. World Health Organization, Geneva, Switzerland.
15. **Baskin, H., Y. Dogan, I. H. Bahar, and N. Yulug.** 2002. Effect of subminimal inhibitory concentrations of three fluoroquinolones on adherence of uropathogenic strains of *Escherichia coli*. *Int J Antimicrob Agents* **19**:79-82.
16. **Bearden, S. W., J. D. Fetherston, and R. D. Perry.** 1997. Genetic organization of the yersiniabactin biosynthetic region and construction of avirulent mutants in *Yersinia pestis*. *Infect Immun* **65**:1659-1668.
17. **Beesley, E. D., R. R. Brubaker, W. A. Janssen, and M. J. Surgalla.** 1967. Pesticins III. Expression of coagulase and mechanism of fibrinolysis. *J Bacteriol* **94**:19-26.
18. **Belvisi, M. G., and D. C. Bolser.** 2002. Summary: animal models for cough. *Pulm Pharmacol Ther* **15**:249-250.

19. **Ben-Efraim, S., M. Aronson, and L. Bichowsky-Slomnicki.** 1961. New antigenic component of *Pasteurella pestis* formed under specified conditions of pH and temperature. *J Bacteriol* **81**:704-714.
20. **Ben-Gurion, R., and A. Shafferman.** 1981. Essential virulence determinants of different *Yersinia* species are carried on a common plasmid. *Plasmid* **5**:183-187.
21. **Bergmann, S., and S. Hammerschmidt.** 2007. Fibrinolysis and host response in bacterial infections. *Thromb Haemost* **98**:512-520.
22. **Bernadac, A., M. Gavioli, J.-C. Lazzaroni, S. Raina, and R. Lloubes.** 1998. *Escherichia coli tol-pal* mutants form outer membrane vesicles. *J Bacteriol* **180**:4872-4878.
23. **Bichowsky-Slomnicki, L., and S. Ben-Efraim.** 1963. Biological activities in extracts of *Pasteurella pestis* and their relation to the "pH 6 antigen". *J Bacteriol* **86**:101-111.
24. **Boland, A., and G. R. Cornelis.** 1998. Role of YopP in suppression of tumor necrosis factor alpha release by macrophages during *Yersinia* infection. *Infect Immun* **66**:1878-1884.
25. **Brice, G. T., N. L. Graber, S. L. Hoffman, and D. L. Doolan.** 2001. Expression of the chemokine MIG is a sensitive and predictive marker for antigen-specific, genetically restricted IFN-[gamma] production and IFN-[gamma]-secreting cells. *J of Immunol Methods* **257**:55-69.
26. **Brubaker, R. R.** 1991. Factors promoting acute and chronic diseases caused by yersiniae. *Clin Microbiol Rev* **4**:309-324.
27. **Brubaker, R. R.** 2007. How the structural gene products of *Yersinia pestis* relate to virulence. *Future Microbiol* **2**:377-385.
28. **Brubaker, R. R.** 1969. Mutation rate to nonpigmentation in *Pasteurella pestis*. *J Bacteriol* **98**:1404-1406.
29. **Brubaker, R. R., E. D. Beesley, and M. J. Surgalla.** 1965. *Pasteurella pestis*: role of pesticin I and iron in experimental plague. *Science* **149**:422-424.

30. **Bubeck, S. S., A. M. Cantwell, and P. H. Dube.** 2007. Delayed inflammatory response to primary pneumonic plague occurs in both outbred and inbred mice. *Infect Immun* **75**:697-705.
31. **Burrows, T. W., and S. Jackson.** 1956. The pigmentation of *Pasteurella pestis* on a defined medium containing haemin. *Br J Exp Pathol* **37**:570-576.
32. **Burrows, T. W., and S. Jackson.** 1956. The virulence-enhancing effect of iron on nonpigmented mutants of virulent strains of *Pasteurella pestis*. *Br J Exp Pathol* **37**:577-583.
33. **Butler, T.** 1983. *Plague and Other Yersinia Infections*. Plenum Press, New York, NY.
34. **Carsiotis, M., D. L. Weinstein, H. Karch, I. A. Holder, and A. D. O'Brien.** 1984. Flagella of *Salmonella typhimurium* are a virulence factor in infected C57BL/6J mice. *Infect Immun* **46**:814-818.
35. **Cascales, E., A. Bernadac, M. Gavioli, J.-C. Lazzaroni, and R. Lloubes.** 2002. Pal lipoprotein of *Escherichia coli* plays a major role in outer membrane integrity. *J Bacteriol* **184**:754-759.
36. **Cathelyn, J. S., S. D. Crosby, W. W. Lathem, W. E. Goldman, and V. L. Miller.** 2006. RovA, a global regulator of *Yersinia pestis*, specifically required for bubonic plague. *Proc Natl Acad Sci* **103**:13514-13519.
37. **Cavanaugh, D. C.** 1971. Specific effect of temperature upon transmission of the plague bacillus by the oriental rat flea, *Xenopsylla cheopis*. *Am J Trop Med Hyg* **20**:264-273.
38. **Cavanaugh, D. C., and R. Randall.** 1959. The role of multiplication of *Pasteurella Pestis* in mononuclear phagocytes in the pathogenesis of flea-borne plague. *J Immunol* **83**:348-363.
39. **CDC** 2006, posting date. CDC Plague Home Page. Centers for Disease Control and Prevention, <http://www.cdc.gov/ncidod/dvbid/plague/>, Accessed January 7, 2007.
40. **Chain, P. S., E. Carniel, F. W. Larimer, J. Lamerdin, P. O. Stoutland, W. M. Regala, A. M. Georgescu, L. M. Vergez, M. L. Land, V. L. Motin, R. R. Brubaker, J. Fowler, J. Hinnebusch, M. Marceau, C. Medigue, M. Simonet, V. Chenal-Francisque, B. Souza, D. Dacheux, J. M. Elliott, A. Derbise, L. J. Hauser, and E. Garcia.** 2004. Insights into the



evolution of *Yersinia pestis* through whole-genome comparison with *Yersinia pseudotuberculosis*. Proc Natl Acad Sci **101**:13826-13831.

41. **Chain, P. S., P. Hu, S. A. Malfatti, L. Radnedge, F. Larimer, L. M. Vergez, P. Worsham, M. C. Chu, and G. L. Andersen.** 2006. Complete genome sequence of *Yersinia pestis* strains Antiqua and Nepal516: evidence of gene reduction in an emerging pathogen. J Bacteriol **188**:4453-4463.
42. **Charnetzky, W. T., and W. W. Shuford.** 1985. Survival and growth of *Yersinia pestis* within macrophages and an effect of the loss of the 47-megadalton plasmid on growth in macrophages. Infect Immun **47**:234-241.
43. **Chauvaux, S., M. L. Rosso, L. Frangeul, C. Lacroix, L. Labarre, A. Schiavo, M. Marceau, M. A. Dillies, J. Foulon, J. Y. Coppee, C. Medigue, M. Simonet, and E. Carniel.** 2007. Transcriptome analysis of *Yersinia pestis* in human plasma: an approach for discovering bacterial genes involved in septicemic plague. Microbiology **153**:3112-3124.
44. **Chen, T. H., and K. F. Meyer.** 1974. Susceptibility and antibody response of *Rattus* species to experimental plague. J Infect Dis **129**:Suppl:S62-71.
45. **Coligan, J., B. Dunn, D. Speicher, and P. Wingfield.** 2002. Current Protocols in Protein Science. John Wiley and Sons, Inc, New York, NY.
46. **Cornelis, G. R.** 2002. *Yersinia* type III secretion: send in the effectors. J Cell Biol **158**:401-408.
47. **Cornelis, G. R.** 2002. The *Yersinia* Ysc-Yop virulence apparatus. Int J Med Microbiol **291**:455-462.
48. **Cornelis, G. R., A. Boland, A. P. Boyd, C. Geuijen, M. Iriarte, C. Neyt, M. P. Sory, and I. Stainier.** 1998. The virulence plasmid of *Yersinia*, an antihost genome. Microbiol Mol Biol Rev **62**:1315-1352.
49. **Darby, C., J. W. Hsu, N. Ghorri, and S. Falkow.** 2002. *Caenorhabditis elegans*: plague bacteria biofilm blocks food intake. Nature **417**:243-244.
50. **DeBord, K. L., D. M. Anderson, M. M. Marketon, K. A. Overheim, R. W. DePaolo, N. A. Ciletti, B. Jabri, and O. Schneewind.** 2006. Immunogenicity and protective immunity

against bubonic plague and pneumonic plague by immunization of mice with the recombinant V10 antigen, a variant of LcrV. *Infect Immun* **74**:4910-4914.

51. **Degen, J. L., T. H. Bugge, and J. D. Goguen.** 2007. Fibrin and fibrinolysis in infection and host defense. *J Thromb Haemost* **5 Suppl 1**:24-31.
52. **Deng, W., V. Burland, G. Plunkett, 3rd, A. Boutin, G. F. Mayhew, P. Liss, N. T. Perna, D. J. Rose, B. Mau, S. Zhou, D. C. Schwartz, J. D. Fetherston, L. E. Lindler, R. R. Brubaker, G. V. Plano, S. C. Straley, K. A. McDonough, M. L. Nilles, J. S. Matson, F. R. Blattner, and R. D. Perry.** 2002. Genome sequence of *Yersinia pestis* KIM. *J Bacteriol* **184**:4601-4611.
53. **Devignat, R.** 1951. Varieties of *Pasteurella pestis*; new hypothesis. *Bull World Health Organ* **4**:247-263.
54. **Doll, J. M., P. S. Zeitz, P. Ettestad, A. L. Bucholtz, T. Davis, and K. Gage.** 1994. Cat-transmitted fatal pneumonic plague in a person who traveled from Colorado to Arizona. *Am J Trop Med Hyg* **51**:109-114.
55. **Drancourt, M., V. Roux, L. V. Dang, L. Tran-Hung, D. Castex, V. Chenal-Francisque, H. Ogata, P. E. Fournier, E. Crubezy, and D. Raoult.** 2004. Genotyping, *Yersinia pestis*-like *Yersinia pestis*, and plague pandemics. *Emerg Infect Dis* **10**:1585-1592.
56. **Duplaix, N.** 1988. Fleas - the lethal leapers. *Natl Geogr* **173**:672-694.
57. **Edwards, R. A., L. H. Keller, and D. M. Schifferli.** 1998. Improved allelic exchange vectors and their use to analyze 987P fimbria gene expression. *Gene* **207**:149.
58. **Eisen, R. J., S. W. Bearden, A. P. Wilder, J. A. Montenieri, M. F. Antolin, and K. L. Gage.** 2006. Early-phase transmission of *Yersinia pestis* by unblocked fleas as a mechanism explaining rapidly spreading plague epizootics. *Proc Natl Acad Sci* **103**:15380-15385.
59. **Eisen, R. J., and K. L. Gage.** 2009. Adaptive strategies of *Yersinia pestis* to persist during inter-epizootic and epizootic periods. *Vet Res* **40**:1.
60. **Ernst, R. K., T. Guina, and S. I. Miller.** 1999. How intracellular bacteria survive: surface modifications that promote resistance to host innate immune responses. *J Infect Dis* **179 Suppl 2**:S326-330.

61. **Fadl, A. A., J. Sha, G. R. Klimpel, J. P. Olano, C. L. Galindo, and A. K. Chopra.** 2005. Attenuation of *Salmonella enterica* serovar Typhimurium by altering biological functions of murein lipoprotein and lipopolysaccharide. *Infect Immun* **73**:8433-8436.
62. **Fadl, A. A., J. Sha, G. R. Klimpel, J. P. Olano, D. W. Niesel, and A. K. Chopra.** 2005. Murein lipoprotein is a critical outer membrane component involved in *Salmonella enterica* serovar Typhimurium systemic infection. *Infect Immun* **73**:1081-1096.
63. **FDA.** 2005. Center for Drug Evaluation and Research: Levaquin (levofloxacin) Information US Food and Drug Administration and the Department and Health and Human Services, <http://www.fda.gov/cder/drug/infopage/levaquin/default.htm>, Accessed October 12, 2007.
64. **Feodorova, V. A., L. N. Pan'kina, E. P. Savostina, L. V. Sayapina, V. L. Motin, S. V. Dentovskaya, R. Z. Shaikhutdinova, S. A. Ivanov, B. Lindner, A. N. Kondakova, O. V. Bystrova, N. A. Kocharova, S. N. Senchenkova, O. Holst, G. B. Pier, Y. A. Knirel, and A. P. Anisimov.** 2007. A *Yersinia pestis* *lpxM*-mutant live vaccine induces enhanced immunity against bubonic plague in mice and guinea pigs. *Vaccine* **25**:7620-7628.
65. **Ferber, D. M., and R. R. Brubaker.** 1979. Mode of action of pesticin: N-acetylglucosaminidase activity. *J Bacteriol* **139**:495-501.
66. **Ferber, D. M., and R. R. Brubaker.** 1981. Plasmids in *Yersinia pestis*. *Infect Immun* **31**:839-841.
67. **Fetherston, J. D., P. Schuetze, and R. D. Perry.** 1992. Loss of the pigmentation phenotype in *Yersinia pestis* is due to the spontaneous deletion of 102 kb of chromosomal DNA which is flanked by a repetitive element. *Mol Microbiol* **6**:2693-2704.
68. **Finegold, M. J., J. J. Petery, R. F. Berendt, and H. R. Adams.** 1968. Studies on the pathogenesis of plague. Blood coagulation and tissue responses of *Macaca mulatta* following exposure to aerosols of *Pasteurella pestis*. *Am J Pathol* **53**:99-114.
69. **Forman, S., A. G. Bobrov, O. Kirillina, S. K. Craig, J. Abney, J. D. Fetherston, and R. D. Perry.** 2006. Identification of critical amino acid residues in the plague biofilm Hms proteins. *Microbiology* **152**:3399-3410.
70. **Frey, J.** 2007. Biological safety concepts of genetically modified live bacterial vaccines. *Vaccine* **25**:5598-5605.

71. **Gage, K. L., and M. Y. Kosoy.** 2005. Natural history of plague: perspectives from more than a century of research. *Annu Rev Entomol* **50**:505-528.
72. **Galimand, M., A. Guiyoule, G. Gerbaud, B. Rasoamanana, S. Chanteau, E. Carniel, and P. Courvalin.** 1997. Multidrug resistance in *Yersinia pestis* mediated by a transferable plasmid. *N Engl J Med* **337**:677-680.
73. **Garcia, E., Y. A. Nedialkov, J. Elliott, V. L. Motin, and R. R. Brubaker.** 1999. Molecular characterization of KatY (antigen 5), a thermoregulated chromosomally encoded catalase-peroxidase of *Yersinia pestis*. *J Bacteriol* **181**:3114-3122.
74. **Gibbs, R. A., G. M. Weinstock, M. L. Metzker, D. M. Muzny, E. J. Sodergren, S. Scherer, G. Scott, D. Steffen, K. C. Worley, P. E. Burch, et al.** 2004. Genome sequence of the Brown Norway rat yields insights into mammalian evolution. *Nature* **428**:493-521.
75. **Glynn, A., C. J. Roy, B. S. Powell, J. J. Adamovicz, L. C. Freytag, and J. D. Clements.** 2005. Protection against aerosolized *Yersinia pestis* challenge following homologous and heterologous prime-boost with recombinant plague antigens. *Infect Immun* **73**:5256-5261.
76. **Grabenstein, J. P., M. Marceau, C. Pujol, M. Simonet, and J. B. Bliska.** 2004. The response regulator PhoP of *Yersinia pseudotuberculosis* is important for replication in macrophages and for virulence. *Infect Immun* **72**:4973-4984.
77. **Gradon, J. D.** 2002. Plague pneumonia. *Curr Infect Dis Rep* **4**:244-248.
78. **Greenfield, R. A. M., D. A. M. Drevets, L. J. M. Machado, G. W. M. Voskuhl, P. M. Cornea, and M. S. M. Bronze.** 2002. Bacterial pathogens as biological weapons and agents of bioterrorism. *Am J Med Sci* **323**:299-315.
79. **Griffiths, E.** 1987. Iron in biological systems, p. 1-25. *In* J. J. Bullen and E. Griffiths (ed.), *Iron and Infection: Molecular, Physiological, and Clinical Aspects*. John Wiley & Sons, New York, NY.
80. **Groisman, E. A.** 2001. The pleiotropic two-component regulatory system PhoP-PhoQ. *J Bacteriol* **183**:1835-1842.

81. **Guiyoule, A., G. Gerbaud, C. Buchrieser, M. Galimand, L. Rahalison, S. Chanteau, P. Courvalin, and E. Carniel.** 2001. Transferable plasmid-mediated resistance to streptomycin in a clinical isolate of *Yersinia pestis*. *Emerg Infect Dis* **7**:43-48.
82. **Guyton, A. C.** 1947. Measurement of the respiratory volumes of laboratory animals. *Am J Physiol* **150**:70-77.
83. **Hall, E., R. Parton, and A. C. Wardlaw.** 1997. Differences in coughing and other responses to intrabronchial infection with *Bordetella pertussis* among strains of rats. *Infect Immun* **65**:4711-4717.
84. **Hantke, K., and V. Braun.** 1973. Covalent binding of lipid to protein. Diglyceride and amide-linked fatty acid at the N-terminal end of the murein-lipoprotein of the *Escherichia coli* outer membrane. *Eur J Biochem* **34**:284-296.
85. **Heath, D. G., G. W. Anderson, Jr., J. M. Mauro, S. L. Welkos, G. P. Andrews, J. Adamovicz, and A. M. Friedlander.** 1998. Protection against experimental bubonic and pneumonic plague by a recombinant capsular F1-V antigen fusion protein vaccine. *Vaccine* **16**:1131-1137.
86. **Heesemann, J.** 1987. Chromosomal-encoded siderophores are required for mouse virulence of enteropathogenic *Yersinia* species. *FEMS Microbiol Lett* **48**:229-233.
87. **Hill, J., J. E. Eyles, S. J. Elvin, G. D. Healey, R. A. Lukaszewski, and R. W. Titball.** 2006. Administration of antibody to the lung protects mice against pneumonic plague. *Infect Immun* **74**:3068-3070.
88. **Hinnebusch, B. J.** 2003. Transmission factors: *Yersinia pestis* genes required to infect the flea vector of plague. *Adv Exp Med Biol* **529**:55-62.
89. **Hinnebusch, B. J., and D. L. Erickson.** 2008. *Yersinia pestis* biofilm in the flea vector and its role in the transmission of plague. *Curr Top Microbiol Immunol* **322**:229-248.
90. **Hinnebusch, B. J., E. R. Fischer, and T. G. Schwan.** 1998. Evaluation of the role of the *Yersinia pestis* plasminogen activator and other plasmid-encoded factors in temperature-dependent blockage of the flea. *J Infect Dis* **178**:1406-1415.

91. **Hinnebusch, B. J., R. D. Perry, and T. G. Schwan.** 1996. Role of the *Yersinia pestis* hemin storage (*hms*) locus in the transmission of plague by fleas. *Science* **273**:367-370.
92. **Hinnebusch, B. J., A. E. Rudolph, P. Cherepanov, J. E. Dixon, T. G. Schwan, and A. Forsberg.** 2002. Role of *Yersinia* murine toxin in survival of *Yersinia pestis* in the midgut of the flea vector. *Science* **296**:733-735.
93. **Hinnebusch, J., P. Cherepanov, Y. Du, A. Rudolph, J. D. Dixon, T. Schwan, and A. Forsberg.** 2000. Murine toxin of *Yersinia pestis* shows phospholipase D activity but is not required for virulence in mice. *Int J Med Microbiol* **290**:483-487.
94. **Hu, P., J. Elliott, P. McCready, E. Skowronski, J. Garnes, A. Kobayashi, R. R. Brubaker, and E. Garcia.** 1998. Structural organization of virulence-associated plasmids of *Yersinia pestis*. *J Bacteriol* **180**:5192-5202.
95. **Huang, X. Z., M. P. Nikolich, and L. E. Lindler.** 2006. Current trends in plague research: from genomics to virulence. *Clin Med Res* **4**:189-199.
96. **Inglesby, T. V., D. T. Dennis, D. A. Henderson, J. G. Bartlett, M. S. Ascher, E. Eitzen, A. D. Fine, A. M. Friedlander, J. Hauer, J. F. Koerner, M. Layton, J. McDade, M. T. Osterholm, T. O'Toole, G. Parker, T. M. Perl, P. K. Russell, M. Schoch-Spana, and K. Tonat.** 2000. Plague as a biological weapon: medical and public health management. Working Group on Civilian Biodefense. *JAMA* **283**:2281-2290.
97. **Iriarte, M., and G. R. Cornelis.** 1995. MyfF, an element of the network regulating the synthesis of fibrillae in *Yersinia enterocolitica*. *J Bacteriol* **177**:738-744.
98. **Janssen, W. A., and M. J. Surgalla.** 1969. Plague bacillus: survival within host phagocytes. *Science* **163**:950-952.
99. **Jones, T., J. J. Adamovicz, S. L. Cyr, C. R. Bolt, N. Bellerose, L. M. Pitt, G. H. Lowell, and D. S. Burt.** 2006. Intranasal Protollin/F1-V vaccine elicits respiratory and serum antibody responses and protects mice against lethal aerosolized plague infection. *Vaccine* **24**:1625-1632.
100. **Kienle, Z., L. Emody, C. Svanborg, and P. W. O'Toole.** 1992. Adhesive properties conferred by the plasminogen activator of *Yersinia pestis*. *J Gen Microbiol* **138 Pt 8**:1679-1687.

101. **Kim, T.-J., S. Chauhan, V. L. Motin, E.-B. Goh, M. M. Igo, and G. M. Young.** 2007. Direct transcriptional control of the plasminogen activator gene of *Yersinia pestis* by the cyclic AMP receptor protein. *J Bacteriol* **189**:8890-8900.
102. **Koornhof, H. J., R. A. Smego, Jr., and M. Nicol.** 1999. Yersiniosis. II: The pathogenesis of *Yersinia* infections. *Eur J Clin Microbiol Infect Dis* **18**:87-112.
103. **Kukkonen, M., K. Lahteenmaki, M. Suomalainen, N. Kalkkinen, L. Emody, H. Lang, and T. K. Korhonen.** 2001. Protein regions important for plasminogen activation and inactivation of alpha2-antiplasmin in the surface protease Pla of *Yersinia pestis*. *Mol Microbiol* **40**:1097-1111.
104. **Kukkonen, M., M. Suomalainen, P. Kyllonen, K. Lahteenmaki, H. Lang, R. Virkola, I. M. Helander, O. Holst, and T. K. Korhonen.** 2004. Lack of O-antigen is essential for plasminogen activation by *Yersinia pestis* and *Salmonella enterica*. *Mol Microbiol* **51**:215-225.
105. **Kutyrev, V., R. J. Mehig, V. L. Motin, M. S. Pokrovskaya, G. B. Smirnov, and R. R. Brubaker.** 1999. Expression of the plague plasminogen activator in *Yersinia pseudotuberculosis* and *Escherichia coli*. *Infect Immun* **67**:1359-1367.
106. **Kutyrev, V. V., A. A. Filippov, O. S. Oparina, and O. A. Protsenko.** 1992. Analysis of *Yersinia pestis* chromosomal determinants Pgm<sup>+</sup> and Pst<sup>s</sup> associated with virulence. *Microb Pathog* **12**:177.
107. **Lahteenmaki, K., M. Kukkonen, S. Jaatinen, M. Suomalainen, H. Soranummi, R. Virkola, H. Lang, and T. K. Korhonen.** 2003. *Yersinia pestis* Pla has multiple virulence-associated functions. *Adv Exp Med Biol* **529**:141-145.
108. **Lahteenmaki, K., R. Virkola, A. Saren, L. Emody, and T. K. Korhonen.** 1998. Expression of plasminogen activator Pla of *Yersinia pestis* enhances bacterial attachment to the mammalian extracellular matrix. *Infect Immun* **66**:5755-5762.
109. **Lathem, W. W., S. D. Crosby, V. L. Miller, and W. E. Goldman.** 2005. Progression of primary pneumonic plague: a mouse model of infection, pathology, and bacterial transcriptional activity. *Proc Natl Acad Sci* **102**:17786-17791.

110. **Lathem, W. W., P. A. Price, V. L. Miller, and W. E. Goldman.** 2007. A plasminogen-activating protease specifically controls the development of primary pneumonic plague. *Science* **315**:509-513.
111. **Lemaitre, N., F. Sebbane, D. Long, and B. J. Hinnebusch.** 2006. *Yersinia pestis* YopJ suppresses tumor necrosis factor alpha induction and contributes to apoptosis of immune cells in the lymph node but is not required for virulence in a rat model of bubonic plague. *Infect Immun* **74**:5126-5131.
112. **Lien-Teh, W.** 1926. A Treatise on Pneumonic Plague. League of Nations Health Organisation, Geneva, Switzerland.
113. **Lillard, J. W., Jr., S. W. Bearden, J. D. Fetherston, and R. D. Perry.** 1999. The haemin storage (Hms+) phenotype of *Yersinia pestis* is not essential for the pathogenesis of bubonic plague in mammals. *Microbiology* **145** ( Pt 1):197-209.
114. **Lindler, L. E., M. S. Klempner, and S. C. Straley.** 1990. *Yersinia pestis* pH 6 antigen: genetic, biochemical, and virulence characterization of a protein involved in the pathogenesis of bubonic plague. *Infect Immun* **58**:2569-2577.
115. **Lindler, L. E., G. V. Plano, V. Burland, G. F. Mayhew, and F. R. Blattner.** 1998. Complete DNA sequence and detailed analysis of the *Yersinia pestis* KIM5 plasmid encoding murine toxin and capsular antigen. *Infect Immun* **66**:5731-5742.
116. **Lindler, L. E., and B. D. Tall.** 1993. *Yersinia pestis* pH 6 antigen forms fimbriae and is induced by intracellular association with macrophages. *Mol Microbiol* **8**:311-324.
117. **Liu, T., R. Konig, J. Sha, S. L. Agar, C. T. Tseng, G. R. Klimpel, and A. K. Chopra.** 2008. Immunological responses against *Salmonella enterica* serovar Typhimurium Braun lipoprotein and lipid A mutant strains in Swiss-Webster mice: potential use as live-attenuated vaccines. *Microb Pathog* **44**:224-237.
118. **Madan Babu, M., and K. Sankaran.** 2002. DOLOP--database of bacterial lipoproteins. *Bioinformatics* **18**:641-643.
119. **Maniatis, T., E. F. Fritsch, and J. Sambrook.** 1982. Molecular Cloning: A Laboratory Manual. Cold Spring Harbor Laboratory, Cold Spring Harbor, NY.



120. **Marketon, M. M., R. W. DePaolo, K. L. DeBord, B. Jabri, and O. Schneewind.** 2005. Plague bacteria target immune cells during infection. *Science* **309**:1739-1741.
121. **McDonough, K. A., and S. Falkow.** 1989. A *Yersinia pestis*-specific DNA fragment encodes temperature-dependent coagulase and fibrinolysin-associated phenotypes. *Mol Microbiol* **3**:767-775.
122. **Mead, R.** 1744. *A Discourse on the Plague*. Printed for A. Miller and J. Brindley, London, England.
123. **Meyer, K. F.** 1961. Pneumonic plague. *Bacteriol Rev* **25**:249-261.
124. **Mizel, S. B., A. H. Graff, N. Sriranganathan, S. Ervin, C. J. Lees, M. O. Lively, R. R. Hantgan, M. J. Thomas, J. Wood, and B. Bell.** 2009. Flagellin-F1-V fusion protein is an effective plague vaccine in mice and two species of nonhuman primates. *Clin. Vaccine Immunol.* **16**:21-28.
125. **Motin, V. L., Y. A. Nedialkov, and R. R. Brubaker.** 1996. V antigen-polyhistidine fusion peptide: binding to LcrH and active immunity against plague. *Infect Immun* **64**:4313-4318.
126. **Nakajima, R., and R. R. Brubaker.** 1993. Association between virulence of *Yersinia pestis* and suppression of gamma interferon and tumor necrosis factor alpha. *Infect Immun* **61**:23-31.
127. **Olsson-Liljequist, B.** 1992. E-Test as a routine MIC tool for reference work. *Diagn Microbiol Infect Dis* **15**:479-482.
128. **Orth, K., L. E. Palmer, Z. Q. Bao, S. Stewart, A. E. Rudolph, J. B. Bliska, and J. E. Dixon.** 1999. Inhibition of the mitogen-activated protein kinase superfamily by a *Yersinia* effector. *Science* **285**:1920-1923.
129. **Oyston, P. C., N. Dorrell, K. Williams, S. R. Li, M. Green, R. W. Titball, and B. W. Wren.** 2000. The response regulator PhoP is important for survival under conditions of macrophage-induced stress and virulence in *Yersinia pestis*. *Infect Immun* **68**:3419-3425.
130. **Parkhill, J., B. W. Wren, N. R. Thomson, R. W. Titball, M. T. Holden, M. B. Prentice, M. Sebahia, K. D. James, C. Churcher, K. L. Mungall, S. Baker, D. Basham, S. D. Bentley, K. Brooks, A. M. Cerdeno-Tarraga, T. Chillingworth, A. Cronin, R. M. Davies,**

**P. Davis, G. Dougan, T. Feltwell, N. Hamlin, S. Holroyd, K. Jagels, A. V. Karlyshev, S. Leather, S. Moule, P. C. Oyston, M. Quail, K. Rutherford, M. Simmonds, J. Skelton, K. Stevens, S. Whitehead, and B. G. Barrell.** 2001. Genome sequence of *Yersinia pestis*, the causative agent of plague. *Nature* **413**:523-527.

131. **Perry, R. D., and J. D. Fetherston.** 1997. *Yersinia pestis*--etiologic agent of plague. *Clin Microbiol Rev* **10**:35-66.
132. **Perry, R. D., T. S. Lucier, D. J. Sikkema, and R. R. Brubaker.** 1993. Storage reservoirs of hemin and inorganic iron in *Yersinia pestis*. *Infect Immun* **61**:32-39.
133. **Peterson, J. W., J. E. Comer, W. B. Baze, D. M. Noffsinger, A. Wenglikowski, K. G. Walberg, J. Hardcastle, J. Pawlik, K. Bush, J. Taormina, S. Moen, J. Thomas, B. M. Chatuev, L. Sower, A. K. Chopra, L. R. Stanberry, R. Sawada, W. W. Scholz, and J. Sircar.** 2007. Human monoclonal antibody AVP-21D9 to protective antigen reduces dissemination of the *Bacillus anthracis* Ames strain from the lungs in a rabbit model. *Infect Immun* **75**:3414-3424.
134. **Peterson, J. W., J. E. Comer, D. M. Noffsinger, A. Wenglikowski, K. G. Walberg, B. M. Chatuev, A. K. Chopra, L. R. Stanberry, A. S. Kang, W. W. Scholz, and J. Sircar.** 2006. Human monoclonal anti-protective antigen antibody completely protects rabbits and is synergistic with ciprofloxacin in protecting mice and guinea pigs against inhalation anthrax. *Infect Immun* **74**:1016-1024.
135. **Philipovskiy, A. V., and S. T. Smiley.** 2007. Vaccination with live *Yersinia pestis* primes CD4 and CD8 T cells that synergistically protect against lethal pulmonary *Y. pestis* infection. *Infect Immun* **75**:878-885.
136. **Pillai, L., J. Sha, T. E. Erova, A. A. Fadl, B. K. Khajanchi, and A. K. Chopra.** 2006. Molecular and functional characterization of a ToxR-regulated lipoprotein from a clinical isolate of *Aeromonas hydrophila*. *Infect Immun* **74**:3742-3755.
137. **Pollitzer, R.** 1954. Plague. WHO Monogr Ser **22**:1-698.
138. **Portnoy, D. A., and S. Falkow.** 1981. Virulence-associated plasmids from *Yersinia enterocolitica* and *Yersinia pestis*. *J Bacteriol* **148**:877-883.

139. **Pouliot, K., N. Pan, S. Wang, S. Lu, E. Lien, and J. D. Goguen.** 2007. Evaluation of the role of LcrV-toll-like receptor 2-mediated immunomodulation in the virulence of *Yersinia pestis*. *Infect Immun* **75**:3571-3580.
140. **Prentice, M. B., and L. Rahalison.** 2007. Plague. *The Lancet* **369**:1196-1207.
141. **Pujol, C., and J. B. Bliska.** 2003. The ability to replicate in macrophages is conserved between *Yersinia pestis* and *Yersinia pseudotuberculosis*. *Infect Immun* **71**:5892-5899.
142. **Pujol, C., and J. B. Bliska.** 2005. Turning *Yersinia* pathogenesis outside in: subversion of macrophage function by intracellular yersiniae. *Clin Immunol* **114**:216-226.
143. **Reed, D. S., and M. J. Martinez.** 2006. Respiratory immunity is an important component of protection elicited by subunit vaccination against pneumonic plague. *Vaccine* **24**:2283-2289.
144. **Reed, L. J., and H. Muench.** 1938. A simple method of estimating fifty per cent endpoint. *Am J Hyg* **27**:493-497.
145. **Riedel, S.** 2005. Plague: from natural disease to bioterrorism. *Proc Bayl Univ Med Cent* **18**:116-124.
146. **Rosqvist, R., A. Forsberg, M. Rimpilainen, T. Bergman, and H. Wolf-Watz.** 1990. The cytotoxic protein YopE of *Yersinia* obstructs the primary host defense. *Mol Microbiol* **4**:657-667.
147. **Rosqvist, R., K. E. Magnusson, and H. Wolf-Watz.** 1994. Target cell contact triggers expression and polarized transfer of *Yersinia* YopE cytotoxin into mammalian cells. *Embo J* **13**:964-972.
148. **Roy, C. J., and M. L. M. Pitt.** 2005. Infectious disease aerobiology: aerosol challenge methods. CRC Press, Boca Raton, FL.
149. **Ruckdeschel, K., S. Harb, A. Roggenkamp, M. Hornef, R. Zumbihl, S. Kohler, J. Heesemann, and B. Rouot.** 1998. *Yersinia enterocolitica* impairs activation of transcription factor NF-kappaB: involvement in the induction of programmed cell death and in the suppression of the macrophage tumor necrosis factor alpha production. *J Exp Med* **187**:1069-1079.

150. **Ruckdeschel, K., O. Mannel, K. Richter, C. A. Jacobi, K. Trulzsch, B. Rouot, and J. Heesemann.** 2001. *Yersinia* outer protein P of *Yersinia enterocolitica* simultaneously blocks the nuclear factor-kappa B pathway and exploits lipopolysaccharide signaling to trigger apoptosis in macrophages. *J Immunol* **166**:1823-1831.
151. **Russell, P., S. M. Eley, S. E. Hibbs, R. J. Manchee, A. J. Stagg, and R. W. Titball.** 1995. A comparison of plague vaccine, USP and EV76 vaccine induced protection against *Yersinia pestis* in a murine model. *Vaccine* **13**:1551-1556.
152. **Saltykova, R. A., and M. M. Faibich.** 1975. Experience from a 30-year study of the stability of the properties of the plague vaccine strain EV in the USSR. *Zh Mikrobiol* **6**:3-8.
153. **Samoilova, S. V., L. V. Samoilova, I. N. Yezhov, I. G. Drozdov, and A. P. Anisimov.** 1996. Virulence of pPst<sup>+</sup> and pPst<sup>-</sup> strains of *Yersinia pestis* for guinea-pigs. *J Med Microbiol* **45**:440-444.
154. **Sample, A. K., and R. R. Brubaker.** 1987. Post-translational regulation of Lcr plasmid-mediated peptides in pesticinogenic *Yersinia pestis*. *Microb Pathog* **3**:239-248.
155. **Sebbane, F., D. Gardner, D. Long, B. B. Gowen, and B. J. Hinnebusch.** 2005. Kinetics of disease progression and host response in a rat model of bubonic plague. *Am J Pathol* **166**:1427-1439.
156. **Sebbane, F., C. O. Jarrett, D. Gardner, D. Long, and B. J. Hinnebusch.** 2006. Role of the *Yersinia pestis* plasminogen activator in the incidence of distinct septicemic and bubonic forms of flea-borne plague. *Proc Natl Acad Sci* **103**:5526-5530.
157. **Sebbane, F., N. Lemaitre, D. E. Sturdevant, R. Rebeil, K. Virtaneva, S. F. Porcella, and B. J. Hinnebusch.** 2006. Adaptive response of *Yersinia pestis* to extracellular effectors of innate immunity during bubonic plague. *Proc Natl Acad Sci* **103**:11766-11771.
158. **Sha, J., S. L. Agar, W. B. Baze, J. P. Olano, A. A. Fadl, T. E. Erova, S. Wang, S. M. Foltz, G. Suarez, V. L. Motin, S. Chauhan, G. R. Klimpel, J. W. Peterson, and A. K. Chopra.** 2008. Braun lipoprotein (Lpp) contributes to the virulence of yersiniae: potential role of Lpp in inducing bubonic and pneumonic plague. *Infect Immun* **76**:1390-1409.
159. **Sha, J., A. A. Fadl, G. R. Klimpel, D. W. Niesel, V. L. Popov, and A. K. Chopra.** 2004. The two murein lipoproteins of *Salmonella enterica* serovar Typhimurium contribute to the virulence of the organism. *Infect Immun* **72**:3987-4003.

160. **Simond, P.-L.** 1898. La propagation de la peste. *Ann Inst Pasteur Paris* **12**:625-687.
161. **Skurnik, M., A. Peippo, and E. Ervela.** 2000. Characterization of the O-antigen gene clusters of *Yersinia pseudotuberculosis* and the cryptic O-antigen gene cluster of *Yersinia pestis* shows that the plague bacillus is most closely related to and has evolved from *Y. pseudotuberculosis* serotype O:1b. *Mol Microbiol* **37**:316-330.
162. **Smego, R., J. Frean, and H. Koornhof.** 1999. Yersiniosis I: microbiological and clinicoepidemiological aspects of plague and non-plague *Yersinia* infections. *Eur J Clin Microbiol Infect Dis* **18**:1-15.
163. **Smiley, S. T.** 2008. Current challenges in the development of vaccines for pneumonic plague. *Expert Rev Vaccines* **7**:209-221.
164. **Smith, P. N.** 1959. Pneumonic plague in mice: gross and histopathology in untreated and passively immunized animals. *J Infect Dis* **104**:78-84.
165. **Smith, P. N., J. McCamish, J. Seely, and G. M. Cooke.** 1957. The development of pneumonic plague in mice and the effect of paralysis of respiratory cilia upon the course of infection. *J Infect Dis* **100**:215-222.
166. **Sodeinde, O. A., and J. D. Goguen.** 1988. Genetic analysis of the 9.5-kilobase virulence plasmid of *Yersinia pestis*. *Infect Immun* **56**:2743-2748.
167. **Sodeinde, O. A., and J. D. Goguen.** 1989. Nucleotide sequence of the plasminogen activator gene of *Yersinia pestis*: relationship to *ompT* of *Escherichia coli* and gene *E* of *Salmonella typhimurium*. *Infect. Immun.* **57**:1517-1523.
168. **Sodeinde, O. A., Y. V. Subrahmanyam, K. Stark, T. Quan, Y. Bao, and J. D. Goguen.** 1992. A surface protease and the invasive character of plague. *Science* **258**:1004-1007.
169. **Song, Y., Z. Tong, J. Wang, L. Wang, Z. Guo, Y. Han, J. Zhang, D. Pei, D. Zhou, H. Qin, X. Pang, J. Zhai, M. Li, B. Cui, Z. Qi, L. Jin, R. Dai, F. Chen, S. Li, C. Ye, Z. Du, W. Lin, J. Yu, H. Yang, P. Huang, and R. Yang.** 2004. Complete genome sequence of *Yersinia pestis* strain 91001, an isolate avirulent to humans. *DNA Res* **11**:179-197.
170. **Straley, S. C., and P. A. Harmon.** 1984. Growth in mouse peritoneal macrophages of *Yersinia pestis* lacking established virulence determinants. *Infect Immun* **45**:649-654.

171. **Straley, S. C., and P. A. Harmon.** 1984. *Yersinia pestis* grows within phagolysosomes in mouse peritoneal macrophages. *Infect Immun* **45**:655-659.
172. **Titball, R. W., and E. D. Williamson.** 2001. Vaccination against bubonic and pneumonic plague. *Vaccine* **19**:4175-4184.
173. **Titball, R. W., and E. D. Williamson.** 2004. *Yersinia pestis* (plague) vaccines. *Expert Opin Biol Ther* **4**:965-973.
174. **Tytler, J.** 1799. A Treatise on the Plague and Yellow Fever: With an Appendix, Containing Histories of the Plague at Athens in the Time of the Peloponnesian War; at Constantinople in the Time of Justinian; at London in 1665; at Marseilles in 1720. J. Cushing, for B.B. Macanulty, Salem, MA.
175. **Une, T., and R. R. Brubaker.** 1984. In vivo comparison of avirulent Vwa- and Pgm- or Pst<sup>f</sup> phenotypes of yersiniae. *Infect Immun* **43**:895-900.
176. **Viboud, G. I., and J. B. Bliska.** 2005. *Yersinia* outer proteins: role in modulation of host cell signaling responses and pathogenesis. *Annu Rev Microbiol* **59**:69-89.
177. **Visser, L. G., A. Annema, and R. van Furth.** 1995. Role of Yops in inhibition of phagocytosis and killing of opsonized *Yersinia enterocolitica* by human granulocytes. *Infect Immun* **63**:2570-2575.
178. **Wake, A., M. Misawa, and A. Matsui.** 1975. Siderochrome production by *Yersinia pestis* and its relation to virulence. *Infect Immun* **12**:1211-1213.
179. **Welkos, S., M. L. Pitt, M. Martinez, A. Friedlander, P. Vogel, and R. Tammariello.** 2002. Determination of the virulence of the pigmentation-deficient and pigmentation-/plasminogen activator-deficient strains of *Yersinia pestis* in non-human primate and mouse models of pneumonic plague. *Vaccine* **20**:2206-2214.
180. **Welkos, S. L., K. M. Davis, L. M. Pitt, P. L. Worsham, and A. M. Freidlander.** 1995. Studies on the contribution of the F1 capsule-associated plasmid pFra to the virulence of *Yersinia pestis*. *Contrib Microbiol Immunol* **13**:299-305.

181. **Welkos, S. L., A. M. Friedlander, and K. J. Davis.** 1997. Studies on the role of plasminogen activator in systemic infection by virulent *Yersinia pestis* strain CO92. *Microb Pathog* **23**:211-223.
182. **WHO Group of Consultants.** 1970. Health Aspects of Chemical and Biological Weapons p. 98-109. Geneva: World Health Organization. Geneva, Switzerland.
183. **Williamson, E. D., H. C. Flick-Smith, E. Waters, J. Miller, I. Hodgson, C. S. Le Butt, and J. Hill.** 2007. Immunogenicity of the rF1+rV vaccine for plague with identification of potential immune correlates. *Microb Pathog* **42**:11-21.
184. **Williamson, E. D., A. J. Stagg, S. M. Eley, R. Taylor, M. Green, S. M. Jones, and R. W. Titball.** 2007. Kinetics of the immune response to the (F1 + V) vaccine in models of bubonic and pneumonic plague. *Vaccine* **25**:1142-1148.
185. **Worsham, P. L., and C. Roy.** 2003. Pestoides F, a *Yersinia pestis* strain lacking plasminogen activator, is virulent by the aerosol route. *Adv Exp Med Biol* **529**:129-131.
186. **Worsham, P. L., M. P. Stein, and S. L. Welkos.** 1995. Construction of defined F1 negative mutants of virulent *Yersinia pestis*. *Contrib Microbiol Immunol* **13**:325-328.
187. **Wyman, W.** 1900. The Bubonic Plague. Government Printing Office; U.S. Treasury Dept.; Marine-Hospital Service; Doc. No. 2165, Washington, DC.
188. **Yamamoto, T., T. Hanawa, S. Ogata, and S. Kamiya.** 1996. Identification and characterization of the *Yersinia enterocolitica* *gsrA* gene, which protectively responds to intracellular stress induced by macrophage phagocytosis and to extracellular environmental stress. *Infect Immun* **64**:2980-2987.
189. **Yamamoto, T., T. Hanawa, S. Ogata, and S. Kamiya.** 1997. The *Yersinia enterocolitica* GsrA stress protein, involved in intracellular survival, is induced by macrophage phagocytosis. *Infect Immun* **65**:2190-2196.
190. **Yang, X., B. J. Hinnebusch, T. Trunkle, C. M. Bosio, Z. Suo, M. Tighe, A. Harmsen, T. Becker, K. Crist, N. Walters, R. Avci, and D. W. Pascual.** 2007. Oral vaccination with *Salmonella* simultaneously expressing *Yersinia pestis* F1 and V antigens protects against bubonic and pneumonic plague. *J Immunol* **178**:1059-1067.

191. **Yersin, A.** 1894. La peste bubonique a Hong Kong. Ann Inst Pasteur Paris **8**:662-667.
192. **Zhang, H., D. W. Niesel, J. W. Peterson, and G. R. Klimpel.** 1998. Lipoprotein release by bacteria: potential factor in bacterial pathogenesis. Infect Immun **66**:5196-5201.
193. **Zhang, H., J. W. Peterson, D. W. Niesel, and G. R. Klimpel.** 1997. Bacterial lipoprotein and lipopolysaccharide act synergistically to induce lethal shock and proinflammatory cytokine production. J Immunol **159**:4868-4878.
194. **Zhou, D., Z. Tong, Y. Song, Y. Han, D. Pei, X. Pang, J. Zhai, M. Li, B. Cui, Z. Qi, L. Jin, R. Dai, Z. Du, J. Wang, Z. Guo, J. Wang, P. Huang, and R. Yang.** 2004. Genetics of metabolic variations between *Yersinia pestis* biovars and the proposal of a new biovar, microtus. J Bacteriol **186**:5147-5152.



## VITA

### STACY LEONA AGAR

Stacy Leona Agar was born on September 2, 1969 in Pasco, Washington to James Darrell Agar and Rae Eleanor Van Water Agar. After obtaining her B.S. degree in chemical engineering at NCSU in 1992, Stacy began employment at FMC Wyoming Corporation in Green River, Wyoming where she worked until 1994. As a process engineer, she gained experience in plant processes and policies, determined the efficiency of equipment to maintain and improve the existing alkali chemical process, and participated in a production foreman training program. After leaving Wyoming in 1994, Stacy began employment at Seattle Veterinary Associates Inc. in Seattle, Washington where she worked until 1997. As a veterinary assistant, Stacy assisted veterinarians with patient exams and surgeries, prepared business reports, employee schedules, and employee payroll, inventoried the pharmacy, and managed patient schedules. She also organized the safety program for the practice. After completing her B.S. degrees at Washington State University in 2000, Stacy began employment at the Virginia Mason Research Center (known now as Benaroya Research Institute) in Seattle, Washington in the laboratory of William W. Kwok. As a research technician, Stacy cloned, produced, and purified MHC class II molecules to further the research of autoimmune diseases. She also isolated mononuclear cells from peripheral blood and produced and purified reagents for the isolation of class II molecules to study the link between class II susceptible alleles and diabetes. Following employment with BRI, Stacy joined the Microbiology and Immunology graduate program at the University of Texas Medical Branch in Galveston, Texas in 2003.

#### Education

B.S., May 2000, Microbiology, Washington State University, Pullman, Washington  
B.S., May 2000, Animal Science, Washington State University, Pullman, Washington  
B.S., May 1992, Chemical Engineering, North Carolina State University, Raleigh, North Carolina

#### Publications

Agar SL, Sha J, Foltz SM, Erova TE, Walberg KG, Parham TE, Baze WB, Suarez G, Peterson JW, Chopra AK. 2008. Characterization of the rat pneumonic plague model: Infection kinetics following aerosolization of *Yersinia pestis* CO92. *Microbes Infect* 2008 Dec 3 [Epub ahead of print].

Agar SL, Sha J, Foltz SM, Erova TE, Walberg KG, Parham TE, Baze WB, Suarez G, Peterson JW, Chopra AK. 2008. Characterization of a mouse model of plague after aerosolization of *Yersinia pestis* CO92. *Microbiology* 154(Pt 7):1939-48.

Kozlova EV, Popov VL, Sha J, Foltz SM, Erova TE, Agar SL, Horneman AJ, Chopra AK. 2008. Mutation in the S-ribosylhomocysteinase (*luxS*) gene involved in quorum sensing affects biofilm formation and virulence in a clinical isolate of *Aeromonas hydrophila*. *Microb Pathog* 45(5-6):343-54.

Zhang F, Sha J, Wood TG, Galindo CL, Garner HR, Burkart MF, Suarez G, Sierra JC, Agar SL, Peterson JW, Chopra AK. 2008. Alteration in the activation state of new inflammation-associated targets by phospholipase A2-activating protein (PLAA). *Cell Signal* 20(5):844-61.

\*Sha J, \*Agar SL, Baze WB, Olano JP, Fadl AA, Erova TE, Wang S, Foltz SM, Suarez G, Motin VL, Chauhan S, Klimpel GR, Peterson JW, Chopra AK. 2008. Braun lipoprotein (Lpp) contributes to virulence of yersiniae: potential role of Lpp in inducing bubonic and pneumonic plague. *Infect Immun* 76(4):1390-409. \*Contributed Equally.

Liu T, König R, Sha J, Agar SL, Tseng CT, Klimpel GR, Chopra AK. 2008. Immunological responses against *Salmonella enterica* serovar Typhimurium Braun lipoprotein and lipid A mutant strains in Swiss-Webster mice: potential use as live-attenuated vaccines. *Microb Pathog* 44(3):224-37.

Reichstetter S, Standifer NE, Geubtner KA, Liu AW, Agar SL, Kwok WW. Cytotoxic herpes simplex type 2-specific, DQ0602-restricted CD4 T-cell clones show alloreactivity to DQ0601. 2006. *Immunology* 117(3): 350-7.

Kwok WW, Gebe JA, Liu A, Agar S, Ptacek N, Hammer J, Koelle DM, Nepom GT. Rapid epitope identification from complex class-II- restricted T-cell antigens. 2001. *Trends in Immunology* 22: 583-588.

### **Summary of Dissertation**

*Yersinia pestis* evolved from *Y. pseudotuberculosis* to become the causative agent of bubonic and pneumonic plague. *Y. pestis* is also a category A select agent based on its potential use as a biological weapon. Currently, there is no vaccine licensed in the United States for use against *Y. pestis* so continued research on understanding the pathogenesis of *Y. pestis* and identifying new virulence factors is warranted. Although the natural route of primary infection with *Y. pestis* results in bubonic plague in humans, it is commonly thought that aerosolized *Y. pestis* will be utilized during a biowarfare attack. Therefore, the purpose of this work was two-fold: to assess the changes in virulence attributable to the deletion of a chromosomal element and a virulence plasmid; and to investigate disease progression following aerosolization of *Y. pestis* in two animal models.

First, Stacy and her colleagues characterized *Y. pestis* strains lacking murein, or Braun, lipoprotein (Lpp), an outer membrane protein conserved within the *Enterobacteriaceae* family. She then cured wild-type and  $\Delta lpp$  mutant strains of virulent *Y. pestis* CO92 of one of the virulence plasmids, pPCP1, and assessed how these deletions attenuated the bacterium. Their data indicated that a significant and possibly synergistic attenuation in bacterial virulence occurred in a mouse model of pneumonic plague when both the *lpp* gene and the virulence plasmid pPCP1 encoding the *pla* gene were deleted from *Y. pestis* CO92.

The second half of this work focused on characterizing the dynamics of pneumonic infection following aerosolization of *Y. pestis* CO92 strain in both the mouse and rat models of infection. They exposed mice and rats in a whole-body Madison chamber to various doses of *Y. pestis* CO92 aerosolized by a Collison nebulizer and determined the LD<sub>50</sub> dose, bacterial dissemination, cytokine/chemokine production, and tissue damage over a 72-h course of infection. Plague in mice and rats mimics disease in humans, and understanding disease progression in these models will facilitate development of improved therapeutics.